

**Polydopamine Chemistry:
Adhesion Mechanism, Copolymerization, and Application**

by

Jiwon Lim

A dissertation submitted in partial fulfillment
of the requirements for the degree of
Doctor of Philosophy
(Macromolecular Science and Engineering)
in the University of Michigan
2024

Doctoral Committee:

Professor Jinsang Kim, Chair
Professor Kevin P. Pipe
Professor Pramod Sangi Reddy
Professor Alan I. Taub

Jiwon Lim

limjw@umich.edu

ORCID iD: 0000-0001-6196-4426

© Jiwon Lim 2024

Acknowledgements

I've had the distinct honor of studying under Prof. Kim's guidance. His mentorship has been invaluable—not only in advancing my academic knowledge but also in influencing my personal development. I am deeply appreciative of your steadfast guidance. Over the past five years, I have found our discussions to be incredibly enriching. Your counsel has consistently provided me with a sense of relief and clarity, especially when I have encountered the inevitable challenges of academic research. While juggling my commitment to my family, he has shown remarkable understanding and generosity. His support has been unwavering, for which I am eternally grateful.

My sincere thanks also go to my collaborators and friends, notably Boonjae, Shuo, Matthew, Deokwon, Jungmoo, John, Joonsoo, Choongman, Mira, Minsang, and many others who shall remain unnamed but not unappreciated. Their camaraderie, intellectual curiosity, and collaborative spirit have significantly enriched my research experience. Their insights and encouragement have been a wellspring of motivation and discovery.

I extend my appreciation to my dissertation committee—Prof. Alan Taub, Prof. Kevin Pipe, and Prof. Pramod Reddy—for their discerning guidance and constructive critiques that were pivotal in refining my research.

My church community has been a cornerstone of support, providing for my family in countless ways during my Ph.D. journey. Their unfailing presence and solidarity have meant the

world to me. They have proven to be far more than friends; they are the family I chose, my true brothers and sisters in spirit.

To my wife, Jihye Ju, words fail to encapsulate my gratitude. Her resilience and unwavering support, being the companion and neighborly friend in the backdrop of Ann Arbor, have been life-affirming. The joy she cultivates, the countless events she has lovingly orchestrated for our children and me, are cherished. My love for her knows no bounds.

And to my beloved children, Dahee, Daeun, and Damin, you are my heart and joy. These past five years in Ann Arbor, being close to you, witnessing your smiles, growth, and devotion, have been the most rewarding. I am immensely proud of each of you and will forever treasure our time together in this chapter of our lives.

With each of you, I share the successes and all the fruits that this journey has yielded. Thank you all.

Jiwon Lim
Ann Arbor, MI
March 2024

Table of Contents

Acknowledgements.....	ii
List of Tables	vii
List of Figures.....	viii
Abstract.....	x
Chapter 1 Introduction to Polydopamine Chemistry	1
1.1 Mussel Foot Protein	1
1.2 Polydopamine Chemistry.....	3
1.2.1 Self-polymerization of Polydopamine	4
1.2.2 Structure of Polydopamine	5
1.2.3 Post-modification.....	8
1.2.4 Applications	9
1.3 Conclusion	13
1.4 Reference	14
Chapter 2 Polydopamine Adhesion: Catechol, Amine, Dihydroxyindole, and Aggregation Dynamics	20
2.1 Introduction.....	21
2.2 Result and Discussion.....	25
2.2.1 Molecular Design Principle	25
2.2.2 Structure Analysis by FTIR, and XPS, and ssNMR	26
2.2.3 Adhesion Mechanism Study	29
2.3 Conclusion	34

2.4 Publication Information	35
2.5 Experimental Section	35
2.5.1 Materials	35
2.5.2 Preparation of the PDA Series Coatings on Various Substrates.....	35
2.5.3 Characterization	35
2.5.4 Quaternized Poly(4-vinylpyridine) Preparation.....	36
2.5.5 PDA1-Quaternized Poly(4-vinylpyridine) Film Preparation.....	36
2.6 Supplementary Information	37
2.6.1 Material Synthesis.....	37
2.6.2 ¹³ C Solid State NMR	38
2.6.3 XPS Spectra of PDA1 Coating on Glass Substrates	39
2.7 Reference	39
Chapter 3 Sequential Self-polymerization of Phenolic Compounds with Alkanedithiol Linkers as a Surface-independent and Solvent-resistant Surface Functionalization Strategy	45
3.1 Introduction.....	46
3.2 Result and Discussion.....	49
3.2.1 Reaction Mechanism and Molecular Structure of Copolymer	49
3.2.2 Surface-independent Coating on Various Phenolic Compounds.....	51
3.2.3 Achieving Solvent Resistance by Crosslinking	56
3.3 Conclusion	59
3.4 Publication Information	60
3.5 Experimental Section	60
3.5.1 Chemicals.....	60
3.5.2 Materials Characterization	60
3.5.3 Self-polymerization of Polyphenols	61
3.5.4 Preparation of Polyphenol-ADT Copolymers Coatings on Various Substrates	61

3.5.5 Preparation of Polyphenol-ODT-TT Copolymers Coatings on Various Substrates	62
3.5.6 Solvent Resistance Test	62
3.6 Supporting Information.....	63
3.7 Reference	65
Chapter 4 Dihydroxy Indole-free Poly(catecholamine) for Smooth Surface Coating with Amine Functionality	75
4.1 Introduction.....	76
4.2 Result and Discussion.....	78
4.2.1 Design of DHI-free PCA	78
4.2.2 Surface Independent Coating of DHI-free PCA and Morphology	83
4.2.3 Primary Amine Functionalization via DHI-free PCA	85
4.2.4 DHI-free PCA-coated Graphene for Polymer Composites with Enhanced Thermal Conductivity.....	87
4.3 Conclusion	92
4.4 Publication Information	92
4.5 Experimental Section	93
4.5.1 Materials	93
4.5.2 Method.....	93
4.6 Supporting Information.....	96
4.6.1 Proposed structure of 3,4-dihydroxybenzylamine Oligomers Based on the ToF Spectrum	96
4.6.2 ¹ H NMR spectra of DHI-free PCA During 7 hrs in NaHCO ₃ /D ₂ O	97
4.6.3 Solid-state NMR Spectroscopy.....	98
4.6.4 Synthesis of 10,12-pentacosadiynoic Acid (PCDA)-NHS	99
4.7 Reference	99
Chapter 5 Summary and Outlook	108

List of Tables

Table 3-1 Atomic ratio of N 1s to S 2s via XPS survey spectra after 24hrs of reaction for various molar feed ratios between ODT and DBA.....	55
Table 3-2 Atomic ratio of N 1s to S 2s over the reaction time after the addition of ODT, as determined by XPS survey spectra (ODT/DBA ratio is 0.5/1).....	55
Table 4-1 Thermal conductivity of graphene nanoplatelet-poly(acrylic acid) composites	91

List of Figures

Figure 1-1 Attachment process of Mytilus mussels to a surface	2
Figure 1-2 Schematic representation of the four main catechol–surface interactions	3
Figure 1-3 Polymerization mechanism of dopamine.	5
Figure 1-4 Amine-based reaction of dopamine monomer	6
Figure 1-5 Some structures of PDA 1–10 and eumelanin 11–14 proposed in the literature.....	7
Figure 1-6 Dopamine oligomers in literatures	8
Figure 1-7 Reactions of N- and S-nucleophiles with <i>o</i> -quinone.....	9
Figure 2-1 Structural analysis of the PDA series by FTIR and XPS	28
Figure 2-2 (A) Evaluation of coating behaviors of the PDA series on different substrates. (B) Particle size analysis by using DLS. (C) SEM images showing the PDA series coating on glass substrates.....	31
Figure 2-3 3D AFM images of the surface morphology of PDA series	32
Figure 2-4 Aggregation induced adhesion via PDA1-qPVP mixture.....	33
Figure S2-1 Solid-state NMR analysis of the PDA series	38
Figure S2-2 High-resolution XPS spectra of the O 1s region for PDA1 drop-casted (Pink) and dip-coated (Gray) on glass substrates	39
Figure 3-1 Reaction mechanism of copolymer and characterization.....	51
Figure 3-2 Copolymerization of various phenolic compounds with ODT	53
Figure 3-3 XPS spectra of copolymers	54
Figure 3-4 Solvent resistance of copolymers.....	58
Figure S3-1 Various oxidation states of 4-ethylcatechol and the proposed structures of its dimer through aryl-aryl coupling	63
Figure S3-2 SEM images showing the copolymer coating on glass substrates.....	64

Figure S3-3 Stability test results of PDBA, PDBA_ODT, and PDBA_EGDT coatings on glass substrates with different ratio of monomer to linker in NaOH(aq.), DMSO and chloroform	64
Figure S3-4 Stability test results of PDBA, PDBA_ODT, and PDBA_EGDT coatings with different ratio of monomer to linker in NaOH(aq.), DMSO and chloroform	65
Figure 4-1 Structure analysis of DHI-free PCA	82
Figure 4-2 Carbon- ¹³ CP-MAS NMR spectra of a powder sample of PDA polymer obtained under 15 kHz MAS	82
Figure 4-3 Surface independent coating of polydopamine and DHI-free PCA.....	84
Figure 4-4 Primary amine functionalization by using DHI-free PCA.....	87
Figure 4-5 DHI-free PCA coating on graphene	89
Figure 4-6 Thermal conductivities of GnP-poly(acrylic acid) composites as a function of graphene content	91
Figure S4-1 H NMR spectra of DHI-free PCA after 0 min	97
Figure S4-2 H NMR spectra of DHI-free PCA after 3 hrs	97
Figure S4-3 H NMR spectra of DHI-free PCA after 7 hrs	98

Abstract

Polydopamine (PDA), inspired by mussel adhesive proteins, has garnered significant interest for its ability to coat surfaces independently of their nature, using a simple and environmentally friendly process in basic aqueous solutions. However, understanding its binding and polymerization mechanisms remains challenging due to the numerous reactive sites of the dopamine monomer and the insoluble nature of the resulting polymer film. Additionally, PDA's short, rigid backbone differs from the long, flexible sequences found in mussel-binding proteins, which limits its effectiveness in achieving the conformal contact necessary for efficient adhesion.

In this dissertation, I systematically investigate the roles of PDA's building blocks—poly(catechol), poly(catecholamine), and PDA—to enhance our understanding of their binding mechanisms. Contrary to initial expectations, we find that PDA's adhesion primarily arises from the solubility limits of catecholamine oligomers in aqueous environments, complemented by catechol's multiple binding modes. Notably, in the absence of amines, poly(catechol) remains in solution or forms minor suspensions without surface coating, emphasizing the crucial role of amines in facilitating insoluble aggregate formation for adhesion. We validate our findings by inducing poly(catechol) aggregation with quaternized poly(4-vinylpyridine) (qPVP), demonstrating adhesion upon agglomerate formation.

Based on these insights, we develop a sequential self-polymerization strategy of phenolic compounds combined with alkanedithiol (ADT) crosslinkers for versatile surface-independent coating and functionalization. The resulting copolymer leverages phenol's diverse binding modes

and ADT's flexible aliphatic chain for conformal substrate contact, with Michael addition reactions yielding solvent-resistant crosslinked polymer films. This approach successfully functionalizes various surfaces with phenolic monomers, overcoming stability issues encountered with conventional polydopamine derivatives.

Furthermore, we achieve 5,6-dihydroxyindole (DHI)-free poly(catecholamine) (PCA) coating using 3,4-dihydroxybenzylamine hydrobromide, yielding smooth, uniform surfaces. The suppressed indole ring formation preserves primary amine groups, offering an alternative surface functionalization strategy, particularly for hydroxyl-containing surfaces. DHI-free PCA modification enhances the thermal conductivity of graphene-polymer composites, achieving a significant increase compared to untreated graphene controls.

Overall, this work advances understanding of PDA's binding mechanisms and offers novel strategies for surface coating and functionalization with broad implications across material science and engineering. By elucidating the intricate processes involved in PDA adhesion and developing innovative coating techniques, this research opens avenues for the design of advanced materials with tailored properties and enhanced performance in various applications.

Chapter 1 Introduction to Polydopamine Chemistry

Bioinspired materials have captivated the field of materials science, presenting innovative solutions to a broad spectrum of engineering obstacles. Nature has crafted materials and methodologies that often exceed the performance and sustainability of their artificial equivalents. Among the notable achievements of natural design are the adhesive proteins located in the holdfasts of mussel byssal threads, which are renowned for their exceptional adhesion qualities, particularly in moist and marine settings.

This chapter is dedicated to exploring the realm of polydopamine chemistry, which draws inspiration from the binding process of mussel adhesive proteins. Initially, I will lay out the historical context of polydopamine and its roots in biological adhesive systems. Subsequent sections will cover the polymerization process of polydopamine, including its structure and potential applications. Despite polydopamine's distinct qualities, its comprehensive understanding is hindered by its complex structure, a challenge that underpins the motivation behind this study.

1.1 Mussel Foot Protein

Mussel foot protein (mfp) has been studied for their unique ability to firmly adhere to substrates in aqueous conditions, which traditionally challenge synthetic adhesives. Intrigued by the extraordinary adhesive properties exhibited by mussels in seawater, researchers initiated a study to understand the biological features of mussel¹, as depicted in Figure 1-1A. Subsequent investigations delved into the binding behaviors of mussels across different substrates and examined various conditions, including the contact angle between the thread, plaque, and

The significance of mussel protein is not limited to underwater adhesion, but a surface-independent adhesion. The catechol side chains of DOPA were found to play a crucial role in the adhesion process through a combination of non-covalent and covalent interactions with the substrate surface.⁵ This unique property is mainly associated with multiple binding modes such as H-bond, π - π interaction, coordination, hydrophobic interaction, and even covalent bonding as shown in Figure 1-2.

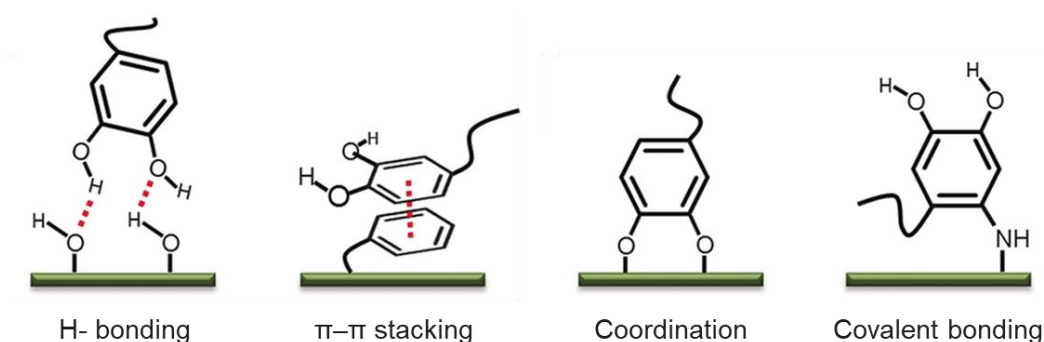


Figure 1-2 Schematic representation of the four main catechol-surface interactions described in this section.⁶

1.2 Polydopamine Chemistry

Since the adhesion property of mussel protein is unique and interesting, many attempts were made to obtain the same adhesion property. However, these efforts often run into issues with scalability and expense, as peptide bond formation is required. Recognizing these limitations, the Messersmith group highlighted PDA as an economically viable and simple substitute to dopa-containing peptides, usually synthesized through the straightforward autoxidation of dopamine in air as depicted in Figure 1-3.⁷ PDA shares structural similarity with mussel proteins, which confer its ability to adhere to a wide range of materials, including ceramics, metals, polymers, and even Teflon. The dopamine monomer, which contains both catechol and amine groups, can form

coatings through oxidative polymerization and the resulting polymer exhibits universal coating capability. Although the process is straightforward and the coating capabilities of PDA are exceptional, a comprehensive understanding of the mechanisms underlying polydopamine formation remains elusive. This is due to the complex reactivity of the dopamine monomer, which has multiple reactive sites, and the formation of various intermediates during polymerization.

1.2.1 Self-polymerization of Polydopamine

The self-polymerization simply initiated by the oxidation and coating layers were formed in aqueous condition in few hours. The presence of the uncyclized, oxidized form of dopamine, which provides primary amine groups on the surface, is observed upon oxidation. This form can undergo dopamine–quinone formation and further react through catechol-to-catechol couplings with either DHI or unoxidized dopamine.⁸ Upon exposure to external stimuli, such as light irradiation, the catechol rings of dopamine can lose an electron to form a dopamine–semiquinone radical. This dopamine–semiquinone radical can then either oxidize intramolecularly to form dopamine–quinone, leading to DHI formation, or oxidize intermolecularly to induce dimerization, resulting in a catechol–catechol dimer.⁹ Research has shown that catechol monomers, even in the absence of nucleophiles like amine groups, can be successfully polymerized on functionalized surfaces through a radical-initiating pathway. Additionally, the formation of 5,6-dihydroxyindole (DHI) through the cyclization reaction of dopaquinone introduces variability in PDA's building blocks. This diversity of building blocks, which possess different oxidation states, contributes to the characteristic dark color of PDA, as it correlates with visible light absorption.

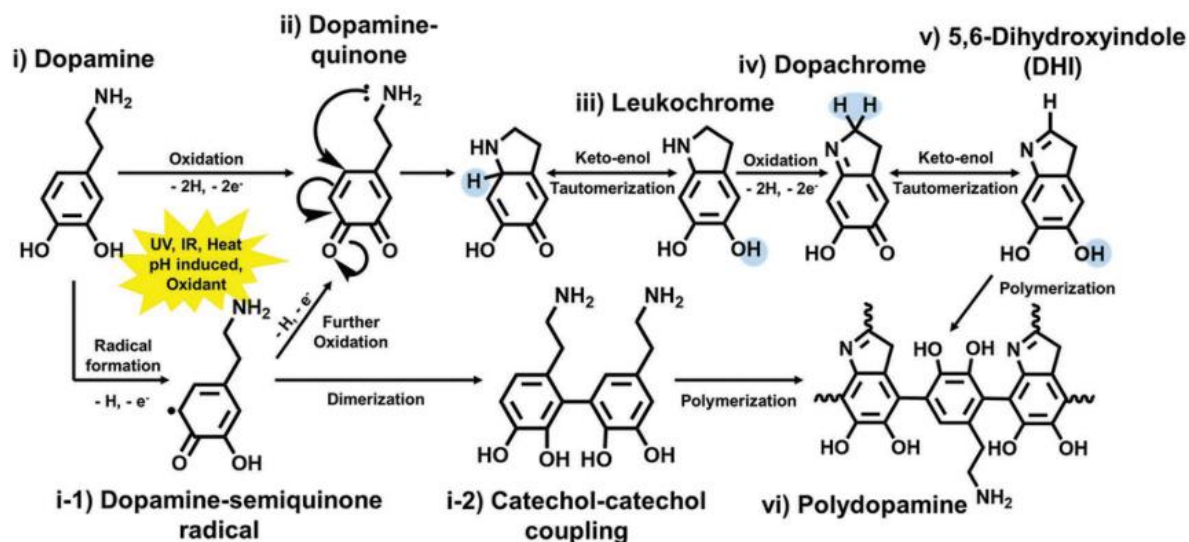
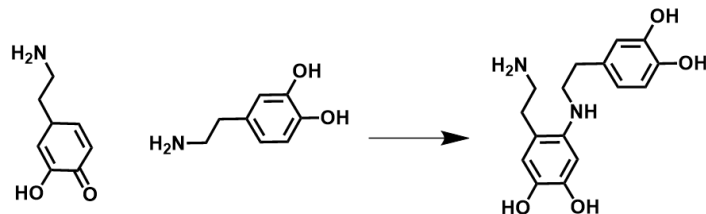


Figure 1-3 Polymerization mechanism of dopamine.¹⁰

1.2.2 Structure of Polydopamine

Unraveling PDA structure has been an enduring pursuit, one that has yet to reach a definitive conclusion—likely due to the inherent complexity of PDA. The structure of PDA is highly dependent on the specifics of its preparation, as well as whether it is formed as a coating on a surface or as particles/aggregates in suspension. The formation of DHI exacerbates the situation by instigating crosslinking and rendering the polymer insoluble, thereby hindering the separation of polymers and impeding structural analysis in a solution state. Moreover, oxidative degradation of the indole structure's phenyl ring results in the production of terminal pyrrole carboxylic acid.^{11,12} Besides, amine functionality could react with the oxidized catechol via Michael addition and Schiff base reaction as shown in Figure 1-4. Therefore, the chemical structure of PDA has not yet been completely elucidated due to its complexity. Although attempts have been made to

1. Michael addition



2. Schiff base reaction

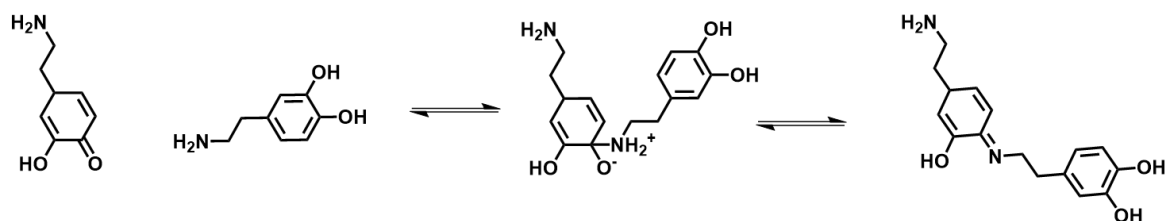


Figure 1-4 Amine-based reaction of dopamine monomer.

characterize its composition, what have primarily been identified using mass spectrometry are oligomeric species or intermediate products rather than the fully formed polymer. Once the PDA polymerizes, the analytical techniques that can be applied are somewhat restricted. These include solid-state nuclear magnetic resonance (NMR) spectroscopy, X-ray crystallography, Fourier-transform infrared (FTIR) spectroscopy, ultraviolet-visible (UV/Vis) spectroscopy, and atomic force microscopy (AFM). These methods allow for the proposal of possible structures, but they do not provide a definitive picture of the polymer's complete structure. These findings have been reported and are exemplified in Figure 1-5.¹³ Another point of contention that has arisen concerns the molecular weight of polydopamine (PDA). As polymerization progresses, the extension of the PDA backbone's π -conjugated system promotes π - π interactions, which in turn increase the hydrophobicity of the molecule and may lead to the exceeding of its solubility threshold in aqueous solutions. Additionally, previous research, which employed matrix-assisted laser desorption/ionization (MALDI) and is depicted in Figure 1-6.¹⁴ predominantly identified oligomeric species, casting doubt on the polymeric nature of PDA. It is worth noting, however,

that there is a singular study asserting the polymeric status of PDA, which is based on evidence from single-molecule force spectroscopy (SMFS).

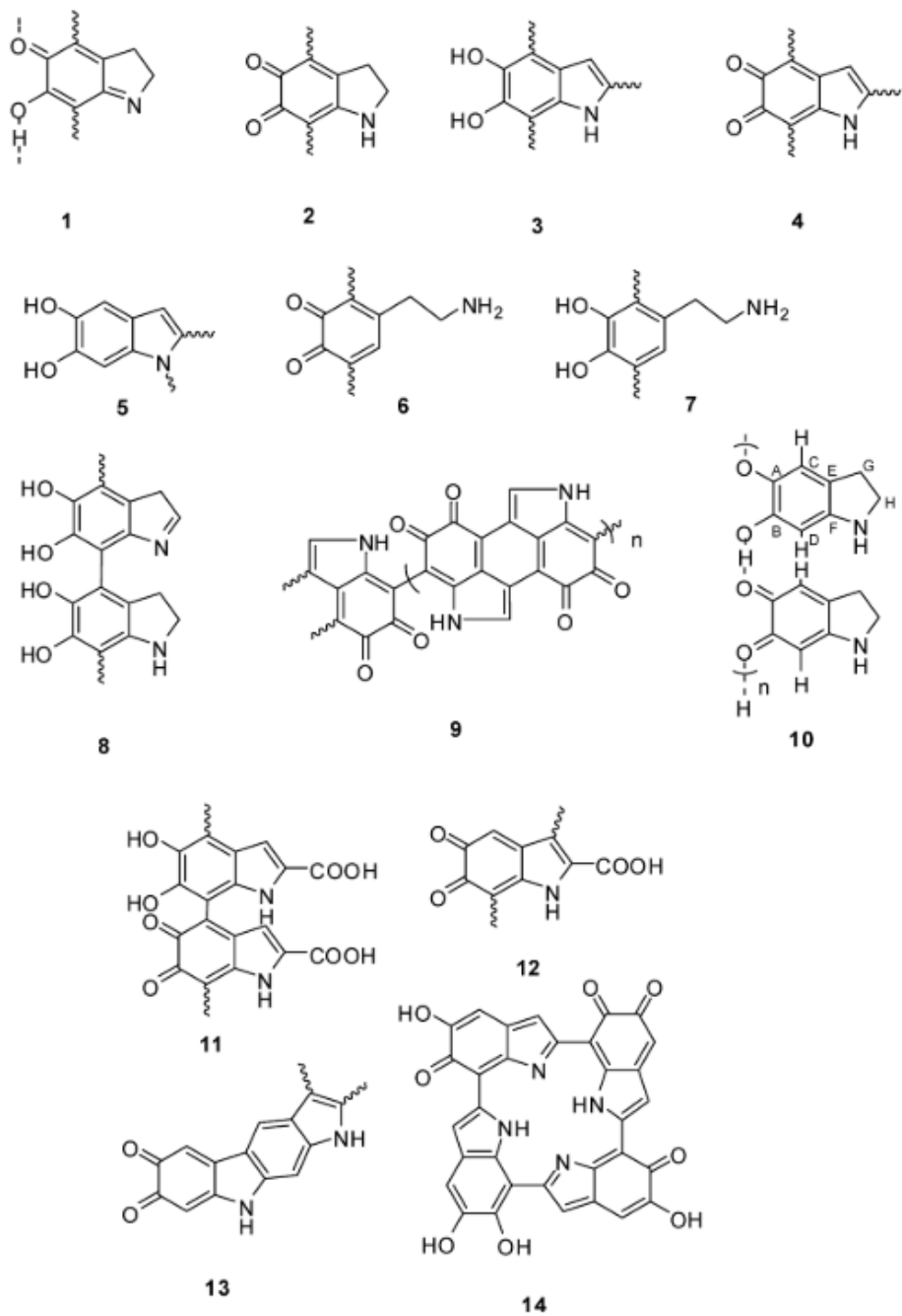


Figure 1-5 Some structures of PDA 1–10 and eumelanin 11–14 proposed in the literature.¹³

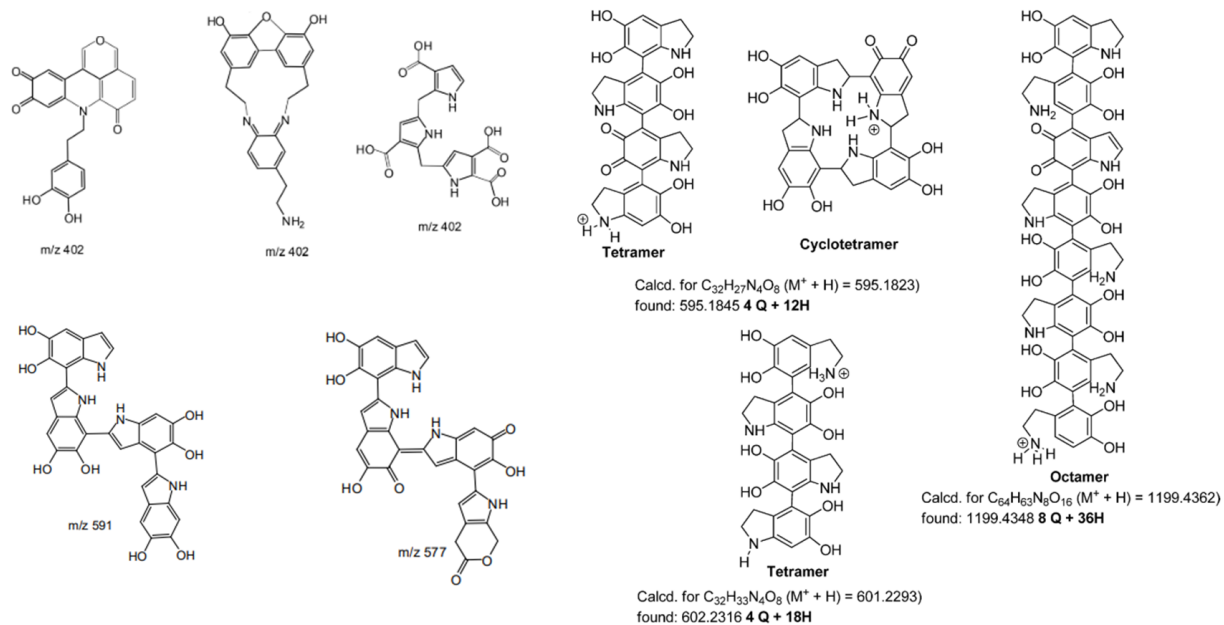


Figure 1-6 Dopamine oligomers in literatures.¹⁴

1.2.3 Post-modification

The *o*-quinone moieties present in polydopamine (PDA), which arise from the oxidation of catechol, introduce additional reactive sites due to their carbonyl functionalities and properties as Michael acceptors. The carbonyl functionalities and Michael acceptor properties of these groups facilitate their participation in nucleophilic addition reactions, which can involve 1,2- and/or 1,4-additions within a basic aqueous solution at room temperature as depicted in Figure 1-7. Each quinone moiety in PDA formally possesses two Michael systems, but it is generally believed that the reaction primarily occurs at the less hindered system. In practical applications, thiol or amine reaction with PDA is highly valued for attaching various functional groups because of the ubiquitous presence of amino and thiol groups in peptides and proteins, or because these groups can be readily introduced to the entity intended for PDA linkage. These applications have been extensively explored.¹⁵⁻¹⁷ Moreover, the in-situ integration of NH_2 or SH containing nucleophiles

during the PDA polymerization process allows for the concurrent formation and functionalization of PDA.¹⁸

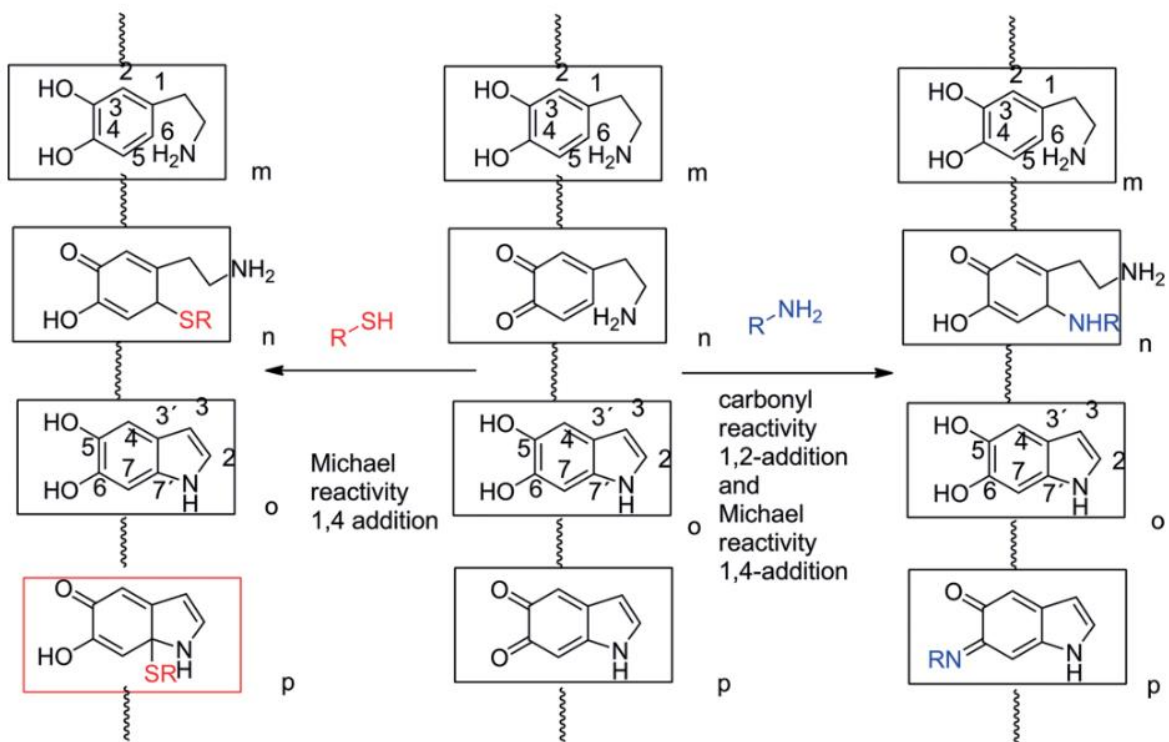


Figure 1-7 Reactions of N- and S-nucleophiles with *o*-quinone.¹⁹

1.2.4 Applications

Enhancing material surfaces is essential for tailoring their properties, improving their performance, and expanding their application scope. Polydopamine (PDA) coatings are remarkably versatile and can be readily applied to a diverse array of surfaces. Moreover, they offer a platform for various post-modifications through Michael addition reactions involving amines and thiols. Before PDA coatings became prevalent, the landscape of surface functionalization was dominated by four principal methods: Silane coupling agents were among the most popular choices, offering a variety of functionalities to modify surfaces containing hydroxy groups. The Layer-by-

Layer (LbL) technique was also prominent but necessitated numerous coating cycles and a meticulous process. Self-Assembled Monolayers (SAMs) required precise matching of surface-adsorbate chemistry, exemplified by the thiol-gold interaction, to be effective. Meanwhile, plasma treatments provided temporary solutions as the beneficial properties imparted to surfaces often deteriorated over time.

In contrast, polydopamine (PDA) coating has gained widespread usage due to its surface independent adhesion and the presence of various functional groups. Unlike the more selective silane coupling agents, LbL assembly, SAMs, and plasma treatments, PDA coating is not confined to substrates like noble metals and metal oxides. It can also effectively bind to materials with inherently low surface energy, including polyolefins. This makes PDA a highly adaptable and durable option for enhancing and customizing the surfaces of an extensive range of materials such as metal oxides, carbon nanomaterials, and polymers.

1.2.4.1 Metal Oxides

Iron (III) oxide, a widely utilized metal oxide for PDA surface modification, is especially valued for its magnetic properties that enable easy collection and purification by external magnetic fields. Mrowczynski et al. coated Fe_3O_4 nanoparticles with a PDA film that have a diameter of about 8 nm. These served as vehicles for drug delivery.²⁰ Similarly, Wu et al. produced PDA-modified Fe_3O_4 nanoparticles, later embedded in natural killer (NK) cells, which exhibited enhanced tumor targeting and growth inhibition when used in conjunction with an external magnetic field.²¹ Expanding beyond single nanoparticles, researchers have also employed PDA with Fe_3O_4 nanoparticle clusters, creating core-shell nanocomposites that exhibited superior

photothermal effects for cancer cell eradication compared to unenhanced clusters. This enhanced effect is partly attributed to the combination of iron oxide and PDA's photothermal properties.²²

In addition to the widely implemented iron oxide, various metal oxides have also been coupled with PDA to develop versatile functional nanoplateforms. Lee et al. produced carbon-coated Mn_3O_4 nanocrystals with a PDA-derived carbon layer, enhancing the electrical conductivity for Pt electrocatalyst support, resulting in significantly improved performance in oxygen reduction reactions.²³ In parallel, Park et al. reported PDA-coated WO_3 nanoparticles conjugated with hyaluronic acid for targeted photothermal therapy with excellent biocompatibility.²⁴

1.2.4.2 Carbon Nanomaterials

Carbon nanomaterials, encompassing carbon dots, nanotubes, fullerenes, graphene, and carbon spheres, possess remarkable physical and chemical properties. However, surfaces with limited functionality and low surface energy pose challenges to effective functionalization. Furthermore, carbon nanomaterials face biomedical application limitations due to toxicity concerns. Addressing this challenge, PDA surface modification are effective strategies, particularly for carbon nanotubes (single-walled and multiwalled), which are extensively researched in nanomedicine and biosensor applications. Liu et al. created an SWNT@PDA nanocomposite for simultaneous radioisotope cancer therapy. The PDA coating enhances SWNT stability and solubility, enables MRI contrast enhancement.²⁵ Moreover, graphene oxide coated with PDA induces N-containing active sites, as investigated by Wang et al., exhibits enhanced electrocatalytic activity for oxygen reduction, outperforming platinum-based catalysts in stability and methanol tolerance.²⁶

1.2.4.3 Polymers

Polymers, particularly common types like polyolefins, typically exhibit low surface energy, which creates obstacles for surface modification. The ability of polydopamine (PDA) to adhere to surfaces regardless of their energy levels presents a viable solution for functionalizing these otherwise inert polymers. For example, poly(lactic-co-glycolic) acid (PLGA) are being coated with PDA to enhance drug delivery systems in nanomedicine. Tao et al. developed a PDA-coated, cholic acid-functionalized PLGA platform for targeted breast cancer therapy with an aptamer conjugated to the PDA layer, facilitating the delivery of the anticancer drug docetaxel. In this application, PDA serves as a linker to introduce the tumor-targeting aptamer.²⁷ Polystyrene (PS) also is modified with polydopamine (PDA) to create novel nanostructures to create raspberry-like nanoparticles are reported by Kohri et al.²⁸ Furthermore, Deng group developed PS/silver nanocomposite particles via PDA coating on PS nanoparticle to improve antibacterial property. Silver precursor $[\text{Ag}(\text{NH}_3)_2]^+$ ions are subsequently attracted to and held by the catechol and amine groups in the PDA coating on the PS/PDA composite spheres.²⁹

1.2.4.4 Other Biomedical Applications

PDA has gained attention for its biocompatibility, adhesive properties, antioxidant capabilities, and efficient photothermal conversion. These features have showcased its vast potential across diverse applications within the field of biomedical applications. PDA functions as a versatile element in regenerative medicine, where it can be utilized as a surface treatment and as an integral part of scaffolding structures to aid in wound healing.³⁰⁻³² In the field of tissue engineering, PDA can promote cell adhesion and proliferation, making it a valuable component in the creation of scaffolds for growing tissues.^{33,34}

1.3 Conclusion

The journey through the realm of polydopamine (PDA) chemistry in this introduction chapter reveals not only the bioinspired origins of PDA but also its transformative impact on materials science. Drawing from the exceptional adhesion capabilities of mussel foot proteins, PDA has emerged as a highly adaptable material capable of universal coating and functionalization across a myriad of substrates without the constraints of surface energy.

The examination of PDA's polymerization process emphasized the complexity and versatility of its structure and highlighted the elusive nature of unraveling its exact molecular makeup. Even so, the utilization of PDA in various applications has not been hindered—its potential continues to be realized in fields ranging from energy conversion and storage to targeted drug delivery and regenerative medicine.

PDA coatings have surpassed traditional methods of surface modification, offering economic and scalable alternatives for enhancing biocompatibility and adhesive strength. Notably, its integration with metal oxides, carbon nanomaterials, and polymers underscores the breadth of its applicability.

This dissertation aims to further dissect the intricacies of PDA chemistry to better harness its potential. Through a comprehensive understanding of PDA's binding mechanism, we can extend its applications and elevate the standard of bioinspired material science to new heights, mirroring nature's own unrivaled designs.

1.4 Reference

- (1) Benedict, C. V.; Waite, J. H. Composition and Ultrastructure of the Byssus of *Mytilus Edulis*. *J. Morphol.* **1986**, *189* (3), 261–270. <https://doi.org/10.1002/jmor.1051890305>.
- (2) Crisp, D. J.; Walker, G.; Young, G. A.; Yule, A. B. Adhesion and Substrate Choice in Mussels and Barnacles. *J. Colloid Interface Sci.* **1985**, *104* (1), 40–50. [https://doi.org/10.1016/0021-9797\(85\)90007-4](https://doi.org/10.1016/0021-9797(85)90007-4).
- (3) Waite, J. H.; Tanzer, M. L. Polyphenolic Substance of *Mytilus Edulis*: Novel Adhesive Containing L-Dopa and Hydroxyproline. *Science* **1981**, *212* (4498), 1038–1040. <https://doi.org/10.1126/science.212.4498.1038>.
- (4) Lee, B. P.; Messersmith, P. B.; Israelachvili, J. N.; Waite, J. H. Mussel-Inspired Adhesives and Coatings. *Annu. Rev. Mater. Res.* **2011**, *41*, 99–132. <http://dx.doi.org/10.1146/annurev-matsci-062910-100429>.
- (5) Waite, J. H. Mussel Adhesion - Essential Footwork. *J. Exp. Biol.* **2017**, *220* (4), 517–530. <https://doi.org/10.1242/jeb.134056>.
- (6) Saiz-Poseu, J.; Mancebo-Aracil, J.; Nador, F.; Busqué, F.; Ruiz-Molina, D. The Chemistry behind Catechol-Based Adhesion. *Angew. Chemie Int. Ed.* **2019**, *58* (3), 696–714. <https://doi.org/10.1002/anie.201801063>.
- (7) Lee, H.; Dellatore, S. M.; Miller, W. M.; Messersmith, P. B. Mussel-Inspired Surface Chemistry for Multifunctional Coatings. *Science*. **2007**, *318* (5849), 426–430. <https://doi.org/10.1126/science.1147241>.
- (8) Hong, S.; Na, Y. S.; Choi, S.; Song, I. T.; Kim, W. Y.; Lee, H. Non-Covalent Self-Assembly and Covalent Polymerization Co-Contribute to Polydopamine Formation. *Adv. Funct. Mater.* **2012**, *22* (22), 4711–4717. <https://doi.org/10.1002/adfm.201201156>.

- (9) Du, X.; Li, L.; Li, J.; Yang, C.; Frenkel, N.; Welle, A.; Heissler, S.; Nefedov, A.; Grunze, M.; Levkin, P. A.; UV-Triggered Dopamine Polymerization: Control of Polymerization, Surface Coating, and Photopatterning. *Adv. Mater.* **2014**, *26* (47), 8029–8033. <https://doi.org/10.1002/adma.201403709>.
- (10) Lee, H. A.; Park, E.; Lee, H. Polydopamine and Its Derivative Surface Chemistry in Material Science: A Focused Review for Studies at KAIST. *Adv. Mater.* **2020**, *32* (35), 1907505. <https://doi.org/10.1002/adma.201907505>.
- (11) Della Vecchia, N. F.; Avolio, R.; Alfè, M.; Errico, M. E.; Napolitano, A.; D'Ischia, M. Building-Block Diversity in Polydopamine Underpins a Multifunctional Eumelanin-Type Platform Tunable Through a Quinone Control Point. *Adv. Funct. Mater.* **2013**, *23* (10), 1331–1340. <https://doi.org/10.1002/adfm.201202127>.
- (12) Ponzio, F.; Barthès, J.; Bour, J.; Michel, M.; Bertani, P.; Hemmerlé, J.; D'Ischia, M.; Ball, V. Oxidant Control of Polydopamine Surface Chemistry in Acids: A Mechanism-Based Entry to Superhydrophilic-Superoleophobic Coatings. *Chem. Mater.* **2016**, *28* (13), 4697–4705. <https://doi.org/10.1021/acs.chemmater.6b01587>.
- (13) Liebscher, J.; Mrówczyński, R.; Scheidt, H. A.; Filip, C.; Haidade, N. D.; Turcu, R.; Bende, A.; Beck, S. Structure of Polydopamine: A Never-Ending Story? *Langmuir* **2013**, *29* (33), 10539–10548. <https://doi.org/10.1021/la4020288>.
- (14) Alfieri, M. L.; Micillo, R.; Panzella, L.; Crescenzi, O.; Oscurato, S. L.; Maddalena, P.; Napolitano, A.; Ball, V.; D'Ischia, M. Structural Basis of Polydopamine Film Formation: Probing 5,6-Dihydroxyindole-Based Eumelanin Type Units and the Porphyrin Issue. *ACS Appl. Mater. Interfaces* **2018**, *10* (9), 7670–7680. <https://doi.org/10.1021/acsami.7B09662>.

- (15) Wei, Y.; Gao, L.; Wang, L.; Shi, L.; Wei, E.; Zhou, B.; Zhou, L.; Ge, B. Polydopamine and Peptide Decorated Doxorubicin-Loaded Mesoporous Silica Nanoparticles as a Targeted Drug Delivery System for Bladder Cancer Therapy. *Drug Deliv.* **2017**, *24* (1), 681–691. <https://doi.org/10.1080/10717544.2017.1309475>.
- (16) Cao, P.; Li, W. W.; Morris, A. R.; Horrocks, P. D.; Yuan, C. Q.; Yang, Y. Investigation of the Antibiofilm Capacity of Peptide-Modified Stainless Steel. *R. Soc. Open Sci.* **2018**, *5* (3). <https://doi.org/10.1098/rsos.172165>.
- (17) Mu, W.; Liu, J.; Wang, J.; Mao, H.; Wu, X.; Li, Z.; Li, Y. Bioadhesion-Inspired Fabrication of Robust Thin-Film Composite Membranes with Tunable Solvent Permeation Properties. *RSC Adv.* **2016**, *6* (106), 103981–103992. <https://doi.org/10.1039/c6ra20341h>.
- (18) Knorr, D. B.; Tran, N. T.; Gaskell, K. J.; Orlicki, J. A.; Woicik, J. C.; Jaye, C.; Fischer, D. A.; Lenhart, J. L. Synthesis and Characterization of Aminopropyltriethoxysilane-Polydopamine Coatings. *Langmuir* **2016**, *32* (17), 4370–4381. <https://doi.org/10.1021/acs.langmuir.6b00531>.
- (19) Liebscher, J. Chemistry of Polydopamine – Scope, Variation, and Limitation. *European J. Org. Chem.* **2019**, *2019* (31–32), 4976–4994. <https://doi.org/10.1002/ejoc.201900445>.
- (20) Mrówczyński, R.; Jurga-Stopa, J.; Markiewicz, R.; Coy, E. L.; Jurga, S.; Woźniak, A. Assessment of Polydopamine Coated Magnetic Nanoparticles in Doxorubicin Delivery. *RSC Adv.* **2016**, *6* (7), 5936–5943. <https://doi.org/10.1039/c5ra24222c>.
- (21) Wu, L.; Zhang, F.; Wei, Z.; Li, X.; Zhao, H.; Lv, H.; Ge, R.; Ma, H.; Zhang, H.; Yang, B.; Li, J.; Jiang, J. Magnetic Delivery of Fe₃O₄@polydopamine Nanoparticle-Loaded

- Natural Killer Cells Suggest a Promising Anticancer Treatment. *Biomater. Sci.* **2018**, *6* (10), 2714–2725. <https://doi.org/10.1039/c8bm00588e>.
- (22) Wu, M.; Zhang, D.; Zeng, Y.; Wu, L.; Liu, X.; Liu, J. Nanocluster of Superparamagnetic Iron Oxide Nanoparticles Coated with Poly (Dopamine) for Magnetic Field-Targeting, Highly Sensitive MRI and Photothermal Cancer Therapy. *Nanotechnology* **2015**, *26* (11). <https://doi.org/10.1088/0957-4484/26/11/115102>.
- (23) Lee, D. G.; Jeong, H.; Jeon, K. W.; Zhang, L.; Park, K.; Ryu, S.; Kim, J.; Lee, I. S. Carbon Thin-Layer-Coated Manganese Oxide Nanocrystals as an Effective Support for High-Performance Pt Electrocatalysts Stabilized at a Metal-Metal Oxide-Carbon Triple Junction. *J. Mater. Chem. A* **2017**, *5* (42), 22341–22351. <https://doi.org/10.1039/c7ta07248a>.
- (24) Sharker, S. M.; Kim, S. M.; Lee, J. E.; Choi, K. H.; Shin, G.; Lee, S.; Lee, K. D.; Jeong, J. H.; Lee, H.; Park, S. Y. Functionalized Biocompatible WO₃ Nanoparticles for Triggered and Targeted in Vitro and in Vivo Photothermal Therapy. *J. Control. Release* **2015**, *217*, 211–220. <https://doi.org/10.1016/j.jconrel.2015.09.010>.
- (25) Zhao, H.; Chao, Y.; Liu, J.; Huang, J.; Pan, J.; Guo, W.; Wu, J.; Sheng, M.; Yang, K.; Wang, J.; Liu, Z. Polydopamine Coated Single-Walled Carbon Nanotubes as a Versatile Platform with Radionuclide Labeling for Multimodal Tumor Imaging and Therapy. *Theranostics* **2016**, *6* (11), 1833–1843. <https://doi.org/10.7150/thno.16047>.
- (26) Wang, D. D.; Gao, X.; Zhao, L.; Zhou, J.; Zhuo, S.; Yan, Z.; Xing, W. Polydopamine-Coated Graphene Nanosheets as Efficient Electrocatalysts for Oxygen Reduction Reaction. *RSC Adv.* **2018**, *8* (29), 16044–16051. <https://doi.org/10.1039/c8ra01027g>.

- (27) Tao, W.; Zeng, X.; Wu, J.; Zhu, X.; Yu, X.; Zhang, X.; Zhang, J.; Liu, G.; Mei, L. Polydopamine-Based Surface Modification of Novel Nanoparticle-Aptamer Bioconjugates for in Vivo Breast Cancer Targeting and Enhanced Therapeutic Effects. *Theranostics* **2016**, *6* (4), 470–484. <https://doi.org/10.7150/thno.14184>.
- (28) Kohri, M.; Nannichi, Y.; Kohma, H.; Abe, D.; Kojima, T.; Taniguchi, T.; Kishikawa, K. Size Control of Polydopamine Nodules Formed on Polystyrene Particles during Dopamine Polymerization with Carboxylic Acid-Containing Compounds for the Fabrication of Raspberry-like Particles. *Colloids Surfaces A Physicochem. Eng. Asp.* **2014**, *449* (1), 114–120. <https://doi.org/10.1016/j.colsurfa.2014.02.049>.
- (29) Cong, Y.; Xia, T.; Zou, M.; Li, Z.; Peng, B.; Guo, D.; Deng, Z. Mussel-Inspired Polydopamine Coating as a Versatile Platform for Synthesizing Polystyrene/Ag Nanocomposite Particles with Enhanced Antibacterial Activities. *J. Mater. Chem. B* **2014**, *2* (22), 3450–3461. <https://doi.org/10.1039/c4tb00460d>.
- (30) Yang, Z.; Huang, R.; Zheng, B.; Guo, W.; Li, C.; He, W.; Wei, Y.; Du, Y.; Wang, H.; Wu, D.; Wang, H. Highly Stretchable, Adhesive, Biocompatible, and Antibacterial Hydrogel Dressings for Wound Healing. *Adv. Sci.* **2021**, *8* (8), 1–12. <https://doi.org/10.1002/advs.202003627>.
- (31) Li, M.; Zhang, Z.; Liang, Y.; He, J.; Guo, B. Multifunctional Tissue-Adhesive Cryogel Wound Dressing for Rapid Nonpressing Surface Hemorrhage and Wound Repair. *ACS Appl. Mater. Interfaces* **2020**, *12* (32), 35856–35872. <https://doi.org/10.1021/acsami.0c08285>.
- (32) Zhou, L.; Zheng, H.; Liu, Z.; Wang, S.; Liu, Z.; Chen, F.; Zhang, H.; Kong, J.; Zhou, F.; Zhang, Q. Conductive Antibacterial Hemostatic Multifunctional Scaffolds Based on

Ti₃C₂TxMXene Nanosheets for Promoting Multidrug-Resistant Bacteria-Infected Wound Healing. *ACS Nano* **2021**, *15* (2), 2468–2480.

<https://doi.org/10.1021/acsnano.0c06287>.

- (33) Cai, S.; Cheng, Y.; Qiu, C.; Liu, G.; Chu, C. The Versatile Applications of Polydopamine in Regenerative Medicine: Progress and Challenges. *Smart Mater. Med.* **2023**, *4* (November 2022), 294–312. <https://doi.org/10.1016/j.smaim.2022.11.005>.
- (34) Qian, Y.; Zhou, X.; Zhang, F.; Diekwisch, T. G. H.; Luan, X.; Yang, J. Triple PLGA/PCL Scaffold Modification Including Silver Impregnation, Collagen Coating, and Electrospinning Significantly Improve Biocompatibility, Antimicrobial, and Osteogenic Properties for Orofacial Tissue Regeneration. *ACS Appl. Mater. Interfaces* **2019**, *11* (41), 37381–37396. <https://doi.org/10.1021/acsami.9b07053>.

Chapter 2 Polydopamine Adhesion: Catechol, Amine, Dihydroxyindole, and Aggregation Dynamics

Contents in this chapter has been submitted to publish in ACS Appl. Mater. Inter. (manuscript ID: adfm.202201256)

Abstract

Polydopamine (PDA) mimics the adhesion of mussel-binding proteins but with a shorter and more rigid backbone, limiting its effectiveness as an adhesive due to reduced conformational contact with surfaces. Our research investigated the adhesion properties of PDA's components: poly(catechol), poly(catecholamine), and PDA itself. Contrary to the expectation that catecholamine oligomers would specifically bind to substrates, we found that PDA's widespread adhesion is due to the oligomers' limited solubility in water and the versatile binding of catechol. Without amines, poly(catechol) failed to adhere, staying in solution or forming negligible suspensions, emphasizing amines' critical role in creating insoluble aggregates that stick to surfaces. We demonstrated this by inducing poly(catechol) to form aggregates with quaternized poly(4-vinylpyridine) (qPVP), which then adhered to surfaces. However, using qPVP with high molecular weight resulted in larger aggregates that remained suspended, not coating the surface, thus illustrating the importance of aggregate size for adhesion.

2.1 Introduction

Mussels exhibit an exceptional adhesion capability even in the challenging environment, seawater. Despite the inhibitory effects of salt water on intermolecular interactions, mussels demonstrate remarkably rapid adhesion with excellent strength and durability to rocks and hull of ships. Extensive research on these organisms has unveiled the critical role played by specific constituents within mussel adhesive plaques, particularly the abundant presence of DOPA (3,4-dihydroxyphenylalanine), lysine, and cysteine units, which feature prominently as catechol and amine moieties.¹⁻³ Although the adhesion mechanism of mussel has not been fully understood, catechol plays a pivotal role by forming various chemical (Metal chelation⁴ and covalent bonding by Michael-type addition and Schiff-base formation) and physical (Hydrogen bonding, π - π interaction, and Van der Waals (VdW) interaction)⁵ interactions with substrates. However, the role of amine in lysine had remained poorly understood until Butler's group unveiled that the amine played a pivotal role in enhancing wet adhesion through surface salt displacement.⁶

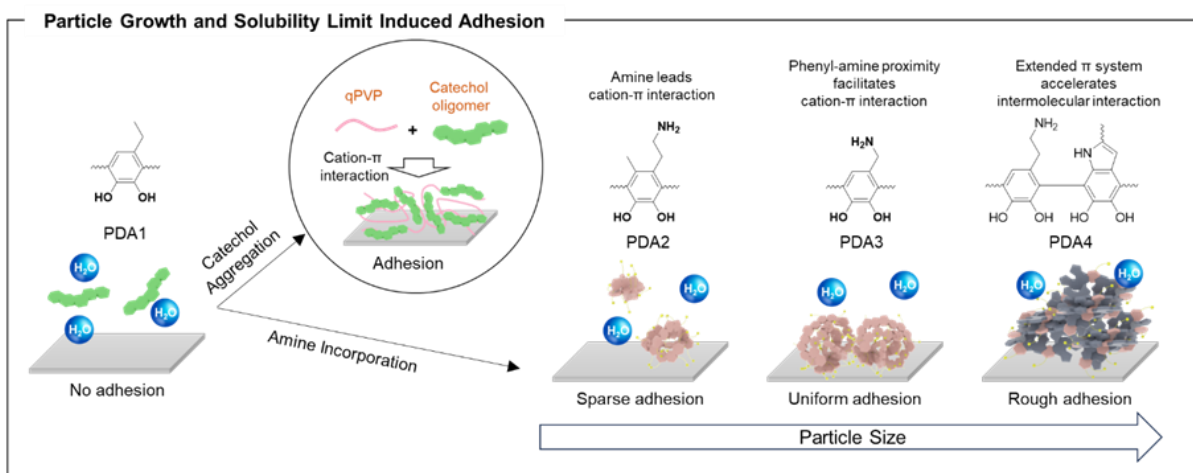
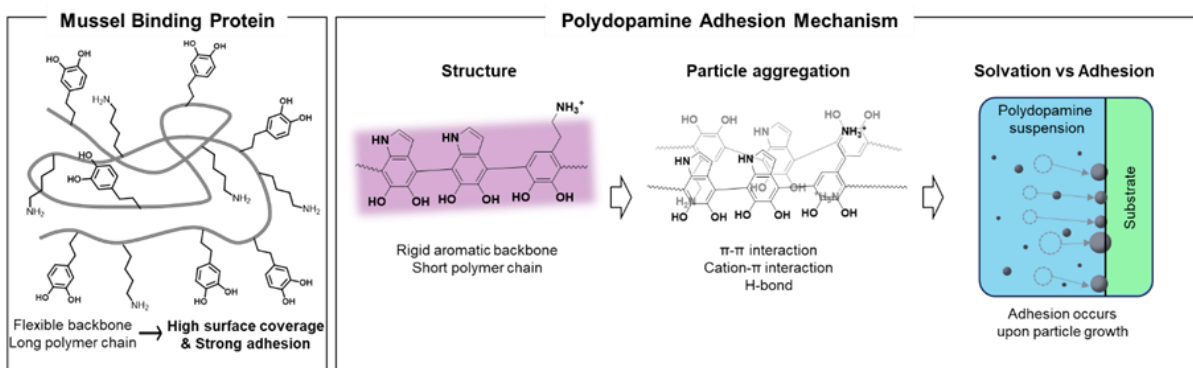
In this context, the pioneering work of Messersmith's group in 2007 led to the development of self-polymerizable polydopamine (PDA), incorporating catecholamine moieties.⁷ PDA's structural similarity to mussel-binding proteins facilitates surface-independent adhesion through simple application methods. This universal applicability sets PDA apart from conventional coating techniques, such as self-assembled monolayers (SAMs),⁸⁻⁹ silane, Langmuir Blodgett, and layer-by-layer polyelectrolyte depositions, which rely heavily on specific surface conditions. However, there are distinct differences between PDA and mussel-binding proteins. Unlike mussel-binding proteins, which possess a long flexible polypeptide backbone, PDA features a rigid aromatic backbone that impedes seamless adhesion to rough surfaces. Furthermore, prior research has consistently reported the oligomeric nature of PDA with the majority being trimers and

tetramers,¹⁰⁻¹³ with the exception of a study conducted by the Messersmith group.¹⁴ The heightened hydrophobicity in the growing PDA chains and consequently developed limited solubility in aqueous solution seem to hinder aryl-aryl coupling reactions, likely ceasing the chain growth at a low molecular weight. Those characteristics of PDA, distinct from mussel-binding proteins, might necessitate supplementary features to compensate its short and rigid backbone structure for a good adhesion. Some prior studies have examined the relationship between aggregation and binding of PDA in the presence of amine-containing compounds, such as PEI¹⁵ or hexamethylenediamine.¹⁶ However, there has been no systematic investigation into the connection between aggregate formation and adhesion in PDA.

The other unique feature of PDA is electron-rich 5,6-dihydroxyindole (DHI) units formed through the annulation of dopamine.¹⁷ Regarding the role of DHI, Zhang et al. investigated adhesion strength of PDA derivatives and found that extended aromaticity of DHI plays a crucial role for cohesion strength by cation- π interaction.¹⁸ Additional intermolecular interactions, such as π - π interactions and cation- π interactions, resulting from DHI, contribute to the enhanced robust coating.¹⁹ While DHI provides cohesive interaction to PDA, surface-independent adhesion stems from its catecholamine moiety as recently Hemmatpour et al. revealed that the early stage of polydopamine deposition is a poly(catecholamine), followed by DHI formation by cyclization, implying the initial binding occurs by catecholamine units.²⁰ Nonetheless, the specific functions of catechol and amine in the PDA adhesion process remained not fully comprehended.

In this study, we proposed that adhesion of PDA is initiated when the solubility limit of PDA agglomerate is reached, and this process is facilitated by the primary amine and DHI components. (Scheme 2-1) We employed a rational design approach to investigate the individual contributions of amine and catechol in the formation of PDA agglomerates. In addition to the

dopamine monomer, we prepared catechol and catecholamine monomers to isolate the role of each unit during particle formation and coating processes. Under oxidative conditions, these compounds undergo self-polymerization, and we subsequently prepared and characterized the corresponding polymer layers. Scanning electron microscopy (SEM), dynamic light scattering (DLS), and atomic force microscopy (AFM) studies revealed the significance of the solubility limit of growing oligomers in relation to their surface coating. Throughout the polymerization process, amine plays a pivotal role by facilitating aggregation, causing the hydrophobic PDA agglomerates to reach their solubility limit in polar solvents. The developed insoluble nature of the agglomerates enhance their affinity for the substrate during the self-coating process. To validate our hypothesis, we prepared poly(catechol)-PVP agglomerates that exhibited particle formation and adhesion while poly(catechol) only did not form any surface coating.



Scheme 2-1 Schematic illustration of the solubility limit triggered adhesion mechanism of PDA. While mussel-binding proteins with their long and flexible polymer sequences as well as catechol side groups, exhibit robust adhesion, the short and rigid structure of PDA is not ideal for conformal coating on substrates. In order to offset this drawback, PDA facilitates intermolecular interactions through π - π interactions, cation- π interactions, and hydrogen bonding. As growing oligomers agglomerate and approach the solubility limit in aqueous solutions, they promote adhesion that is thermodynamically stable. We have elucidated the relationship between particle size and adhesion in the PDA series through a rational design approach. Finally, the formation of qPVP/PDA1 agglomerates has confirmed that catechol is primarily responsible for adhesion, while the aggregation of qPVP/PDA1 in aqueous solutions leads to reaching the solubility limit.

2.3 Result and Discussion

2.3.1 Molecular Design Principle

Initially, we investigated the role of primary amine in PDA by using poly(4-ethylcatechol) (PDA1), which does not have amine functionality. Interestingly, catechol has been understood as an adhesion part of mussel-binding protein, and catechol-containing polymers have exhibited surface-independent adhesion without amine.²¹⁻²⁶ In the majority of these systems, catechol is incorporated as a side group on a flexible polymer backbone. Furthermore, the role of amines in mussel-binding proteins was originally investigated not primarily for adhesion but within the context of underwater adhesion and the reinforcement of PDA cohesion through cation- π interactions.²⁷⁻²⁸ Nevertheless, within PDA, amines hold a significance beyond mere salt cleaning. This study systematically compared poly(catechol), poly(catecholamine), and PDA, shedding light on the role of amines in PDA during both aggregation and adhesion processes.

One significant distinction between PDA and mussel-binding proteins lies in the absence of DHI in the latter. Even though DHI exclusively exists in PDA, it provides unique features to PDA through its extended aromaticity. Consequently, it becomes essential to investigate the surface-independent adhesive characteristics of DHI-free poly(catecholamine). The chemical structures of the catechol-containing monomers used in this study are shown in Scheme 2-1. We pursued two distinct design strategies to obtain poly(catecholamine). PDA2 incorporates a methyl group at position 5 to prevent the ring closure to make DHI while preserving the catechol-ethylamine structure. On the other hand, PDA3 features a 4-aminomethylcatechol unit where the amine cannot reach the benzene ring for annulation due to the one-carbon short linker length. Therefore, in the absence of DHI, PDA2 and PDA3 allowed us to isolate and study the binding

properties of catecholamine exclusively. To better understand the role of DHI, we added conventional polydopamine (PDA4).

Scheme 2-1 provides a schematic illustration of our understandings. Poly(catechol) (PDA1) exhibits a lack of strong intermolecular interactions, leading to particle dispersion in polar solvents due to solvation effects. Poly(catecholamine) (PDA2 and PDA3) possesses larger polarity than PDA1 due to the presence of amine groups. However, under mild basic conditions (pH 8.5), the positively charged ammonium ($-\text{NH}_3^+$) groups of PDA2 and PDA3 engage in cation- π interactions, resulting in particle aggregation. Furthermore, the cyclization of catecholamine of PDA4 leads to the formation of DHI, which possesses an increased number of π electrons. This facilitates both π - π interactions and cation- π interactions, leading to the formation of larger aggregates which is thermodynamically unstable in polar solvents and thereby causing adhesion to substrates.

2.3.2 Structure Analysis by FTIR, and XPS, and ssNMR

The polymerization of the DA series was conducted in a Tris-HCl aqueous solution with a pH of 8.5, rendering the generation of polymers with different oxidation states. We purchased DA1, DA3, and DA4 monomers and synthesized DA2. Self-polymerization of polydopamine, poly(catechol), and poly(catecholamine) were reported²⁹ and we confirmed the structures via spectroscopic methods. To investigate the chemical structures of the PDA series, we examined the coated film on glass substrates. However, because the lack of amine functionality of PDA1 did not make film formation, we analyzed a drop-casted film on a glass substrate instead. First, we investigated the oxidation state of the PDA series since it determines binding modes, such as catechol forms hydrogen bonding while quinone facilitates coordination bonding with metals. The FTIR spectra of PDA1, PDA2, PDA3, and PDA4 (Figure 2-1A) exhibited a broad band at

3600–3200 cm^{-1} that is assigned to $\nu(\text{N-H})$ or $\nu(\text{O-H})$ stretching modes. The peak at 1650 cm^{-1} corresponding to $\nu(\text{C=O})$ groups was observed in PDA1, while PDA2, PDA3, and PDA4 exhibited weak stretching modes in this region indicating variations in oxidation states within the PDA series likely due to the difference in the form of amine group. The high-resolution XPS spectra of O 1s (Figure 2-1B) and C 1s (Figure 2-1C) were consistent with the FTIR results that exhibit the coexistence of catechol and quinone that allow multiple bonding to the substrates. FTIR and XPS spectra of PDA1 exhibited a notably different ratio between catechol and quinone compared to the others because DA1 monomer is neutral while the other monomers are acid salt form, which would decrease the pH of the buffer solution, leading to a relatively weaker oxidation condition and consequently larger portion of catechol than quinone. This implies that we can manipulate the catechol/quinone ratio by pH control. We also examined nitrogen functionalities through the FTIR (Figure 2-1A) that exhibits an aromatic C-C/C=C band (1608 cm^{-1}) associated with DHI and catechol, whereas the amine band is detected as well at 1510 cm^{-1} . The presence of DHI in PDA4 is confirmed by the increase in the peak intensity at 1608 cm^{-1} , characterized by the augmented aromaticity. Meanwhile, PDA2 and PDA3 showed relatively reduced peak intensity at the aromatic region due to the lack of DHI. Furthermore, the N 1s region of the high-resolution XPS spectra confirmed the absence of DHI in PDA2 and PDA3. (Figure 2-1D)

We further investigated the polymer structure via ^{13}C CP-MAS NMR. Based on the structural features observed within each PDA series, as depicted in Figure S2-1a, it is reasonable to infer that the ^{13}C peaks within the chemical shift range of 100-150 ppm primarily correspond to carbon atoms of aromatic rings (Figure S2-1b) and 0- 50 ppm correspond to the aliphatic carbon atoms. The chemical shift distribution exhibits broadening because of variations in polymer chain length. A contact time of 2 ms facilitates magnetization transfer from abundant protons to natural-

abundance ^{13}C enabling not only the transfer of magnetization from directly bonded C-H protons but also for C-O-H groups. The line-broadening observed for ~ 160 to ~ 180 ppm could be attributed to a combination of heterogeneous structure and slow motion of the corresponding chemical groups. The up-field shifts in chemical shift values can be attributed to extended π - π stacking interactions present in both PDA1 and PDA4 (parallel, anti-parallel, slipped parallel, and slipped anti-parallel, etc.), which could also contribute to the heterogeneous line-broadenings.³⁰ In summary, the ^{13}C CP-MAS NMR spectra of the synthesized PDA powder samples suggest the presence of structurally intricate oligomers.

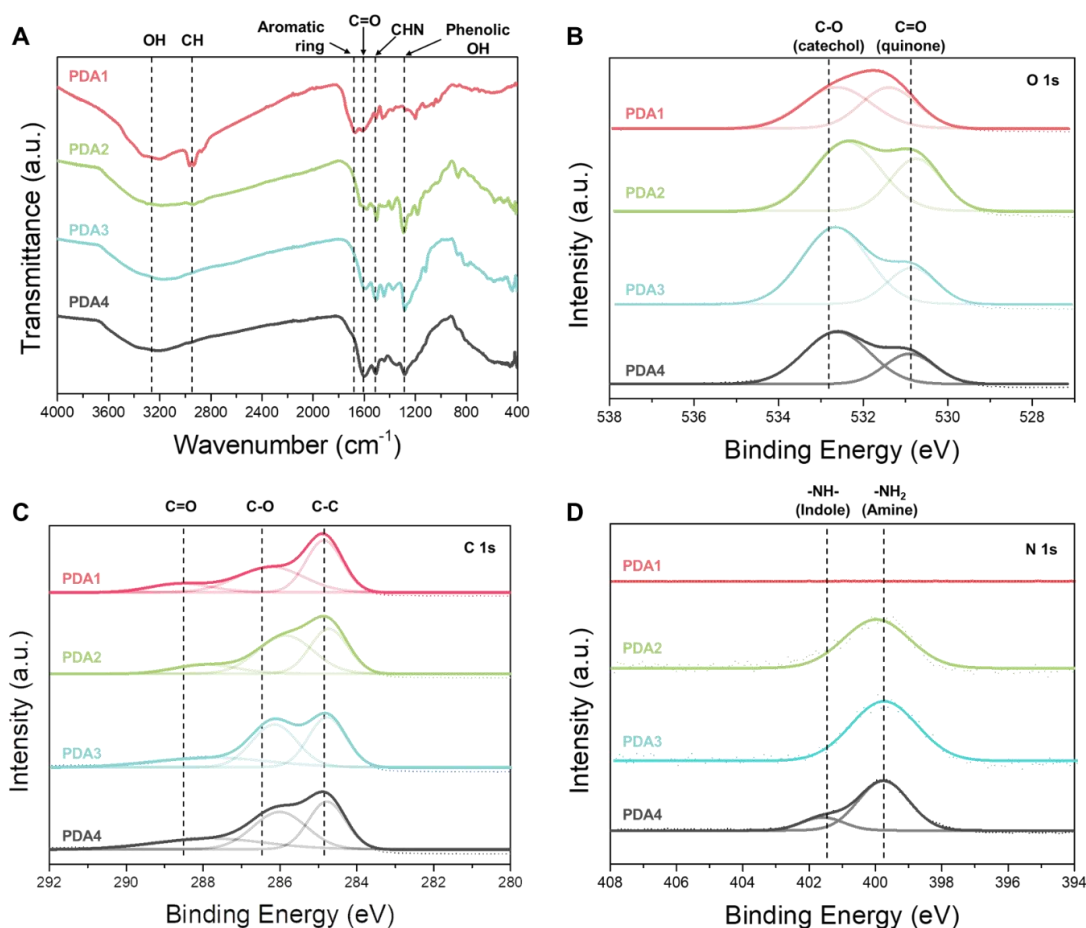


Figure 2- 1 Structural analysis of the PDA series by FTIR and XPS. (A) FTIR spectra of PDA1, PDA2, PDA3, and PDA4. (B) High-resolution XPS spectra of O 1s region for PDA1, PDA2, PDA3, and PDA4. (C) High-resolution XPS spectra of C 1s region for PDA1, PDA2, PDA3, and PDA4 (D) High-resolution XPS spectra of N 1s region for PDA1, PDA2, PDA3, and PDA4.

2.3.3 Adhesion Mechanism Study

Despite the surface independent coating behavior of PDA is indisputable, roles of catechol, amine, and DHI in PDA are not clear during the adhesion process. To understand the coating mechanism, the PDA series were deposited on polyamide (nylon), polyethylene terephthalate (PET), and glass, representing hydrophilic, hydrophobic, and ceramic substrates, respectively. As depicted in Figure 2-2A, the entire PDA series successfully coated the nylon substrate, regardless of the presence of amine functionality. This suggests that catechol alone is capable of forming effective interactions with high surface energy substrates. However, it's important to note that only amine-containing polymers were able to form coatings on glass and PET substrates. The high-resolution XPS spectra of O 1s confirmed the absence of PDA1 on glass substrate as shown in Figure S2-2. On the contrary, the other PDA analogs having amine functionality showed an efficient coating on all substrates and were confirmed by the high-resolution XPS of N 1s (Figure 2-1C). As we discussed, some catechol-containing polymeric adhesives have an unconditional coating property like PDA due to the various binding modes (H-bonding, π - π interaction, metal chelation and etc.) even without amine functionality.^{22,24} However, we observed that the presence of amines is pivotal for achieving universal adhesion in the PDA analogues, as they compensate for the limited cohesion strength of PDA caused by its short polymer chain. These results support the notion that surface-independent adhesion is initiated by catecholamine units, while particle aggregation through π - π interactions and cation- π interactions plays an important role.²⁰ We conducted additional water contact angle measurements on dip-coated PDA series on glass substrates, as illustrated in Figure S2-3. The lack of a PDA1 layer on the glass led to similar angles as the pristine glass, measuring 55° and 54°, respectively. For PDA2, PDA3, and PDA4, the angles were 22°, 7°, and 23°, indicating hydrophilic properties of the PDA series. Interestingly, PDA3

exhibited the lowest water contact angle, attributed to the absence of DHI units and a uniform coating, as explained below.

Following the verification of the coating layers using spectroscopic methods and water contact angle measurement, we proceeded with a surface morphology analysis using DLS and SEM, as illustrated in Figure 2-2B and Figure 2-2C. As the XPS results confirmed, PDA1 did not adhere to the glass and PET substrates, whereas PDA4 coated all substrates successfully. Interestingly, the two poly(catecholamine) variants, PDA2 and PDA3, demonstrated different coating capabilities on glass substrates. PDA2 exhibited sparse attachment, while PDA3 formed a uniform coating, indicating poly(catecholamine)s do not assure a universally effective coating. We investigated the particle size and adhesion relationship by employing DLS analysis to gain some insights. As shown in the DLS and SEM data consistently, the particle size exhibited a gradual increase from the amine-free poly(catechol) (PDA1) to DHI-free poly(catecholamine)s (PDA2 and PDA3), and finally to polydopamine (PDA4). The presence of larger particles in PDA4 (1590 nm) can be attributed to the efficient intra- and intermolecular interactions of DHI units. Additionally, the existence of medium-sized particles in PDA3 (410 nm), which has catecholamine unit, contributes to its universal adhesion. It is worth noting that the absence of DHI in PDA3 resulted in a smooth coating. Conversely, the formation of small particles in PDA2 (230 nm) and PDA1 (137 nm) results in only sparse coating or no adhesion. The extended conjugation of DHI results in substantial aggregation, whereas the cation- π interaction between NH_3^+ and catechol of the DHI-free catecholamines was comparatively weaker than that of DHI. Although large agglomerates were loosely adhered to the surface, they could be detached through ultrasonication.²⁹

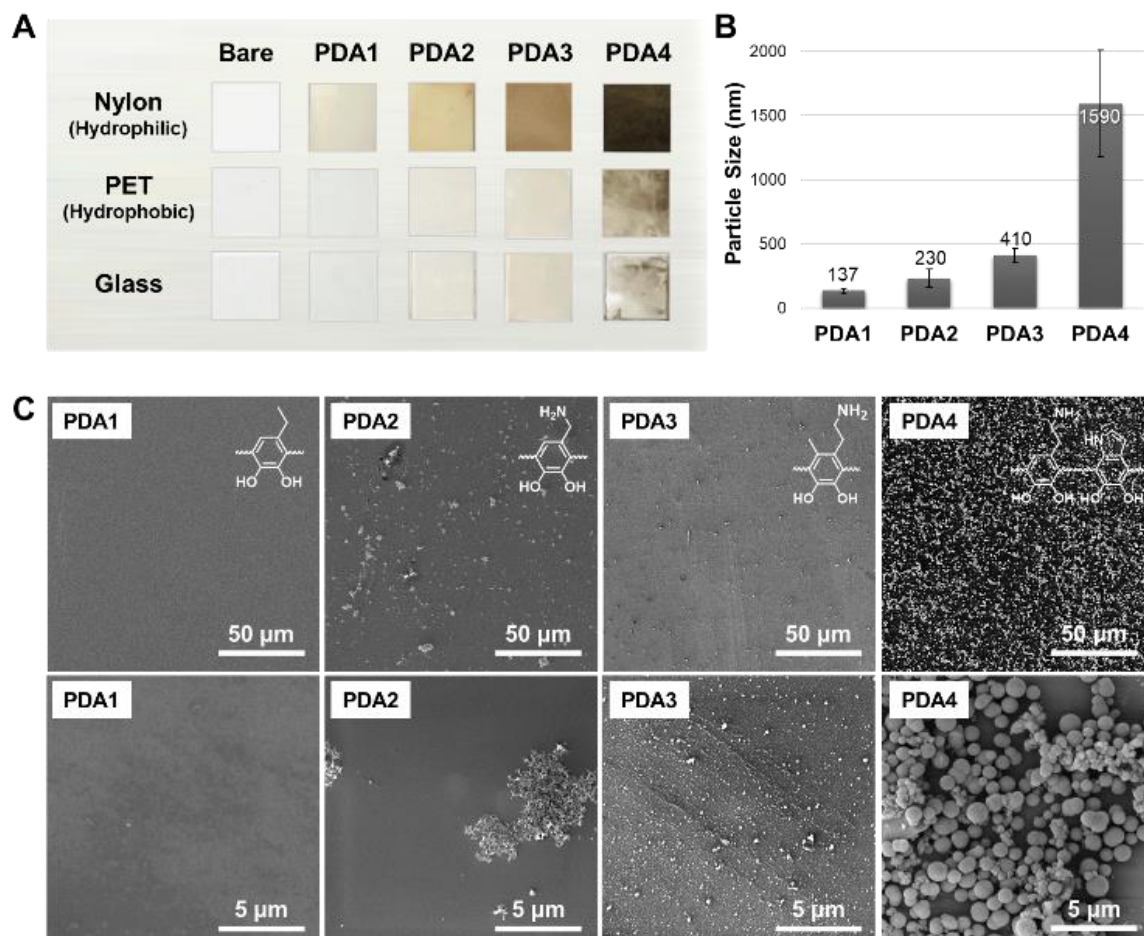


Figure 2- 2 Coating behavior and morphology. (A) Evaluation of coating behaviors of the PDA series on different substrates. (B) Particle size analysis by using DLS. (C) SEM images showing the PDA series coating on glass substrates.

In addition to the SEM analysis, we conducted a more in-depth examination of the surface morphologies beneath these coated agglomerates using atomic force microscopy. Following the removal of agglomerates via ultrasonication for 10 min in DI water, we assessed the surface morphologies using the tapping mode of AFM as shown in Figure 2-3. First, the absence of a poly(catechol) (PDA1) coating was verified by the low average roughness (R_a) of 0.1 nm. Adhesion began to manifest gradually with PDA2, which displayed a sparse coating due to the weak intra- and intermolecular interaction. In contrast, PDA3 and PDA4, possessing strong intra- and intermolecular interactions, appeared to adhere thoroughly. We subsequently hypothesized

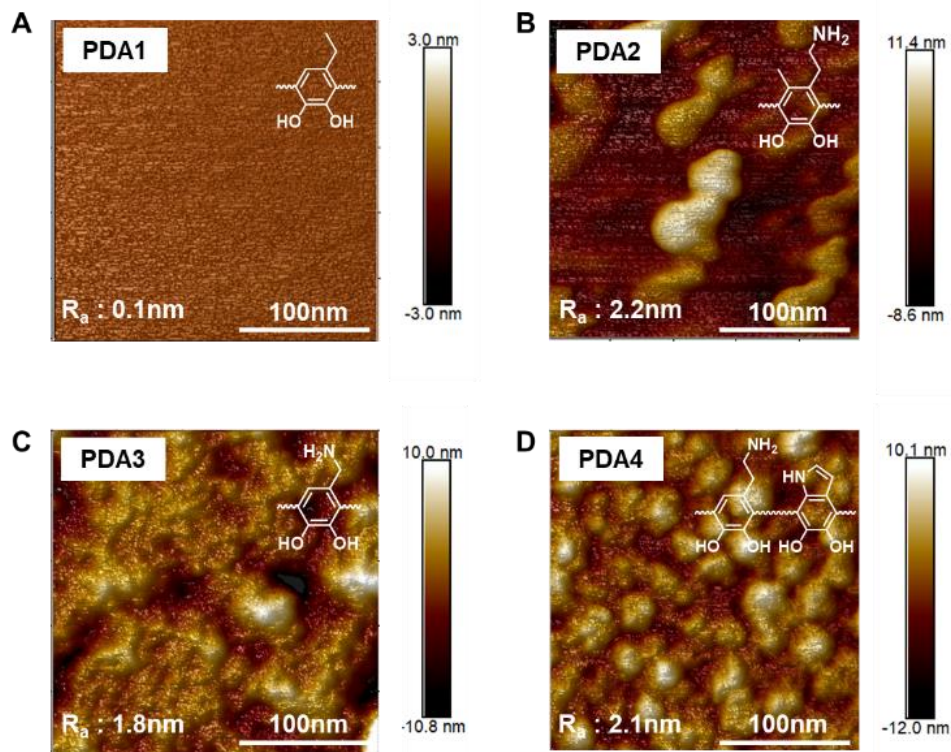


Figure 2- 3 3D AFM images of the surface morphology of PDA series: (A) PDA1, (B) PDA2, (C) PDA3, and (D) PDA4 after applying 10 minutes of ultrasonication in DI water. Scan size $250 \times 250 \text{ nm}^2$. The average roughness (R_a) for the full image is shown in each figure.

that approaching the solubility limit of growing PDA agglomerates in polar protic solvents facilitates adhesion. In contrast, when the intra-intermolecular interaction of catechol oligomers is not strong enough to reach their solubility limit in mild basic conditions the oligomers either remain in solution or exist as a minor suspension.

To validate the concept of aggregation-induced solubility limit-based adhesion mechanism, we incorporated quaternized poly(4-vinyl pyridine) (qPVP) in the amine-free poly(catechol) (PDA1) solution at pH 8 to ensure cation- π interactions and coulombic interactions^{27,28} as depicted in Figure 2-4A. Both PDA1 and qPVP are soluble in water, and none of them can establish coating on glass separately. Nevertheless, upon the interaction of PDA1 with qPVP, the resulting agglomerates formed a coating layer via multiple binding modes of catechol as shown in Figure

2-4B. The presence of the coating layer was confirmed through SEM images and high-resolution N 1s XPS spectra from quarternary amine, as illustrated in Figure 2-4C and Figure 2-4D, respectively. While qPVP could potentially form a binding with a negatively charged glass under mild basic conditions, the absence of quarternary amine in XPS suggests that qPVP is solvated in the aqueous solution rather than deposited on the glass. To further explore the impact of particle size, we varied the molecular weights of qPVP. As we raised the molecular weights of qPVP from 1400 Da to 60 kDa, the particle size of the agglomerates also increased up to 3050 nm (Figure 2-4E). Large agglomerates induced by high-molecular-weight polymers formed precipitated particles rather than forming surface coatings due to their bulky and heavy characteristics. (Figure 2-4F) In summary, the aggregation of PDA1 leads to adhesion unless the particles are excessively large and heavy.

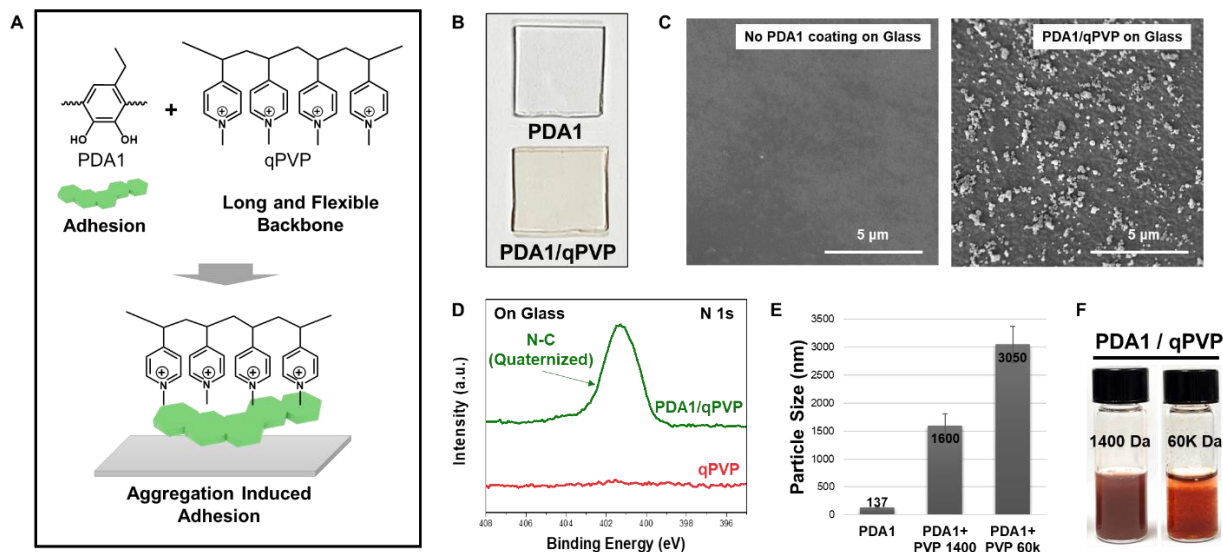


Figure 2-4 Aggregation induced adhesion via PDA1-qPVP mixture. Aggregation process of PDA1/ qPVP. Solubilized PDA1 and qPVP engaged in cation- π interactions and coulombic interactions, subsequently leading to aggregation-induced adhesion. B Coating test of PDA1 and PDA1/qPVP agglomerate on glass substrates. C SEM images reveal the absence of a coating when PDA1 is applied to a glass substrate, while the combination of PDA1/qPVP (Mw1400) demonstrates adhesion on the glass substrate. D High-resolution N 1s XPS spectra of PDA1/qPVP agglomerates and qPVP (Mw1400) on the glass substrate. E DLS analysis of PDA1/qPVP agglomerates with various molecular weight range. F PDA1/qPVP agglomerates suspension in water. Large molecular weight of qPVP (60K Da) lead large particle formation (3050 nm), followed by precipitation without coating.

2.4 Conclusion

We explored the binding mechanism of polydopamine (PDA) by a rationally designed PDA derivative. These analogs are designed to investigate the role of catechol, amine functionality, and DHI in the unique material-independent surface coating feature of PDA. Our investigation encompassing various substrate materials unveiled an important distinction: amine-containing polymers exhibited an exceptional capacity for surface-independent adhesion, whereas amine-free poly(catechol) exclusively yielded coating layers on only hydrophilic substrates, exemplified by nylon. Furthermore, our SEM, DLS, and AFM analyses elucidated the role of aggregation formation in initiating surface adhesion. While the monomeric catechol derivatives used in this study are all soluble in aqueous solution, as the molecular weight increases by self-polymerization, the growing oligomers reach an insoluble length limit, haltering further growth. The size of the insoluble oligomers without having amine group is small enough to stably stay in solution while protonated amine groups (NH_3^+) of poly(catecholamine)s form cation- π interactions with catechol or DHI, making the resulting aggregates to coat on a substrate. Notably, the particle size emerged as a critical factor influencing this process, as exemplified by the contrasting behavior of PDA2 and PDA3; while smaller aggregates of PDA2 (240nm) gave only sparse coating, larger aggregates (410nm) of PDA3 made a uniform surface coating. To substantiate the observed solubility limit effect on surface coating, we induced the aggregation of amine-free poly(catechol), PDA1, by means of adding quaternized poly(4-vinylpyridine) (qPVP). This strategic blending of cationic qPVP and poly(catechol) in solution fostered cation- π and coulombic interactions among them, ultimately resulting in the formation of agglomerates that constituted a coating layer, supporting our proposed aggregation-induced solubility limit-based adhesion mechanism of PDA.

2.5 Publication Information

Jiwon Lim, Shuo Zhang, Jung-Moo Heo, Kalitha C. Dickwella Widanage, Ayyalusamy Ramamoorthy and Jinsang Kim*, "Polydopamine Adhesion: Catechol, Amine, Dihydroxyindole, and Aggregation Dynamics" revision submitted.

2.6 Experimental Section

2.6.1 Materials

All the chemicals and solvents for the synthesis were purchased from commercial suppliers (TCI, Acros, Sigma-Aldrich, and Fisher Sci. and 4-Ethylcatechol (DA1), 3,4-Dihydroxybenzylamine hydrobromide (DA3), and Dopamine hydrochloride (DA4), were purchased from Sigma-Aldrich. 2-(4,5-dihydroxy-2-methylphenyl)ethan-1-aminium bromide (DA2) was synthesized as shown in Scheme S2-2.

2.6.2 Preparation of the PDA Series Coatings on Various Substrates

First, a monomer solution (2 mg/mL) dissolved in tris buffer (pH 8.5) was prepared (DA/Tris solution). Then various substrates (1x1 cm²) were placed in a petri dish containing 5 mL of the monomer/Tris solution. After 24h, the coated substrates were rinsed with DI water and methanol and then dried by blowing air.

2.6.3 Characterization

Scanning electron microscope (SEM) was carried out by using Tescan Mira3 FEGSEM. Atomic force microscope (AFM) was carried out by using Veeco Dimension Icon Atomic Force

Microscope. AFM images were acquired in amplitude modulated AC mode (aka tapping mode) in air, under ambient conditions, with silicon tip SCANASYST-AIR (Bruker). X-Ray photoelectron spectroscopy (XPS) spectra were obtained by Kratos Axis Ultra XPS using Monochromatic Al source. The base pressure in the analysis chamber was typically 1×10^{-9} mbar. All spectra were collected with the charge neutralization. The collected data were processed using the CasaXPS software package. Spectral charge correction was performed using the main C 1s peak due to hydrocarbon (C-C/C-H bonds) set to 284.5 eV. FTIR was conducted by using NicoletTM iS20 FT-IR spectrometer. The Adv ATR mode of OMNIC software was used for the baseline collection. XPS and FT-IR spectra were collected from dip-coated surfaces for all samples except PDA1. Due to the poor coating capability of PDA1, the spectra for PDA1 were obtained from a drop-casted film. DLS were conducted by using Malvern zetasizer nano ZSP.

2.6.4 Quaternized Poly(4-vinylpyridine) Preparation

200 mg of Poly(4-vinylpyridine)(1.9 mmol) was dissolved into 20ml of methanol, and the solution was refluxed in the presence of 0.23 mL (3.8 mmol) of iodomethane for 24 h. The obtained polymer were precipitated from the reaction mixtures using diethyl ether, filtered, and washed with methanol and diethyl ether to yield a yellowish polymer product. The obtained polymer product was dried in the oven (60°C) for overnight.

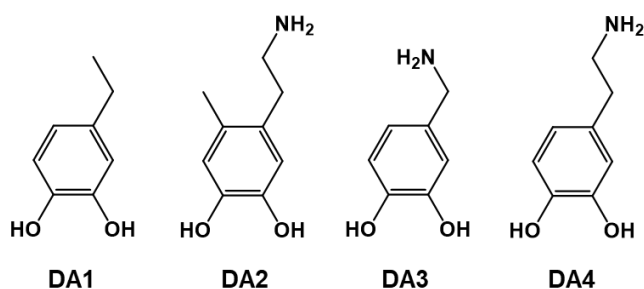
2.6.5 PDA1-Quaternized Poly(4-vinylpyridine) Film Preparation

First, DA1 monomer (2 mg/mL) dissolved in tris buffer (pH 8.5) was prepared (DA/Tris solution). Glass substrate was placed in a vial containing 2 mL of the DA1/Tris solution for 1 day.

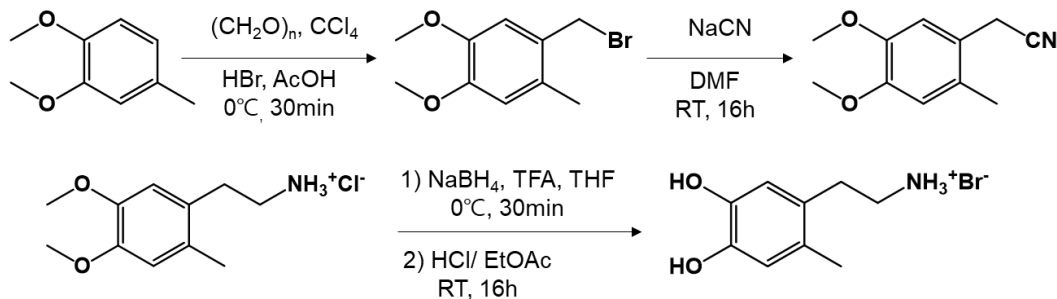
Then qPVP (2 mg/ml) was dissolved in water, and 0.5 ml of qPVP solution was added to the DA/Tris solution. After 24h, the coated substrate was rinsed with DI water and methanol and then dried by blowing air.

2.7 Supplementary Information

2.7.1 Material Synthesis



Scheme S2- 1 Monomer structures of PDA series.



Scheme S2- 2 Synthetic route of a monomer for DA2

2-(4,5-dihydroxy-2-methylphenyl)ethan-1-aminium bromide (DA2) was synthesized by previously described synthetic routes.³¹

2.7.2 ^{13}C Solid State NMR

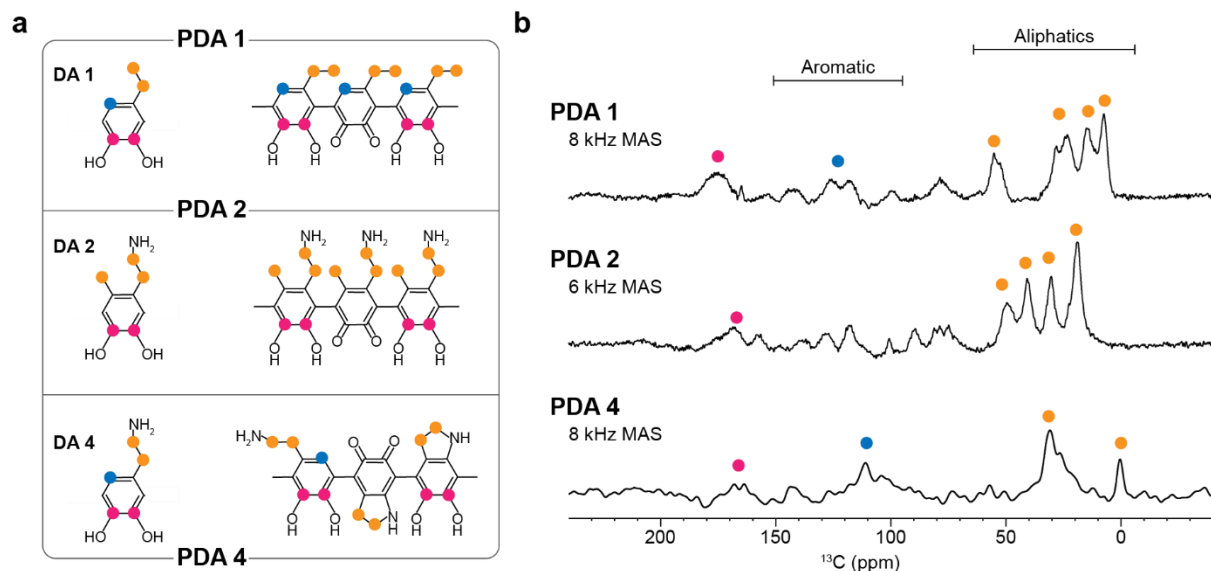


Figure S2- 1 Solid-state NMR analysis of the PDA series. a, Chemical structures of monomers and polymers in PDA series. b, Proton-decoupled ^{13}C Ramp-CP spectra of powered PDA complexes under 6-8 kHz MAS. c, Possible structural oligomers of PDA series. Carbon atoms that are discernible through the utilization of the cross-polarization (CP) MAS experiments are color-coded as follows: yellow for aliphatic, cyan for aromatic, and magenta for those linked to -OH groups.

Solid-state NMR experiments were carried out on a 600 MHz (14.1 T) Bruker Avance NMR spectrometer operating at 600.12 MHz and 150.91 MHz resonance frequencies for ^1H and ^{13}C nuclei, respectively. A 3.2 mm HCN triple-resonance MAS probe was used to acquire ^{13}C CP-MAS NMR spectra under 8-9 kHz MAS at room temperature. The ramp-cross-polarization³² was used with the experimental parameters: a 83.3 kHz ^1H 90° pulse followed by a simultaneous ^1H spin-lock field of 62.5 kHz and ^{13}C RF field ramped from 53 to 76 kHz for 2 ms, with 10,000-21,000 scans and a recycle delay of 3.5 s. Protons were decoupled using 83.3 kHz RF SPINAL64 pulse sequence. The ^{13}C chemical shifts were externally referenced to adamantane's CH_2 peak at 38.48 ppm with 0 ppm for ^{13}C peak of tetramethylsilane (TMS). ^{13}C CP-MAS NMR of PDA3 was assigned in our previous study.¹³

2.7.3 XPS Spectra of PDA1 Coating on Glass Substrates

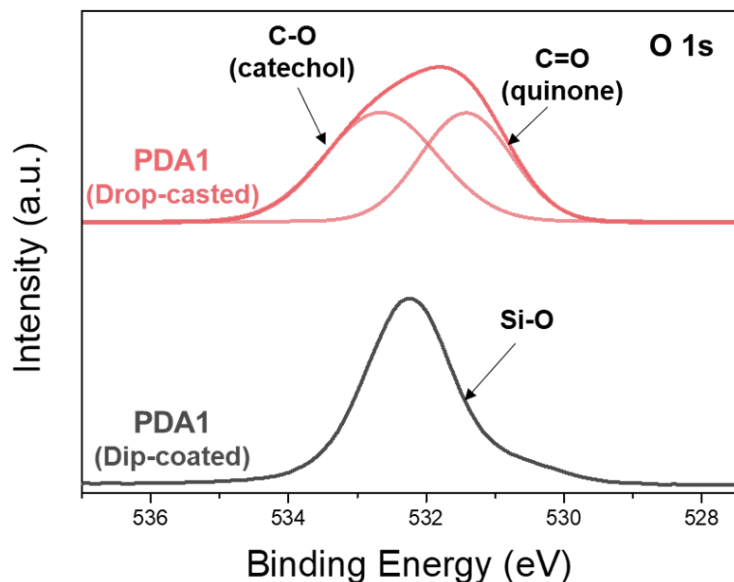


Figure S2- 2 High-resolution XPS spectra of the O 1s region for PDA1 drop-casted (Pink) and dip-coated (Gray) on glass substrates reveal that PDA1 did not bind to the glass substrate.

2.8 Reference

- (1) Burzio, L. A.; Waite, J. H. Cross-Linking in Adhesive Quinoproteins: Studies with Model Decapeptides. *Biochemistry* **2000**, *39* (36), 11147–11153. <https://doi.org/10.1021/bi0002434>.
- (2) Waite, J. H.; Qin, X. Polyphosphoprotein from the Adhesive Pads of *Mytilus Edulis*. *Biochemistry* **2001**, *40* (9), 2887–2893. <https://doi.org/10.1021/bi002718x>.
- (3) Waite, J. H.; Tanzer, M. L. Polyphenolic Substance of *Mytilus Edulis*: Novel Adhesive Containing L-Dopa and Hydroxyproline. *Science* **1981**, *212* (4498), 1038–1040. <https://doi.org/10.1126/science.212.4498.1038>.
- (4) Im, K. M.; Kim, T. W.; Jeon, J. R. Metal-Chelation-Assisted Deposition of Polydopamine on Human Hair: A Ready-to-Use Eumelanin-Based Hair Dyeing

- Methodology. *ACS Biomater. Sci. Eng.* **2017**, *3* (4), 628–636.
<https://doi.org/10.1021/acsbiomaterials.7b00031>.
- (5) Liebscher, J. Chemistry of Polydopamine – Scope, Variation, and Limitation. *European J. Org. Chem.* **2019**, *2019* (31–32), 4976–4994. <https://doi.org/10.1002/ejoc.201900445>.
- (6) Maier, G. P.; Rapp, M. V.; Waite, J. H.; Israelachvili, J. N.; Butler, A. Adaptive Synergy between Catechol and Lysine Promotes Wet Adhesion by Surface Salt Displacement. *Science.* **2015**, *349* (6248), 628–632. <https://doi.org/10.1126/scienceAAB0556>.
- (7) Lee, H.; Dellatore, S. M.; Miller, W. M.; Messersmith, P. B. Mussel-Inspired Surface Chemistry for Multifunctional Coatings. *Science.* **2007**, *318* (5849), 426–430.
<https://doi.org/10.1126/science.1147241>.
- (8) Love, J. C.; Estroff, L. A.; Kriebel, J. K.; Nuzzo, R. G.; Whitesides, G. M. Self-Assembled Monolayers of Thiolates on Metals as a Form of Nanotechnology. *Chem. Rev.* **2005**, *105* (4), 1103–1169. <https://doi.org/10.1021/CR0300789>.
- (9) Ulman, A. Formation and Structure of Self-Assembled Monolayers. *Chem. Rev.* **1996**, *96* (4), 1533–1554. <https://doi.org/10.1021/cr9502357>.
- (10) Della Vecchia, N. F.; Avolio, R.; Alfè, M.; Errico, M. E.; Napolitano, A.; D’Ischia, M. Building-Block Diversity in Polydopamine Underpins a Multifunctional Eumelanin-Type Platform Tunable Through a Quinone Control Point. *Adv. Funct. Mater.* **2013**, *23* (10), 1331–1340. <https://doi.org/10.1002/adfm.201202127>.
- (11) Liebscher, J.; Mrówczyński, R.; Scheidt, H. A.; Filip, C.; Haidade, N. D.; Turcu, R.; Bende, A.; Beck, S. Structure of Polydopamine: A Never-Ending Story? *Langmuir* **2013**, *29* (33), 10539–10548. <https://doi.org/10.1021/la4020288>.

- (12) Alfieri, M. L.; Micillo, R.; Panzella, L.; Crescenzi, O.; Oscurato, S. L.; Maddalena, P.; Napolitano, A.; Ball, V.; D'Ischia, M. Structural Basis of Polydopamine Film Formation: Probing 5,6-Dihydroxyindole-Based Eumelanin Type Units and the Porphyrin Issue. *ACS Appl. Mater. Interfaces* **2018**, *10* (9), 7670–7680.
<https://doi.org/10.1021/acsami.7b09662>.
- (13) Lim, J.; Zhang, S.; Wang, L.; Seo, D.; Dickwella Widanage, M. C.; Pipe, K. P.; Ramamoorthy, A.; Kim, J. Dihydroxy Indole (DHI)-Free Poly(Catecholamine) for Smooth Surface Coating with Amine Functionality. *ACS Appl. Polym. Mater.* **2023**.
- (14) Delparastan, P.; Malollari, K. G.; Lee, H.; Messersmith, P. B. Direct Evidence for the Polymeric Nature of Polydopamine. *Angew. Chemie Int. Ed.* **2019**, *58* (4), 1077–1082.
<https://doi.org/10.1002/anie.201811763>.
- (15) Lv, Y.; Yang, S. J.; Du, Y.; Yang, H. C.; Xu, Z. K. Co-Deposition Kinetics of Polydopamine/Polyethyleneimine Coatings: Effects of Solution Composition and Substrate Surface. *Langmuir* **2018**, *34* (44), 13123–13131.
<https://doi.org/10.1021/acs.langmuir.8B02454>.
- (16) Argenziano, R.; Alfieri, M. L.; Arntz, Y.; Castaldo, R.; Liberti, D.; Maria Monti, D.; Gentile, G.; Panzella, L.; Crescenzi, O.; Ball, V.; Napolitano, A.; d'Ischia, M. Non-Covalent Small Molecule Partnership for Redox-Active Films: Beyond Polydopamine Technology. *J. Colloid Interface Sci.* **2022**, *624*, 400–410.
<https://doi.org/10.1016/j.jcis.2022.05.123>.
- (17) Ding, Y.; Weng, L.-T.; Yang, M.; Yang, Z.; Lu, X.; Huang, N.; Leng, Y. Insights into the Aggregation/Deposition and Structure of a Polydopamine Film. **2014**.
<https://doi.org/10.1021/la5026608>.

- (18) Zhang, C.; Xiang, L.; Zhang, J.; Liu, C.; Wang, Z.; Zeng, H.; Xu, Z. K. Revisiting the Adhesion Mechanism of Mussel-Inspired Chemistry. *Chem. Sci.* **2022**, *13* (6), 1698–1705. <https://doi.org/10.1039/d1sc05512g>.
- (19) Lyu, Q.; Song, H.; Yakovlev, N. L.; Tan, W. S.; Chai, C. L. L. In Situ Insights into the Nanoscale Deposition of 5,6-Dihydroxyindole-Based Coatings and the Implications on the Underwater Adhesion Mechanism of Polydopamine Coatings. *RSC Adv.* **2018**, *8* (49), 27695–27702. <https://doi.org/10.1039/c8ra04472d>.
- (20) Hemmatpour, H.; De Luca, O.; Crestani, D.; Stuart, M. C. A.; Lasorsa, A.; van der Wel, P. C. A.; Loos, K.; Giouisis, T.; Haddadi-Asl, V.; Rudolf, P. New Insights in Polydopamine Formation via Surface Adsorption. *Nat. Commun.* **2023**, *14* (1), 1–12. <https://doi.org/10.1038/s41467-023-36303-8>.
- (21) Saiz-Poseu, J.; Mancebo-Aracil, J.; Nador, F.; Busqué, F.; Ruiz-Molina, D. The Chemistry behind Catechol-Based Adhesion. *Angew. Chemie Int. Ed.* **2019**, *58* (3), 696–714. <https://doi.org/10.1002/anie.201801063>.
- (22) Matos-Pérez, C. R.; White, J. D.; Wilker, J. J. Polymer Composition and Substrate Influences on the Adhesive Bonding of a Biomimetic, Cross-Linking Polymer. *J. Am. Chem. Soc.* **2012**, *134* (22), 9498–9505. <https://doi.org/10.1021/JA303369P>.
- (23) North, M. A.; Del Grosso, C. A.; Wilker, J. J. High Strength Underwater Bonding with Polymer Mimics of Mussel Adhesive Proteins. *ACS Appl. Mater. Interfaces* **2017**, *9* (8), 7866–7872. <https://doi.org/10.1021/acsami.7b00270>.
- (24) Burke, S. A.; Ritter-Jones, M.; Lee, B. P.; Messersmith, P. B. Thermal Gelation and Tissue Adhesion of Biomimetic Hydrogels. *Biomed. Mater.* **2007**, *2* (4), 203. <https://doi.org/10.1088/1748-6041/2/4/001>.

- (25) Lee, H.; Lee, B. P.; Messersmith, P. B. A Reversible Wet/Dry Adhesive Inspired by Mussels and Geckos. *Nature* **2007**, *448* (7151), 338–341.
<https://doi.org/10.1038/nature05968>.
- (26) Gan, D.; Xing, W.; Jiang, L.; Fang, J.; Zhao, C.; Ren, F.; Fang, L.; Wang, K.; Lu, X. Plant-Inspired Adhesive and Tough Hydrogel Based on Ag-Lignin Nanoparticles-Triggered Dynamic Redox Catechol Chemistry. *Nat. Commun.* **2019**, *10* (1), 1–10.
<https://doi.org/10.1038/s41467-019-09351-2>.
- (27) Gebbie, M. A.; Wei, W.; Schrader, A. M.; Cristiani, T. R.; Dobbs, H. A.; Idso, M.; Chmelka, B. F.; Herbert Waite, J.; Israelachvili, J. N. Tuning Underwater Adhesion with Cation- π Interactions. *Nat. Chem.* **2017**, *9* (5), 473–479.
<https://doi.org/10.1038/nchem.2720>.
- (28) Shin, M.; Park, Y.; Jin, S.; Jung, Y. M.; Cha, H. J. Two Faces of Amine-Catechol Pair Synergy in Underwater Cation- π Interactions. *Chem. Mater.* **2021**, *33* (9), 3196–3206.
<https://doi.org/10.1021/acs.chemmater.1c00079>.
- (29) Yang, J.; Saggiomo, V.; Velders, A. H.; Stuart, M. A. C.; Kamperman, M. Reaction Pathways in Catechol/Primary Amine Mixtures: A Window on Crosslinking Chemistry. **2016**. <https://doi.org/10.1371/journal.pone.0166490>.
- (30) Saitô, H.; Ando, I.; Ramamoorthy, A. Chemical Shift Tensor – The Heart of NMR: Insights into Biological Aspects of Proteins. *Prog. Nucl. Magn. Reson. Spectrosc.* **2010**, *57* (2), 181–228. <https://doi.org/https://doi.org/10.1016/j.pnmrs.2010.04.005>.
- (31) Milhazes, N.; Cunha-Oliveira, T.; Martins, P.; Garrido, J.; Oliveira, C.; Rego, A. C.; Borges, F. Synthesis and Cytotoxic Profile of 3,4-Methylenedioxyamphetamine (“ecstasy”) and Its Metabolites on Undifferentiated PC12 Cells: A Putative Structure-

Toxicity Relationship. *Chem. Res. Toxicol.* **2006**, *19* (10), 1294–1304.

<https://doi.org/10.1021/tx060123i>.

- (32) Metz, G.; Wu, X.; Smith, S. O. Ramped-Amplitude Cross Polarization in Magic-Angle-Spinning NMR. *J. Magn. Reson. Ser. A* **1994**, *110* (2), 219–227.

<https://doi.org/10.1006/jmra.1994.1208>.

Chapter 3 Sequential Self-polymerization of Phenolic Compounds with Alkanedithiol Linkers as a Surface-independent and Solvent-resistant Surface Functionalization Strategy

Contents in this chapter has been submitted to publish in *Angewandte Chemie*. (manuscript ID: 202319088)

Abstract

We developed a versatile surface coating technique based on sequential self-polymerization of phenolic compounds with alkanedithiol (ADT) crosslinkers. This method utilizes the synergy of phenol's diverse binding and ADT's flexible aliphatic chain to ensure conformal substrate contact. Michael addition between the components creates crosslinked polymer films, enhancing solvent resistance of the coatings. We applied this technique to various surfaces, including glass, aluminum, polyethylene, and Teflon, using different phenolic monomers like dopamine and tannic acid. The hydrophobic nature of ADT grants the copolymer insolubility in polar solvents, ensuring substrate adhesion during the coating process. X-ray photoelectron spectroscopy (XPS) analysis confirmed the presence of functional groups (amine, carboxylic acid, aldehyde) with at least a 0.35:0.65 ratio of phenol monomer to ADT linker on the substrates, using a monomer to ADT feed ratio of 1:0.5. The copolymer exhibited impressive solvent resistance, including against NaOH (aq.), DMSO, and chloroform, providing a solution to the stability challenges of traditional polydopamine-based coatings.

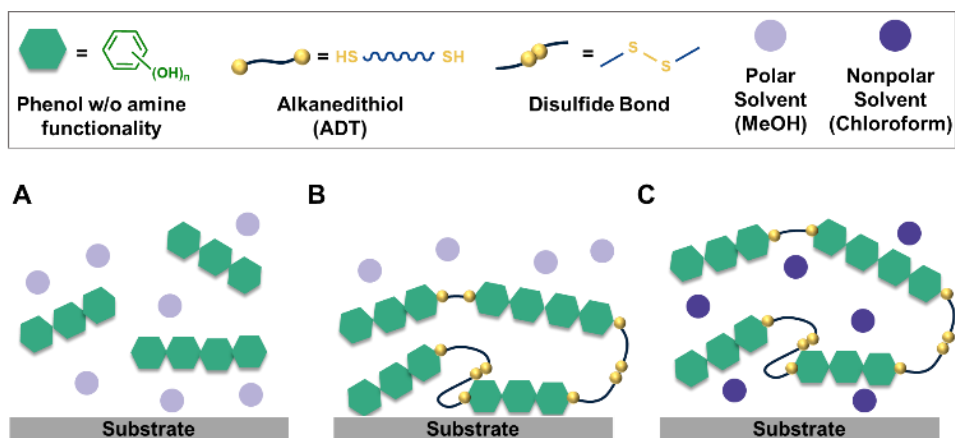
3.1 Introduction

Phenolic compounds are a diverse group of phytochemicals that are ubiquitous in nature and over 8000 polyphenol families have been identified so far. In addition to plant-based phenolic compounds, various living organisms contain catecholamines like dopamine and melanin. Messersmith group utilized polyphenols as a universal coating material by leveraging the self-polymerization of dopamine in 2007.¹ Due to its structural similarity to mussel binding protein (catechol and amine), polydopamine exhibits surface-independent coating behavior allowing wide adoption as a surface functionalization method in energy, environmental, and biomedical.²⁻⁵ The unique binding properties of polydopamine mainly arise from the physical interactions (π - π interaction, H-bonding, and Van der Waals interaction) and chemical bonding (ionic bonding and covalent bonding) of catechol.⁶⁻¹¹ Moreover, Caruso group introduced metal-phenolic networks (MPN) as a rapid and low cost coating methodology in 2013. Nonetheless, the selection of phenols is predominantly confined to tannic acid.¹²⁻¹³ Interestingly, various phenolic compounds, not just dopamine, can undergo self-polymerization by oxidative coupling that was first discovered in 1959.¹⁴⁻¹⁶ However, simply forming polyphenols is not enough to render the substrate coating capability.¹⁷ Although phenolic compounds can bind to substrates through multiple binding modes, their hydrophilic nature enables them to remain in a thermodynamically stable solution state. The addition of an amine group can promote the surface coating of catechol, as evidenced by previous studies utilizing polydopamine, poly(levodopa),¹⁸ poly(catecholamine)^{19,20}, and polynorepinephrine.²¹ Hong et al revealed that the presence of amine plays a crucial role in promoting aggregation of polydopamine (PDA) through cation- π interaction.²² Furthermore, we recently discovered that the aggregation of dopamine oligomer is crucial to reach their solubility limit in the solution for initiating the surface coating. Building upon the polydopamine adhesion

mechanism driven by the solubility limit, we anticipated that utilizing a hydrophobic crosslinker to bridge phenolic oligomers could lead surface-independent adhesion even in the absence of amine functionality. This approach potentially extends the unique surface-independent coating of polydopamine to encompass general phenolic compounds.

Taking into account reactivity with phenols, amine and thiol emerged as suitable candidates for serving as crosslinkers, owing to their potential covalent linkage with the phenol through Michael addition or Schiff base reactions.²³⁻²⁶ Along with oxidation of phenols, the electron-withdrawing property of carbonyl groups lead Michael addition with nucleophiles such as amine and thiol. This chemistry has been introduced as a post-modification method of polydopamine coating, allowing additional functionalities at the coating surface.²⁷⁻²⁹ Amine-based Michael addition with polydopamine has been extensively studied with polyethylene imine (PEI) for membrane applications.³⁰⁻³² Besides, thiol-modified PDA coating has been adopted in surface post-modification,³³⁻³⁵ catalyst,³⁶ membrane,^{37,38} hydrogel,^{39,40} and drug delivery.⁴¹ However, this chemistry hasn't been recognized as a crosslinking strategy for connecting phenolic oligomers for solvent resistive surface coating. Among amine and thiol crosslinkers, thiol possesses advantages due to its rapid reaction with phenol facilitated by its inherent weak sulfur-hydrogen bond and the high electron density of sulfur, promoting efficient Michael addition with alkenes.^{42,43} Additionally, the formation of disulfide bonds enables the extension of hydrophobic portions, resulting in rapidly built insolubility in a polar environment.^{44,45}

Herein, we present a versatile polyphenol-alkanedithiol (ADT) copolymer system that can be easily applied to a wide range of phenolic compounds using a simple sequential addition method and provides solvent-resistive stability to the resulting surface coating. Our sequential one-pot



Scheme 3-1 Binding mechanism of polyphenol-alkanedithiol copolymers. (A) Solubilized phenolic oligomer in polar solvents. (B) Hydrophobic nature of the alkanedithiol (ADT) linker causes the copolymer to reach its solubility limit in polar solvent. (C) Solubilized copolymer films in nonpolar solvent.

reaction scheme involves self-polymerization of phenols, particularly catechol and gallol compounds, self-polymerization of ADT, and covalent linkage of ADT to polyphenol via Michael addition, resulting in a copolymer with universal coating capability for various substrates. Self-polymerization of ADT increases hydrophobicity of the copolymer promptly, which makes the resulting polyphenol-ADT copolymer to reach its solubility limit in the polar solvent as well as gives backbone flexibility. Consequently, the combined effects lead to the adhesion of the copolymer to various substrates as illustrated in Scheme 3-1. We extended this strategy to a series of phenolic compounds such as dopamine, 3,4-dihydroxybenzylamine, 4-ethylcatechol, levodopa, tannic acid, caffeic acid, and 3,4-dihydroxybenzylaldehyde and demonstrated the universal coating capability of the resulting copolymers with ADT. Qualitative and quantitative analysis using XPS confirmed the functionalization of the surface. Furthermore, the resulting copolymer coating exhibited robust solvent resistivity in strong base (pH 14), DMSO, and chloroform whereas the stability of the surface coating from polydopamine derivatives was notably lower. We conducted solvent-resistance tests of the copolymer films to assess their stability and robustness arising from the covalent linkage under various conditions.

3.2 Result and Discussion

3.2.1 Reaction Mechanism and Molecular Structure of Copolymer

We aimed to develop a copolymer system comprising phenolic compounds and ADTs to achieve solvent resistivity of the resulting film as well as surface-independent coating capability because conventional phenol-based surface coating, such as dopamine chemistry, is fragile in a wide range of solvents. It is worth noting that the reaction conditions for the self-polymerization of phenolic compound, dithiol self-polymerization, and thiol-phenol Michael addition are similar to each other as shown in Figure 3-1A. The self-polymerization of catechol has been extensively reported in the synthesis of polydopamine under mild alkaline conditions.^{1,46} Under basic conditions, oxidation creates a radical that initiates the polymerization of catechol via aryl-aryl coupling as shown in Figure S3-1.^{47,48} Moreover, the diverse oxidation states of catechol cause increased structural complexity.⁴⁹⁻⁵¹ In this study, we opted for simplified polymer structures. In the same condition, oxidation of sulfhydryl group of alkanedithiol (ADT) yields a thiyl radical, and undergo dimerization with another thiyl radical to create a disulfide bond,⁵² and consequently form polyalkanedithiol (PADT).^{53,54} In addition, the thiol-Michael addition reaction connects polyphenols and PADTs. Although position 5 of catechol is more favorable for the formation of a covalent linkage with ADT through oxidative coupling with a thiyl radical.^{55,56} the steric effects of phenolic oligomers may hinder thiol linkage at position 5, necessitating consideration of linkage at position 6 through Michael addition as well. While these three reactions occur simultaneously, their distinct reaction kinetics may impede the formation of the catechol-alkanedithiol copolymers. Initially, we anticipated that the copolymer could be formed through a one-pot reaction. However, we later realized that thiol acts as a radical scavenger,⁵⁷ inhibiting the polymerization of phenolic

compounds. Eventually, we employed a sequential addition method, where we initiated the formation of polyphenol first, and after an hour added ADT to prepare the copolymer.

We prepared the desired copolymer using 4-ethylcatechol (EC) and 1,8-octanedithiol (ODT) in a mild basic methanol solution. The reaction yielded a yellowish solid, which we identified as PEC_ODT (Figure 3-1A). Fourier-transform infrared spectra (FTIR) of PEC_ODT exhibited a broad band at 3600-3200 cm^{-1} that is assigned to O-H stretching modes, an aromatic hydrocarbon region at 1587 cm^{-1} , and a C-O region at 1231 cm^{-1} from the catechol unit. Moreover, strong aliphatic C-H signals of ODT were detected at 2923 cm^{-1} and 2854 cm^{-1} (Figure 3-1B). The FTIR analysis confirmed the presence of EC and ODT units. However, it was challenging to assign the thioether (C-S-C) stretching vibrations due to the weak signal resulting from the relatively small amount in the copolymer. Hence, we conducted the thermogravimetric analysis (TGA) and differential scanning calorimetry (DSC) to verify the copolymer formation. The TGA results showed that PEC starts to decompose at 178 °C, while PODT and PEC_ODT start to decompose at around 284 °C. PEC_ODT did not show the decomposition at 178 °C, indicating the absence of PEC homopolymer in the resulting copolymers (Figure 3-1C). Additionally, the 2nd heating DSC curve of PEC_ODT did not exhibit the melting peaks of PODT at around 50 °C, confirming the successful formation of the copolymers having chemically connected PEC and ODT (Figure 3-1D).

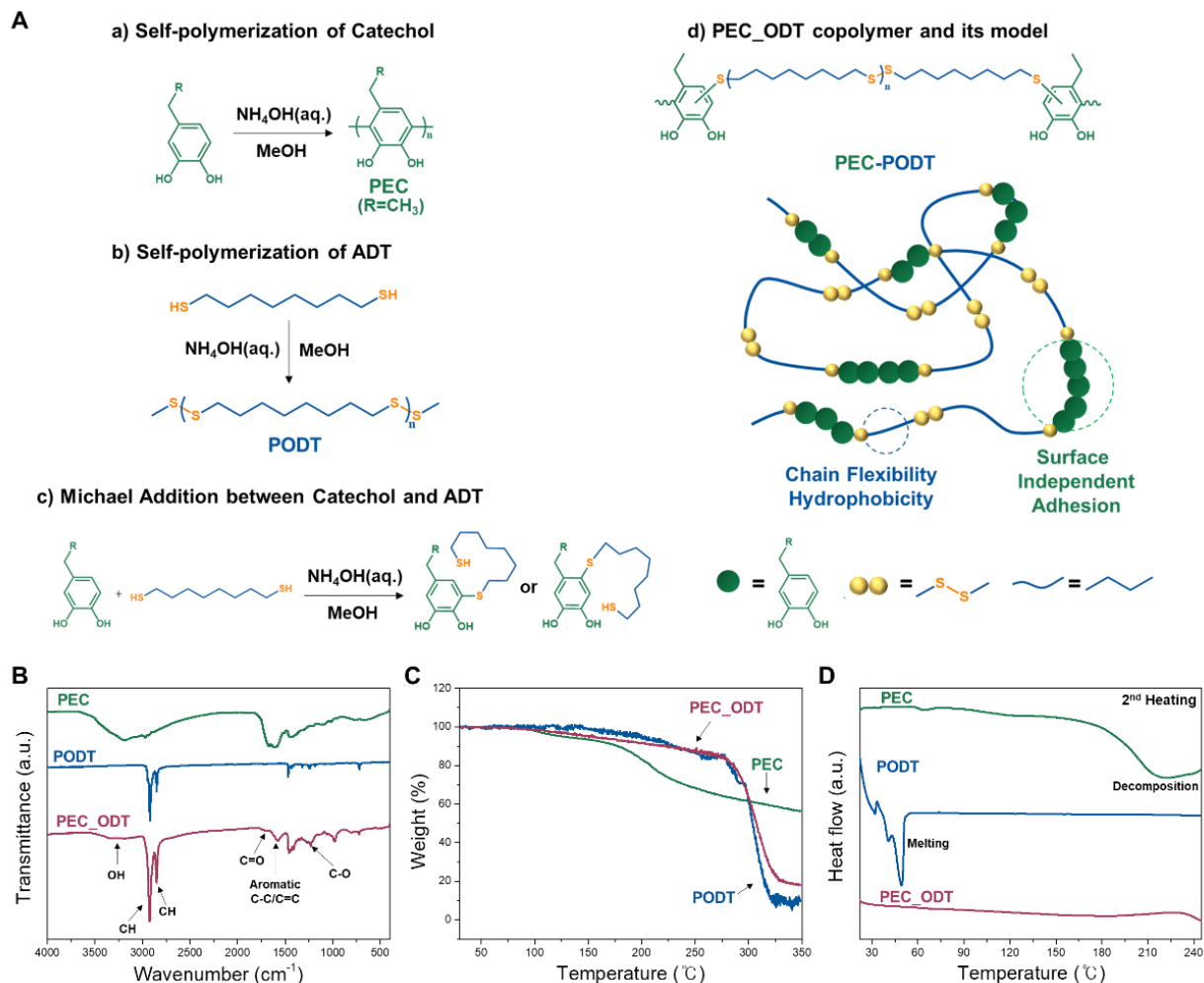


Figure 3-1 Reaction mechanism of copolymer and characterization. (A) a) poly(catechol), b) poly(alkanedithiol), and c) Michael addition between catechol and thiol. d) PEC_ODT structure. e) Suggested structure of the catechol-alkanedithiol copolymer. (B) FTIR spectra of polyethylcatechol (PEC), polyoctanedithiol (PODT), and polyethylcatechol_octanedithiol (PEC_ODT). (C) Thermogravimetric analysis (TGA) for PEC, PODT, and PEC_ODT. (D) 2nd Heating dynamic scanning calorimetry (DSC) plots of PEC, PODT, and PEC_ODT.

3.2.2 Surface-independent Coating on Various Phenolic Compounds

We prepared a series of phenolic compounds including dopamine (DA), 3,4-dihydroxybenzylamine (DBA), ethylcatechol (EC), caffeic acid (CAC), tannic acid (TA), levodopa (LD), and catecholaldehyde (CAD), and conducted coating tests on various substrates (Figure 3-2A). First, we monitored the self-polymerization of the phenolic monomers by observing the color change in methanol/ammonia solutions. All monomer solutions were initially transparent and gradually developed a color over time, indicating a reduced bandgap change due to the

formation of conjugated oligo-phenolic compounds during the self-polymerization (Figure 3-2B).⁵⁸ Then we polymerized those polyphenols in the same condition but with a glass substrate in the vials, and observed that only the amine-containing phenols made the glass substrate coating as shown in the top row of the photos in Figure 3-2C. Interestingly, additional incorporation of ODT made all tested phenolic compounds to adhere to the glass substrate (the bottom row of the photos in Figure 3-2C). The surface morphology of the coating layer on glass substrates was examined via SEM, as depicted in Figure S3-2. Particle merging observed on the surface indicated adhesion based on the solubility limit, as revealed in our previous study.¹⁷ We further explored the surface-independent adhesion of the polyphenol-ADT copolymer on glass, aluminum (Al), polyethylene (PE), which represent ceramic, metal, and polymer with low surface energy, respectively (Figure 3-2D). The results clearly demonstrated that with the ODT linker the polyphenols regardless of having amine functionality have surface-independent universal adhesion properties.

We utilized X-ray photoelectron spectroscopy (XPS) to analyze the surface functionalities of the resulting coating of polyphenol-ODT copolymers as shown in Figure 3-3. High-resolution C 1s spectra of PCAC_ODT, PTA_ODT, and PLD_ODT revealed the presence of carboxylic acid (-COOH) or ester (-COO-) groups, indicated by the peaks at 284.4 eV (C-C), 286.2 eV (C=O), and 288.4 eV (O-C=O). The C-C and C=O peaks of PCAD_ODT confirmed the presence of aldehyde (-CHO) groups, as depicted in Figure 3-3A. High-resolution N 1s spectra showed primary amine (-NH₂) or secondary amine (-NH-) bonds at 399.4 eV and 401.1 eV, respectively, indicating the

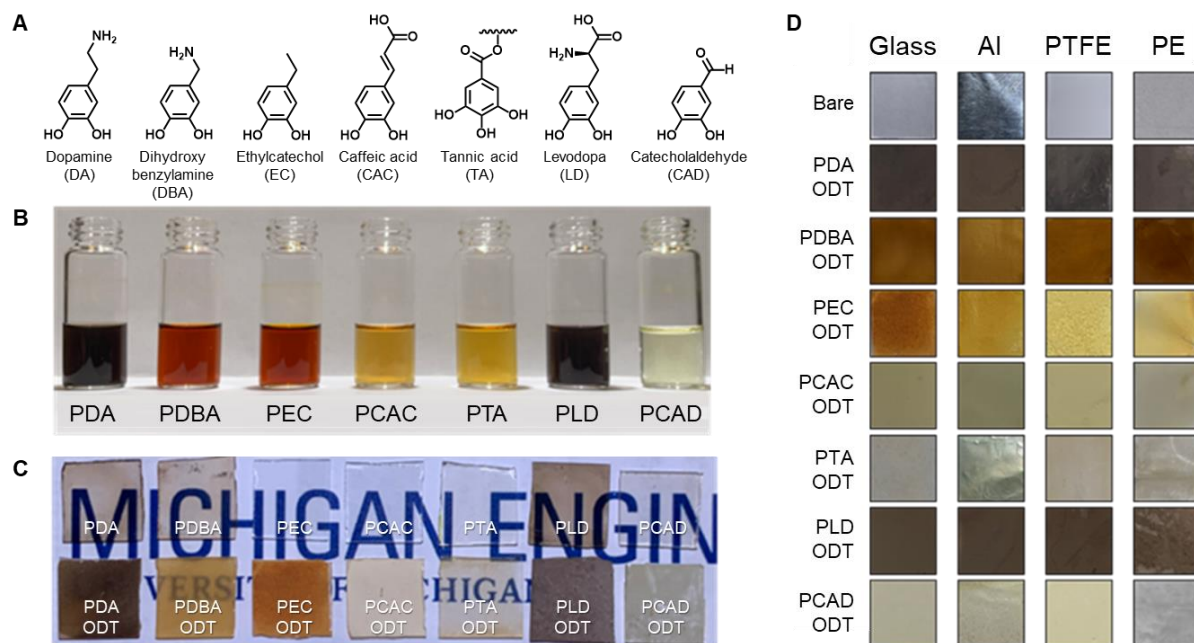


Figure 3-2 Copolymerization of various phenolic compounds with ODT. (A) Chemical structure of the phenolic monomers and (B) their corresponding polymers formed in mild alkaline solution (NH_4OH in MeOH). (C) Coating behaviors of the polyphenols and polyphenol-ADT copolymers on glass substrates. (D) Surface-independent Coating of polyphenol-ADT copolymers on Glass, Aluminum (Al), Teflon (PTFE), and Polyethylene (PE) substrates.

presence of amine functionalities (Figure 3-3B). PDBA_ODT possessed only primary amine, while PDA_ODT had both primary and secondary amine due to the formation of 5,6-dihydroxyindole (DHI). PLD_ODT could have both primary and secondary amine due to DHI formation as outlined by the Raper-Mason scheme for melanin synthesis in the body.^{59,60} Under synthetic conditions, however, the primary amine is the predominant species present in PLD_ODT, as evidenced by earlier research.⁶¹

We further conducted quantitative analysis through XPS survey scans and compared N 1s and S 2s signals from PDBA_ODT to quantify the effective functional groups on the copolymer surface. We varied the molar feed ratio between DBA and ODT and found a direct proportional trend of surface amine with the amount of DBA (Figure 3-3C and Table 3-1). We also studied coating uniformity through a time-study of PDBA_ODT, as described in Figure 3-3D. We

collected PDBA_ODT copolymer films at different time intervals after the addition of ODT (2h, 4h, 6h, 8h, and 10h) with a fixed DBA:ODT feed ratio of 1:0.5 considering that each DBA has one amine group whereas ODT has two thiols. The XPS results showed a sulfur-rich composition for the first 8hrs, indicating that ODT polymerization was faster than Michael addition. However, the relative amount of sulfur peak gradually decreased after 6hrs, implying that once majority of ODT was consumed, PDBA became the major component in the later stage of the copolymerization. Although the chemical composition of the film was not perfectly uniform, more than 35% of amine functionality was maintained on the surface regardless of the reaction time (see Table 3-2 for details).

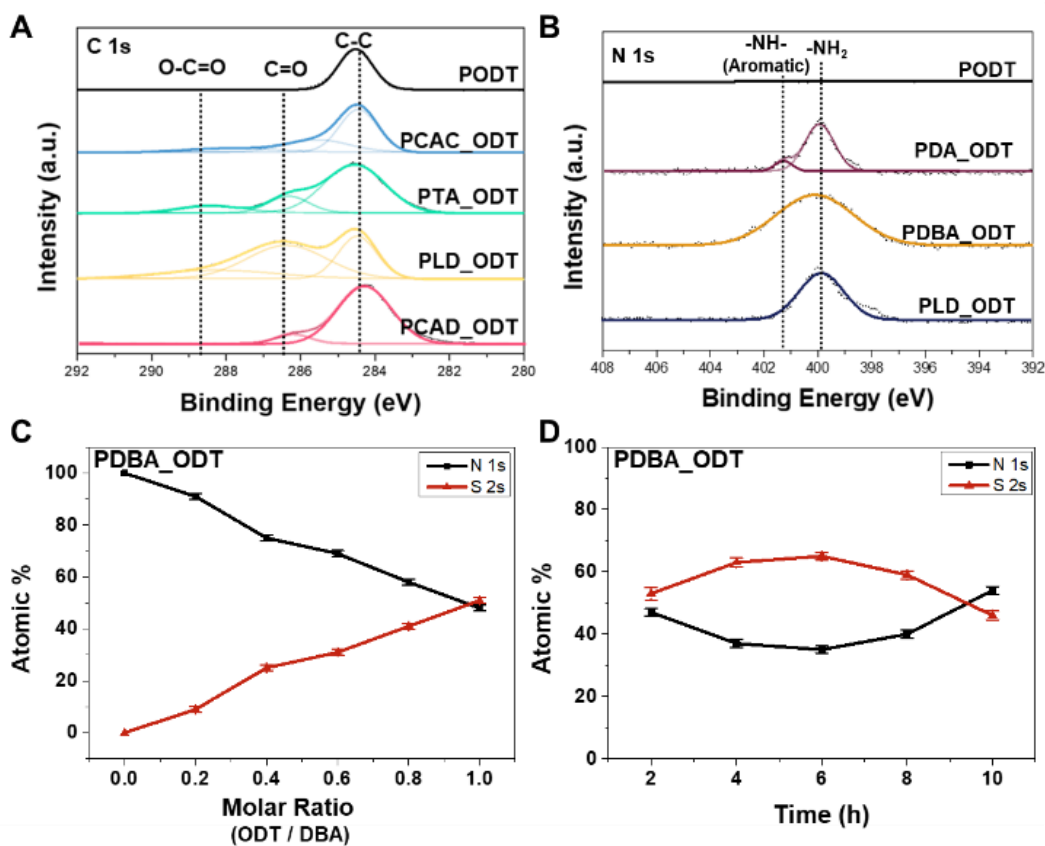


Figure 3-3 XPS spectra of copolymers. (A) High-resolution C 1s in polyphenol-ODT copolymers. (B) High-resolution XPS spectra of N 1s in polyphenol-ODT copolymers. (C) Atomic ratio of N 1s to S 2s via XPS survey spectra after 24hrs of reaction for various molar ratios between ODT and DBA. (D) Atomic ratio of N 1s to S 2s over the reaction time after the addition of ODT, as determined by XPS survey spectra (ODT/DBA feed ratio is 0.5/1).

Table 3-1 Atomic ratio of N 1s to S 2s via XPS survey spectra after 24hrs of reaction for various molar feed ratios between ODT and DBA

DBA:ODT Ratio	Atomic ratio, At% (σ)	
	N 1s	S 2s
1:0	100 (0)	0 (0)
1:0.2	91 (1.1)	9 (1.2)
1:0.4	75 (1.2)	25 (1.2)
1:0.6	69 (1.2)	31 (1.2)
1:0.8	58 (1.2)	41 (1.2)
1:1	48 (1.2)	51 (1.2)

Table 3-2 Atomic ratio of N 1s to S 2s over the reaction time after the addition of ODT, as determined by XPS survey spectra (ODT/DBA ratio is 0.5/1)

Time after ODT addition	Atomic ratio, At% (σ)	
	N 1s	S 2s
2h	47 (1.1)	53 (2.0)
4h	37 (1.3)	63 (1.4)
6h	35 (1.1)	65 (1.2)
8h	41 (1.3)	59 (1.3)
10h	54 (1.3)	46 (1.4)

3.2.3 Achieving Solvent Resistance by Crosslinking

PDA coating mainly relies on cation - π interactions between ammonium cation (NH_3^+) and DHI, leading to coating stability issues in highly basic conditions and in certain organic solvents like DMSO or DMF.⁵⁷ Hong et al. demonstrated the delamination of the PDA coating under basic conditions (pH \sim 9.8). This delamination was triggered by the disappearance of cation- π interactions due to the deprotonation of ammonium cation (NH_3^+) within the PDA coating.²⁰ Furthermore, Yang et al performed a stability test of PDA coating on gold with ten organic solvents and showed that DMSO can trigger the serious detachment of PDA coating by hyper-solvation of PDA.⁶² Moreover, Park et al found that DMSO can disrupt the hydrogen bonding between PDA and specific substrates such as SiO_2 , leading to selective PDA coating on metals through coordination bonding.⁶³ This problem can be exacerbated in the linear structure of polyphenols when compared to the crosslinked structure of amine-containing PDA.

Unlike the secondary interaction observed in PDA coating, the introduction of ADT into polyphenol enhances copolymer stability through covalent linkage, as depicted in Figure 3-4A. To conduct a quantitative analysis of solvent resistance, we applied PDA and PDBA copolymer coatings onto aluminum and glass substrates. The chemical structure of the monomers and linkers used in this study is shown in Figure 3-4B. Subsequently, we conducted the stability test by measuring weight changes of the samples before and after exposure to NaOH (aq.), DMSO, and chloroform treatments using both a microbalance and TGA and the results are summarized in Figure 3-4C. Initially, we immersed PDA and PDA_ODT coated glass substrates in a 1N sodium hydroxide aqueous solution. The PDA coating was delaminated due to the nullified cation- π interaction, resulting in only 30% of the PDA coating remaining. Nevertheless, PDA still exhibited solvent resistance in DMSO and chloroform with 76% and 84% of the coating remaining,

respectively. The incorporation of ODT into PDA leads to extended crosslinking through DHI and ODT, resulting in robustness across all conditions. Unlike PDA, other polyphenols are mostly linear due to the lack of DHI or amine functionality and can be easily detached under certain conditions. For instance, the PDBA layer exhibited significant detachment from the substrates in both sodium hydroxide aqueous solution and DMSO. While copolymerization of PDBA with ODT appeared to resolve the stability issue, we discovered that the linear PDBA_ODT could be solubilized in organic solvents like chloroform as illustrated in Scheme 3-1C and shown in Figure 3-4C. Although the Michael addition occurs, the short chain length of phenolic oligomers impedes the creation of an effective network structure, resulting in the prevalence of linear polymers. We explored the correlation between the monomer:linker ratio and solvent resistance. In the case of PDBA_ODT, we noted a distinct trend wherein the coating exhibited increased stability in sodium hydroxide aqueous solution and DMSO as the amount of ODT linker was raised from 1:0.5 to 1:5, as depicted in Figure S3-3 and Figure S3-4. Nevertheless, with the increase in ODT linker concentration, the resulting copolymer became soluble in chloroform, indicating the solubility issue of a hydrophobic linker in chloroform. Consequently, we further investigated a hydrophilic ethylene glycol type dithiol (EGDT) linker, 3,6-Dioxa-1,8-octane-dithiol, to manipulate the stability of PDBA-based copolymer in non-polar organic solvents. Even though PDBA_EGDT exhibited poor stability in DMSO, it showed enhanced stability in chloroform as shown in Figure S3-3 and Figure S3-4. These findings support the proposition that the polyphenol-ADT copolymers exhibit a linear polymer structure rather than a crosslinked network. To transition from a linear to a network polymer structure with enhanced solvent resistance under diverse conditions, we introduced trimethylolpropane tris(3-mercaptopropionate) (TT) as a multi-functional crosslinker and prepared a copolymer using a 1:1:1 molar ration of monomer:ODT:TT. The

solvent resistance tests on the resulting copolymer on aluminum demonstrated exceptional robustness in NaOH(aq.), DMSO, and chloroform. The same test results on glass substrates are presented in Figure 3-4D. The exceptional solvent-resistance of this coating indirectly verifies the successful formation of a network polymer, achieved through the extension of polyphenols facilitated by the trithiol crosslinkers.

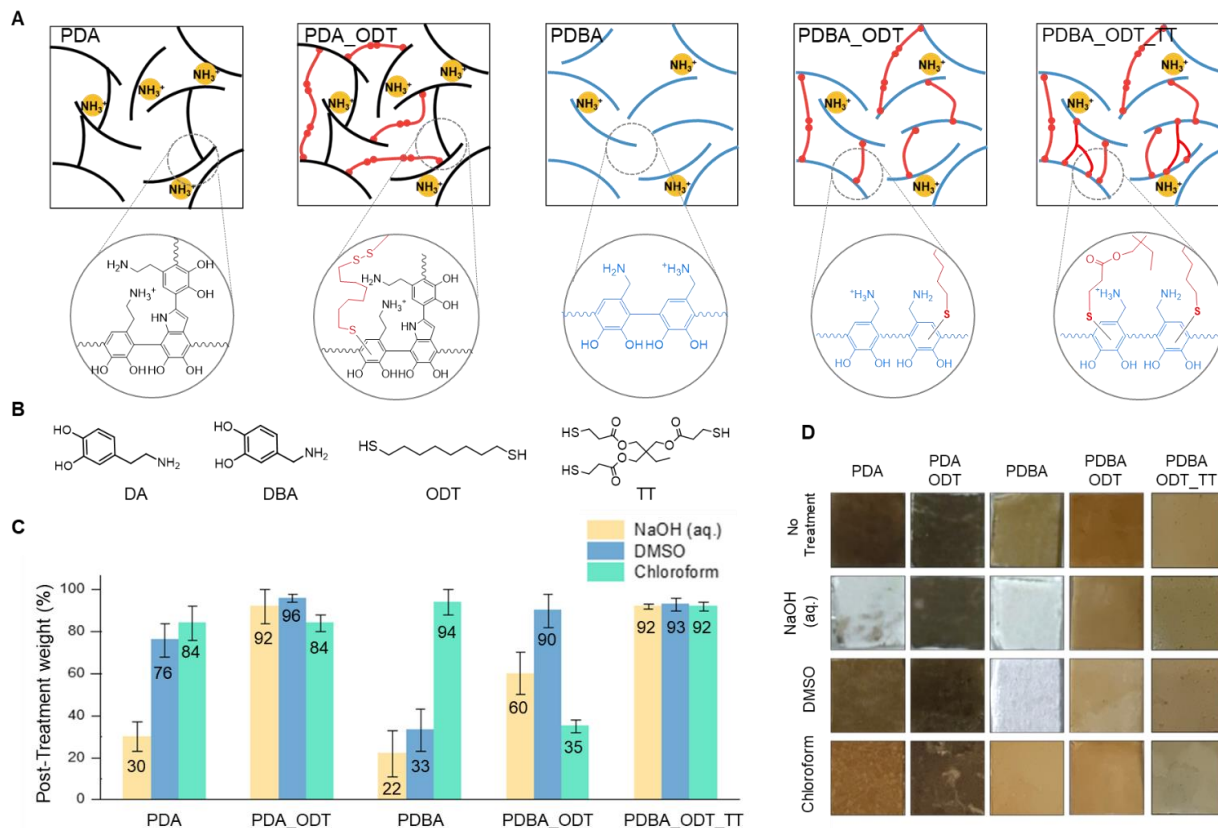


Figure 3-4 Solvent resistance of copolymers. (A) Schematic illustration of copolymer structures alongside their corresponding chemical structures. (B) Chemical structure of monomers and linkers in the solvent resistance study. (C) Solvent resistance test results of PDA, PDA_ODT, PDBA, PDBA_ODT, and PDA_ODT_TT coatings in NaOH(aq.), DMSO and chloroform. The molar ratio between monomer and ODT is 1:1. The PDBA_ODT_TT sample was prepared using a 1:1:1 molar ratio of monomer, ODT, and trithiol (TT) crosslinker. (D) Solvent resistance test results of PDA, PDA_ODT, PDBA, PDBA_ODT, and PDA_ODT_TT coatings on glass substrates.

3.3 Conclusion

We developed a sequential polymerization of polyphenol-ADT copolymer via thiol-Michael addition under mild alkaline conditions to achieve solvent-resistive robust as well as substrate-independent surface coating and functionalization. The aliphatic groups of ODT provide flexibility to the rigid aromatic backbone of polyphenol, while the catechol groups of polyphenols render unique multiple binding modes (H-bond, van der Waals, π - π interaction, and metal chelation) with substrates, resulting in a robust and enhanced adhesion. By introducing flexible aliphatic linkers, this work extends the surface-independent coating capability previously limited to catecholamines to various amine-free phenolic compounds. We applied the phenol-ADT copolymer strategy to various phenolic monomers (DBA, EC, TA, CAC, and CAD), providing coating with diverse functionality, such as carboxylic acid, amine, and aldehyde on ceramic (glass), metal (Al), polymer (PE) and even Teflon. The covalently bound PEC and PODT exhibited remarkable robustness in strong basic conditions, unlike polydopamine coatings that are removed due to disassembled cation- π interaction. ADT selection and content were optimized in various solvents conditions. Ultimately, the synergy between ADT and trimethylolpropane tris(3-mercaptopropionate) crosslinkers results in robust solvent resistance against NaOH(aq.), DMSO, and chloroform. The developed strategy is readily applicable for various surface modification schemes.

3.4 Publication Information

Jiwon Lim, Meng-Hsun Lee, Abigail Ahn, and Jinsang Kim, “Sequential Self-polymerization of Phenolic Compounds with Alkanedithiol Linkers as a Surface-independent and Solvent-resistant Surface Functionalization Strategy” revision submitted.

3.5 Experimental Section

3.5.1 Chemicals

Dopamine hydrochloride, 3,4-dihydroxybenzylamine hydrobromide, 4-ethylcatechol, caffeic acid, tannic acid, 3,4-dihydroxybenzaldehyde, 1,8-octanedithiol 3,6-Dioxa-1,8-octane-dithiol, Trimethylolpropane tris(3-mercaptopropionate), and Ammonia solution 25% were purchased from Millipore Sigma. 3-(3,4-Dihydroxyphenyl)-L-alanine was purchased from TCI America. All chemicals and solvents were used without further purification.

3.5.2 Materials Characterization

FT-IR was conducted by using Nicolet iS20 spectrometer with a platinum ATR accessory. The FTIR spectra were performed with 64 scans at 4 cm^{-1} resolution. The Adv ATR mode of OMNIC software was used for the baseline collection. The thermal properties of the copolymer were investigated using a Discovery Differential Scanning Calorimeter (DSC) from TA Instrument. Prior to analysis, the samples were dried in vacuum oven at 40°C for overnight. Measurements were performed over a temperature range from 25°C to 250°C at a heating rate of $10^{\circ}\text{C}/\text{min}$. An initial equilibration period of 5 min was allowed before each run. Thermogravimetric Analysis (TGA) was conducted with TA Instrument Discovery TGA. Measurements were performed over

a temperature range from 25°C to 350°C at a heating rate of 10°C/min. X-Ray photoelectron spectroscopy (XPS) spectra were obtained by Kratos Axis Ultra XPS using monochromatic Al source. The base pressure in the analysis chamber was typically 1×10^{-9} mbar. All spectra were collected with the charge neutralization. The collected data were processed using the CasaXPS software package. Spectral charge correction was performed using the main C 1s peak due to hydrocarbon (C-C/C-H bonds) set to 284.5 eV.

3.5.3 Self-polymerization of Polyphenols

The polyphenol coatings were prepared using the following methods. Firstly, glass slides were rinsed with acetone and methanol before use. Next, dopamine hydrochloride, 3,4-dihydroxybenzylamine hydrobromide, 4-ethylcatechol, caffeic acid, Tannic acid, 3-(3,4-dihydroxyphenyl)-L-alanine, and 3,4-dihydroxybenzylaldehyde were each dissolved separately in methanol at a concentration of 40mg/20ml. The glass slides were then immersed in the dopamine solution, followed by the addition of 0.8ml of 25% ammonium solution to the solution. The solution was allowed to react for one day with stirring, and then rinsed with methanol. Due to the poor coating capability, PEC was prepared by reprecipitation with methanol (good solvent) and tetrahydrofuran (bad solvent) for the further analysis.

3.5.4 Preparation of Polyphenol-ADT Copolymers Coatings on Various Substrates

The polyphenol-ODT copolymers were prepared using the following methods. Firstly, dopamine hydrochloride, 3,4-dihydroxybenzylamine hydrobromide, 4-ethylcatechol, caffeic acid, Tannic acid, 3-(3,4-dihydroxyphenyl)-L-alanine, and 3,4-dihydroxybenzylaldehyde were each dissolved separately in methanol at a concentration of 40mg/20ml. Next, slide glass, aluminum foil, polyethylene film, and PTFE film were immersed in the monomer solution, followed by the addition of 0.8ml of 25% ammonium solution to the solution. The solution was allowed to react for one hour, after which 1,8-octanedithiol was added with stirring. The molar ratio of monomer to ODT used were 1:0.2, 1:0.4, 1:0.5, 1:0.6, 1:0.8, 1:1, and 1:5. The solution was then allowed to react for one day, and then rinsed with methanol.

3.5.5 Preparation of Polyphenol-ODT-TT Copolymers Coatings on Various Substrates

3,4-dihydroxybenzylamine hydrobromide was dissolved in methanol at a concentration of 40mg/20ml, followed by the addition of 0.8ml of 25% ammonium solution to the mixture. The solution was allowed to react for one hour, then 1,8-octanedithiol was added while stirring. After 12h, slide glass and aluminum foil were immersed in the solution, followed by 72mg of trimethylolpropane tris(3-mercaptopropionate) addition. After 12h, the substrates were rinsed with methanol and then dried by blowing air.

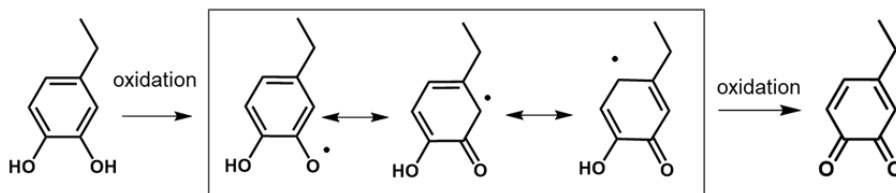
3.5.6 Solvent Resistance Test

Glass and aluminum foil substrates measuring 1x1 cm² were prepared with PDA, PCA, PDA_ODT, PCA_ODT, and PCA_EGDT coatings using the previously described method. The total weight of each substrate was measured using a microbalance of TGA. The substrates were then immersed in 1N NaOH(aq.), DMSO, and chloroform, and stirred for 1 minute. After rinsing the substrates with acetone and MeOH, they were dried in a vacuum oven for 2 hours at 50°C. To determine the stability of the coatings, the coating layers were completely decomposed using TGA at a heating rate of 10°C/min from 30°C up to 600°C. The weight of the aluminum substrate was measured by TGA before treatment, after treatment, and at the end of the experiment. The stability was calculated as follows.

$$\text{Stability (\%)} = (1 - \text{Weight}_{\text{initial}} - \text{Weight}_{\text{treated}} + 2\text{Weight}_{\text{final}}) / (\text{Weight}_{\text{initial}} - \text{Weight}_{\text{final}}) * 100$$

3.6 Supporting Information

Oxidation states



Aryl-aryl coupling

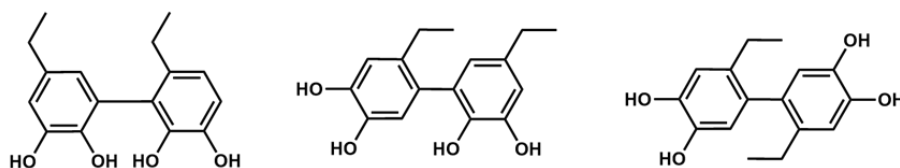


Figure S3-1 Various oxidation states of 4-ethylcatechol and the proposed structures of its dimer through aryl-aryl coupling.

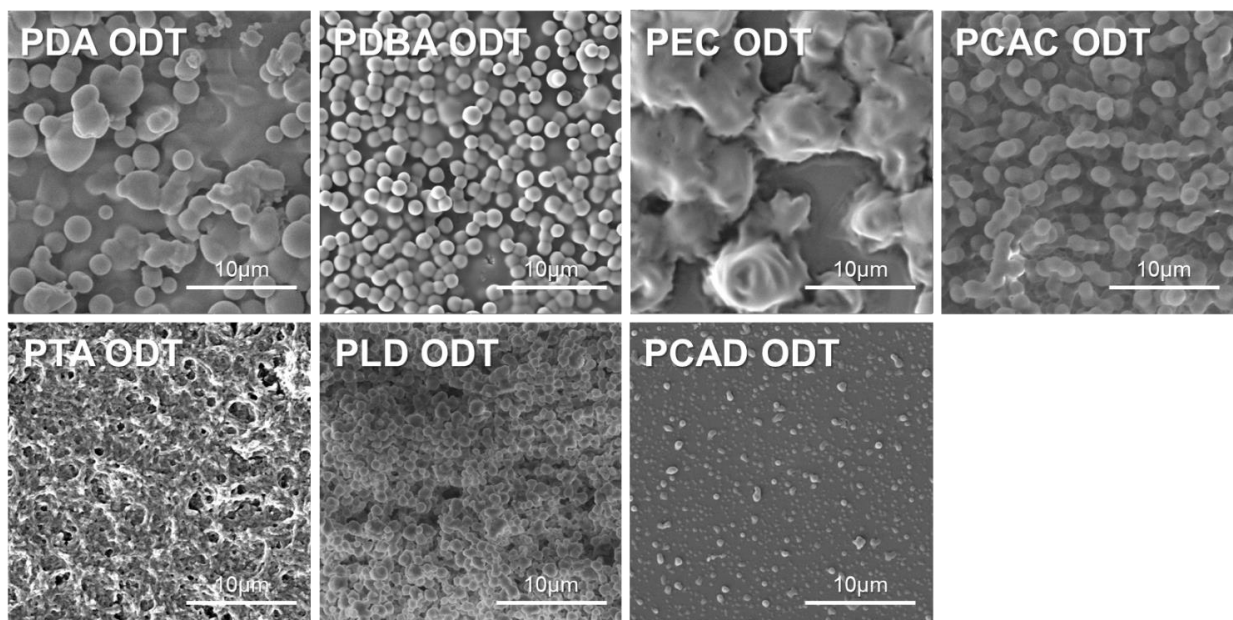


Figure S3-2 SEM images showing the copolymer coating on glass substrates.

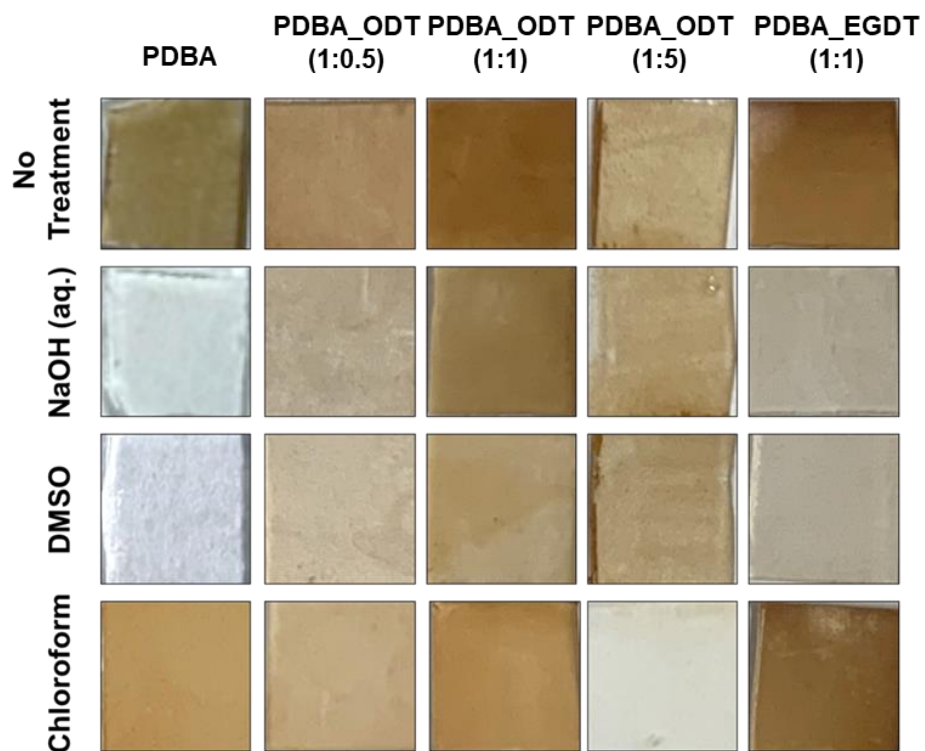


Figure S3-3 Stability test results of PDBA, PDBA_ODT, and PDBA_EGDT coatings on glass substrates with different ratio of monomer to linker in NaOH(aq.), DMSO and chloroform.

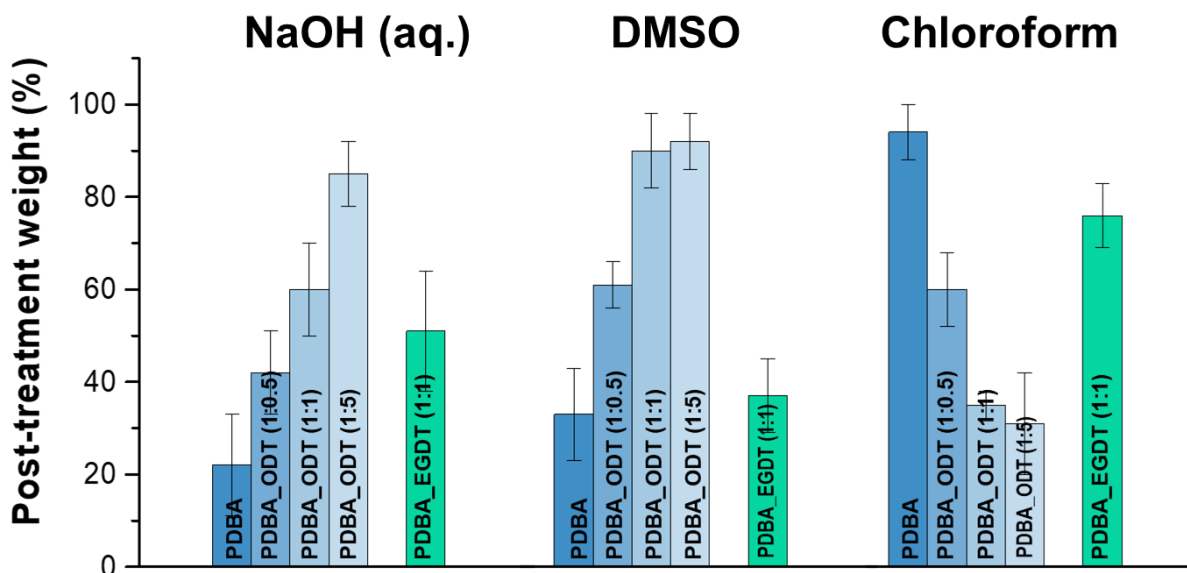


Figure S3-4 Stability test results of PDBA, PDBA_ODT, and PDBA_EGDT coatings with different ratio of monomer to linker in NaOH(aq.), DMSO and chloroform.

3.7 Reference

- (1) Lee, H.; Dellatore, S. M.; Miller, W. M.; Messersmith, P. B. Mussel-Inspired Surface Chemistry for Multifunctional Coatings. *Science*. **2007**, *318* (5849), 426–430. <https://doi.org/10.1126/science.1147241>.
- (2) Hu, M.; Mi, B. Enabling Graphene Oxide Nanosheets as Water Separation Membranes. *Environ. Sci. Technol.* **2013**, *47* (8), 3715–3723. <https://doi.org/10.1021/es400571g>.
- (3) Liu, Y.; Ai, K.; Lu, L. Polydopamine and Its Derivative Materials: Synthesis and Promising Applications in Energy, Environmental, and Biomedical Fields. *Chem. Rev.* **2014**, *114* (9), 5057–5115. <https://doi.org/10.1021/cr400407a>.
- (4) Ye, Q.; Zhou, F.; Liu, W. Bioinspired Catecholic Chemistry for Surface Modification. *Chem. Soc. Rev.* **2011**, *40* (7), 4244–4258. <https://doi.org/10.1039/c1cs15026f>.

- (5) Lee, H. A.; Park, E.; Lee, H. Polydopamine and Its Derivative Surface Chemistry in Material Science: A Focused Review for Studies at KAIST. *Adv. Mater.* **2020**, *32* (35), 1907505. <https://doi.org/10.1002/adma.201907505>.
- (6) Saiz-Poseu, J.; Mancebo-Aracil, J.; Nador, F.; Busqué, F.; Ruiz-Molina, D. The Chemistry behind Catechol-Based Adhesion. *Angew. Chemie Int. Ed.* **2019**, *58* (3), 696–714. <https://doi.org/10.1002/anie.201801063>.
- (7) Lee, H.; Lee, B. P.; Messersmith, P. B. A Reversible Wet/Dry Adhesive Inspired by Mussels and Geckos. *Nat.* **2007**, *448* (7151), 338–341. <https://doi.org/10.1038/nature05968>.
- (8) Burke, S. A.; Ritter-Jones, M.; Lee, B. P.; Messersmith, P. B. Thermal Gelation and Tissue Adhesion of Biomimetic Hydrogels. *Biomed. Mater.* **2007**, *2* (4), 203. <https://doi.org/10.1088/1748-6041/2/4/001>.
- (9) Westwood, G.; Horton, T. N.; Wilker, J. J. Simplified Polymer Mimics of Cross-Linking Adhesive Proteins. *Macromolecules* **2007**, *40*, 3960-3964. <https://doi.org/10.1021/ma0703002>.
- (10) North, M. A.; Del Grosso, C. A.; Wilker, J. J. High Strength Underwater Bonding with Polymer Mimics of Mussel Adhesive Proteins. *ACS Appl. Mater. Interfaces* **2017**, *9* (8), 7866–7872. <https://doi.org/10.1021/acsami.7b00270>.
- (11) White, J. D.; Wilker, J. J. Underwater Bonding with Charged Polymer Mimics of Marine Mussel Adhesive Proteins. *Macromolecules* **2011**, *44*, 5085–5088. <https://dx.doi.org/10.1021/ma201044x> |
- (12) Ejima, H.; Richardson, J. J.; Liang, K.; Best, J. P.; Van Koeveden, M. P.; Such, G. K.; Cui, J.; Caruso, F. One-Step Assembly of Coordination Complexes for Versatile Film and

- Particle Engineering. *Science* **2013**, *341* (6142), 154–157.
<https://doi.org/10.1126/science.1237265>.
- (13) Ejima, H.; Richardson, J. J.; Caruso, F. Metal-Phenolic Networks as a Versatile Platform to Engineer Nanomaterials and Biointerfaces. *Nano Today* **2017**, *12*, 136–148.
<https://doi.org/10.1016/j.nantod.2016.12.012>.
- (14) Hay, A. S.; Blanchard, H. S.; Endriss, G. F.; Eustance, J. W. Polymerization by Oxidative Coupling. *J. Am. Chem. Soc.* **1959**, *81* (23), 6335–6336.
<https://doi.org/10.1021/ja01532A062>.
- (15) Kobayashi, S.; Higashimura, H. Oxidative Polymerization of Phenols Revisited. *Prog. Polym. Sci.* **2003**, *28* (6), 1015–1048. [https://doi.org/10.1016/S0079-6700\(03\)00014-5](https://doi.org/10.1016/S0079-6700(03)00014-5).
- (16) Rahim, M. A.; Kristufek, S. L.; Pan, S.; Richardson, J. J.; Caruso, F. Phenolic Building Blocks for the Assembly of Functional Materials. *Angew. Chemie - Int. Ed.* **2019**, *58* (7), 1904–1927. <https://doi.org/10.1002/anie.201807804>.
- (17) J. Lim, S. Zhang, J. Heo, M. Dickwella Widanage, A. Ramamoorthy, J. Kim “Polydopamine Adhesion: Catechol, Amine, Dihydroxyindole, and Aggregation Dynamics” unpublished results.
- (18) Tan, X.; Gao, P.; Li, Y.; Qi, P.; Liu, J.; Shen, R.; Wang, L.; Huang, N.; Xiong, K.; Tian, W.; Tu, Q. Poly-Dopamine, Poly-Levodopa, and Poly-Norepinephrine Coatings: Comparison of Physico-Chemical and Biological Properties with Focus on the Application for Blood-Contacting Devices. *Bioact. Mater.* **2021**, *6* (1), 285–296.
<https://doi.org/10.1016/j.bioactmat.2020.06.024>.
- (19) Lim, J.; Zhang, S.; Wang, L.; Seo, D.; Dickwella Widanage, M. C.; Pipe, K. P.; Ramamoorthy, A.; Kim, J. Dihydroxy Indole (DHI)-Free Poly(Catecholamine) for

- Smooth Surface Coating with Amine Functionality. *ACS Appl. Polym. Mater.* **2023**, *5*, 6133–6142. <https://doi.org/10.1021/acsapm.3c00803>.
- (20) Petran, A.; Filip, C.; Bogdan, D.; Zimmerer, C.; Beck, S.; Radu, T.; Liebscher, J. Oxidative Polymerization of 3,4-Dihydroxybenzylamine—The Lower Homolog of Dopamine. *Langmuir* **2023**, *39*, 5610-5620. <https://doi.org/10.1021/acs.langmuir.3c00604>.
- (21) Hong, S.; Kim, J.; Na, Y. S.; Park, J.; Kim, S.; Singha, K.; Im, G.-I.; Han, D.-K.; Kim, W. J.; Lee, H. Poly(Norepinephrine): Ultrasoother Material-Independent Surface Chemistry and Nanodepot for Nitric Oxide. *Angew. Chemie Int. Ed.* **2013**, *52* (35), 9187–9191. <https://doi.org/10.1002/anie.201301646>.
- (22) Hong, S.; Wang, Y.; Park, S. Y.; Lee, H. Progressive Fuzzy Cation- Assembly of Biological Catecholamines. *Sci. Adv.* **2018**, *4* (9), 1–11. <https://doi.org/10.1126/sciadv.aat7457>.
- (23) Alfieri, M. L.; Panzella, L.; Oscurato, S. L.; Salvatore, M.; Avolio, R.; Errico, M. E.; Maddalena, P.; Napolitano, A.; d'Ischia, M. The Chemistry of Polydopamine Film Formation: The Amine-Quinone Interplay. *Biomimetics* **2018**, *3* (3), 26. <https://doi.org/10.3390/biomimetics3030026>.
- (24) Xue, P.; Sun, L.; Li, Q.; Zhang, L.; Guo, J.; Xu, Z.; Kang, Y. PEGylated Polydopamine-Coated Magnetic Nanoparticles for Combined Targeted Chemotherapy and Photothermal Ablation of Tumour Cells. *Colloids Surfaces B Biointerfaces* **2017**, *160*, 11–21. <https://doi.org/10.1016/j.colsurfb.2017.09.012>.
- (25) Miao, Z.-H.; Wang, H.; Yang, H.; Li, Z.-L.; Zhen, L.; Xu, C.-Y. Intrinsically Mn²⁺-Chelated Polydopamine Nanoparticles for Simultaneous Magnetic Resonance Imaging

- and Photothermal Ablation of Cancer Cells. *ACS Appl. Mater. Interfaces* **2015**, *7* (31), 16946–16952. <https://doi.org/10.1021/acsami.5b06265>.
- (26) Polymerization, M.; Krüger, J. M.; Bçrner, H. G. Accessing the Next Generation of Synthetic Mussel-Glue Polymers Via Mussel-Inspired Polymerization. *Angew. Chem. Int. Ed.*, **2021**, *60* (12), 6408–6413. <https://doi.org/10.1002/anie.202015833>.
- (27) Liebscher, J. Chemistry of Polydopamine – Scope, Variation, and Limitation. *European J. Org. Chem.* **2019**, 4976–4994. <https://doi.org/10.1002/ejoc.201900445>.
- (28) Mrówczyński, R.; Markiewicz, R.; Liebscher, J. Chemistry of Polydopamine Analogues. *Polym. Int.* **2016**, *65* (11), 1288–1299. <https://doi.org/10.1002/pi.5193>.
- (29) Chen, L.; Guo, Z. A Facile Method to Mussel-Inspired Superhydrophobic Thiol-Textiles @ Polydopamine for Oil / Water Separation. *Colloids Surfaces A* **2018**, *554*, 253–260. <https://doi.org/10.1016/j.colsurfa.2018.06.059>.
- (30) Yang, H. C.; Liao, K. J.; Huang, H.; Wu, Q. Y.; Wan, L. S.; Xu, Z. K. Mussel-Inspired Modification of a Polymer Membrane for Ultra-High Water Permeability and Oil-in-Water Emulsion Separation. *J. Mater. Chem. A* **2014**, *2* (26), 10225–10230. <https://doi.org/10.1039/c4ta00143e>.
- (31) Lv, Y.; Yang, H. C.; Liang, H. Q.; Wan, L. S.; Xu, Z. K. Nanofiltration Membranes via Co-Deposition of Polydopamine/Polyethylenimine Followed by Cross-Linking. *J. Memb. Sci.* **2015**, *476*, 50–58. <https://doi.org/10.1016/j.memsci.2014.11.024>.
- (32) Lv, Y.; Yang, S. J.; Du, Y.; Yang, H. C.; Xu, Z. K. Co-Deposition Kinetics of Polydopamine/Polyethyleneimine Coatings: Effects of Solution Composition and Substrate Surface. *Langmuir* **2018**, *34* (44), 13123–13131. <https://doi.org/10.1021/acs.langmuir.8b02454>.

- (33) Xu, L. Q.; Yang, W. J.; Neoh, K. G.; Kang, E. T.; Fu, G. D. Dopamine-Induced Reduction and Functionalization of Graphene Oxide Nanosheets. *Macromolecules* **2010**, *43* (20), 8336–8339. <https://doi.org/10.1021/ma101526k>.
- (34) Liu, X.; Gu, W.; Wang, K.; Zhang, W.; Xia, C.; Shi, S. Q.; Li, J. Thiol-Branched Graphene Oxide and Polydopamine-Induced Nanofibrillated Cellulose to Strengthen Protein-Based Nanocomposite Films. *Cellulose* **2019**, *26* (12), 7223–7236. <https://doi.org/10.1007/S10570-019-02609-4/tables/3>.
- (35) Lee, D.; Bae, H.; Ahn, J.; Kang, T.; Seo, D.; Soo, D. Acta Biomaterialia Catechol-Thiol-Based Dental Adhesive Inspired by Underwater Mussel Adhesion. *Acta Biomater.* **2020**, *103*, 92–101. <https://doi.org/10.1016/j.actbio.2019.12.002>.
- (36) Du, Y.; Yang, H. C.; Xu, X. L.; Wu, J.; Xu, Z. K. Polydopamine as a Catalyst for Thiol Coupling. *ChemCatChem* **2015**, *7* (23), 3822–3825. <https://doi.org/10.1002/cctc.201500643>.
- (37) Yang, H.; Lan, Y.; Zhu, W.; Li, W.; Xu, D.; Cui, J.; Shen, D.; Li, G. Polydopamine-Coated Nanofibrous Mats as a Versatile Platform for Producing Porous Functional Membranes. *J. Mater. Chem.* **2012**, *22* (33), 16994–17001. <https://doi.org/10.1039/c2jm33251e>.
- (38) Shahkaramipour, N.; Cheng,; Lai, K.; Venna, S. R.; Sun, H.; Cheng, C.; Lin, H. Membrane Surface Modification Using Thiol-Containing Zwitterionic Polymers via Bioadhesive Polydopamine. *Ind. Eng. Chem. Res.* **2018**, *57* (6), 2336–2345. <https://doi.org/10.1021/acs.iecr.7B05025>.
- (39) Lee, Y.; Chung, H. J.; Yeo, S.; Ahn, C. H.; Lee, H.; Messersmith, P. B.; Park, T. G. Thermo-Sensitive, Injectable, and Tissue Adhesive Sol–Gel Transition Hyaluronic

- Acid/Pluronic Composite Hydrogels Prepared from Bio-Inspired Catechol-Thiol Reaction. *Soft Matter* **2010**, *6* (5), 977–983. <https://doi.org/10.1039/b919944f>.
- (40) Yu, Q.-H.; Zhang, C.-M.; Jiang, Z.-W.; Qin, S.-Y.; Zhang, A.-Q.; Yu, Q.-H.; Zhang, C.-M.; Jiang, Z.-W.; Qin, S.-Y. A.; Zhang, -Q. Mussel-Inspired Adhesive Polydopamine-Functionalized Hyaluronic Acid Hydrogel with Potential Bacterial Inhibition. *Glob. Challenges* **2020**, *4* (2), 1900068. <https://doi.org/10.1002/gch2.201900068>.
- (41) Yegappan, R.; Selvaprithiviraj, V.; Mohandas, A.; Jayakumar, R. Nano Polydopamine Crosslinked Thiol-Functionalized Hyaluronic Acid Hydrogel for Angiogenic Drug Delivery. *Colloids Surfaces B Biointerfaces* **2019**, *177*, 41–49. <https://doi.org/10.1016/j.colfurfb.2019.01.035>.
- (42) Nair, D. P.; Podgórski, M.; Chatani, S.; Gong, T.; Xi, W.; Fenoli, C. R.; Bowman, C. N. The Thiol-Michael Addition Click Reaction: A Powerful and Widely Used Tool in Materials Chemistry. *Chem. Mater.* **2014**, *26* (1), 724–744. <https://doi.org/10.1021/cm402180t>.
- (43) Hoyle, C. E.; Bowman, C. N. Thiol–Ene Click Chemistry. *Angew. Chemie Int. Ed.* **2010**, *49* (9), 1540–1573. <https://doi.org/10.1002/anie.200903924>.
- (44) Zhang, Q.; Qu, D. H.; Feringa, B. L.; Tian, H. Disulfide-Mediated Reversible Polymerization toward Intrinsically Dynamic Smart Materials. *J. Am. Chem. Soc.* **2022**, *144* (5), 2022–2033. <https://doi.org/10.1021/jacs.1c10359>.
- (45) Zhou, J.; Penna, M.; Lin, Z.; Han, Y.; Lafleur, R. P. M.; Qu, Y.; Richardson, J. J.; Yarovsky, I.; Jokerst, J. V.; Caruso, F. Robust and Versatile Coatings Engineered via Simultaneous Covalent and Noncovalent Interactions Communications *Angew. Chemie Int. Ed.* **2021**, *92093*, 20225–20230. <https://doi.org/10.1002/anie.202106316>.

- (46) Ryu, J. H.; Messersmith, P. B.; Lee, H. Polydopamine Surface Chemistry: A Decade of Discovery. *ACS Appl. Mater. Interfaces* **2018**, *10* (9), 7523–7540.
<https://doi.org/10.1021/acsami.7b19865>.
- (47) Yu, M.; Hwang, J.; Deming, T. J. Role of 1-3,4-Dihydroxyphenylalanine in Mussel Adhesive Proteins. *J. Am. Chem. Soc.* **1999**, *121* (24), 5825–5826.
<https://doi.org/10.1021/ja990469y>.
- (48) Sedó, J.; Saiz-Poseu, J.; Busqué, F.; Ruiz-Molina, D.; Sedó, J.; Ruiz-Molina, D.; Saiz-Poseu Fundació Privada Ascamm, J.; Busqué, F. Catechol-Based Biomimetic Functional Materials. *Adv. Mater.* **2013**, *25* (5), 653–701. <https://doi.org/10.1002/adma.201202343>.
- (49) Della Vecchia, N. F.; Avolio, R.; Alfè, M.; Errico, M. E.; Napolitano, A.; D’Ischia, M. Building-Block Diversity in Polydopamine Underpins a Multifunctional Eumelanin-Type Platform Tunable Through a Quinone Control Point. *Adv. Funct. Mater.* **2013**, *23* (10), 1331–1340. <https://doi.org/10.1002/adfm.201202127>.
- (50) Liebscher, J.; Mrówczyński, R.; Scheidt, H. A.; Filip, C.; Haidade, N. D.; Turcu, R.; Bende, A.; Beck, S. Structure of Polydopamine: A Never-Ending Story? *Langmuir* **2013**, *29* (33), 10539–10548. <https://doi.org/10.1021/la4020288>.
- (51) Dreyer, D. R.; Miller, D. J.; Freeman, B. D.; Paul, D. R.; Bielawski, C. W. Elucidating the Structure of Poly(Dopamine). *Langmuir* **2012**, *28* (15), 6428–6435.
<https://doi.org/10.1021/la204831b>.
- (52) Shigeru Oae; Joyce Doi. *Organic Sulfur Chemistry: Structure and Mechanism*; CRC Press, 1991.

- (53) Goethals, E. J.; Sillis, C. Oxidation of Dithiols to Polydisulfides by Means of Dimethylsulfoxide. *Die Makromol. Chemie* **1968**, *119* (1), 249–251.
<https://doi.org/10.1002/macp.1968.021190129>.
- (54) Meng, Y. Z.; Liang, Z. A.; Lu, Y. X.; Hay, A. S. Aromatic Disulfide Polymers Back to Macrocyclic Disulfide Oligomers via Cyclo-Depolymerization Reaction. *Polyme* **2005**, *46* (24), 11117–11124. <https://doi.org/10.1016/j.polymer.2005.08.067>.
- (55) Al, M. L.; Cariola, A.; Panzella, L.; Napolitano, A.; Ischia, M.; Valgimigli, L.; Crescenzi, O. Disentangling the Puzzling Regiochemistry of Thiol Addition to o - Quinones. **2022**.
<https://doi.org/10.1021/acs.joc.1c02911>.
- (56) Mancebo-aracil, J.; Casagualda, C.; Moreno-villa, Ø.; Nador, F.; Busqu, F. Ø. Ø.; Ø, R. A.; Esplandiu, J. Ø.; Ruiz-molina, D.; Sed, J. Bioinspired Functional Catechol Derivatives through Simple Thiol Conjugate Addition. **2019**, 12367–12379.
<https://doi.org/10.1002/chem.201901914>.
- (57) Winterbourn, C. C. Radical Scavenging by Thiols and the Fate of Thiyl Radicals. *Oxidative Stress Redox Regul.* **2013**, *9789400757875*, 43–58. https://doi.org/10.1007/978-94-007-5787-5_2.
- (58) Beaujuge, P. M.; Reynolds, J. R. Color Control in π -Conjugated Organic Polymers for Use in Electrochromic Devices. *Chem. Rev.* **2010**, *110* (1), 268–320.
<https://doi.org/10.1021/cr900129a>.
- (59) Mason, H. S.; Wright, C. I. The Chemistry of Melanin. *J. Biol. Chem.* **1949**, *180* (1), 235–247. [https://doi.org/10.1016/s0021-9258\(18\)56739-9](https://doi.org/10.1016/s0021-9258(18)56739-9).
- (60) Prota, G. Recent Advances in the Chemistry of Melanogenesis in Mammals. *J. Invest. Dermatol.* **1980**, *75* (1), 122–127. <https://doi.org/10.1111/1523-1747.ep12521344>.

- (61) Belcarz, A.; Michalicha, A.; Roguska, A.; Przekora, A.; Budzy, B. Poly (Levodopa) - Modified β -Glucan as a Candidate for Wound Dressings. *Carbohydrate Polymers* **2021**, 272 (15), 118485. <https://doi.org/10.1016/j.carbpol.2021.118485>.
- (62) Yang, W.; Liu, C.; Chen, Y. Stability of Polydopamine Coatings on Gold Substrates Inspected by Surface Plasmon Resonance Imaging. *Langmuir* **2018**, 34 (12), 3565–3571. <https://doi.org/10.1021/acs.langmuir.7b03143>.
- (63) Park, H. K.; Park, J. H.; Lee, H.; Hong, S. Material-Selective Polydopamine Coating in Dimethyl Sulfoxide. *ACS Appl. Mater. Interfaces* **2020**, 12 (43), 49146–49154. <https://doi.org/10.1021/acsami.0c11440>.

Chapter 4 Dihydroxy Indole-free Poly(catecholamine) for Smooth Surface Coating with Amine Functionality

Contents in this chapter was published in *ACS Appl. Polym. Mater.* **2023**, 5, 8, 6133–6142.

Abstract

The catecholamine of polydopamine (PDA) is associated with adhesion and self-polymerization. However, 5,6-dihydroxyindole (DHI) of polydopamine inevitably consumes primary amine groups. Furthermore, DHI leads to particle aggregation by causing $\pi - \pi$ interaction and cation- π interaction. Here, we used 3,4-dihydroxybenzylamine hydrobromide to achieve DHI-free poly(catecholamine) (PCA) coating by self-polymerization. The DHI-free nature renders a smooth and uniform surface. Moreover, the suppressed indole ring formation preserves the primary amine groups after the DHI-free PCA coating, suggesting an alternative surface amine functionalization strategy to the conventional silane-based. Surface amine functionality of DHI-free poly(catecholamine) is confirmed by fluorescence image of the tethered NHS ester-functionalized polydiacetylene liposome by NHS ester-amine coupling reaction. Furthermore, DHI-free PCA was used to modify the surface properties of graphene to enhance the thermal conductivity of graphene-polymer composites. Graphene nanoplatelets (GnP) coated with DHI-free PCA formed adequate intermolecular bonding with poly(acrylic acid) (PAA) matrix, which reduces interfacial thermal resistance. The resulting graphene-polymer composites achieved a sharp increase in thermal conductivity, reaching 2.9W/mK at 15wt% of graphene content, which is 87% larger than the thermal conductivity of control composites with untreated graphene.

4.1 Introduction

Dopamine, a catechol-containing monomer, was demonstrated to undergo self-polymerization to form substrate-independent adhesive coatings by the Messersmith group in 2007.

¹ Compared to other coating methods based on self-assembled monolayers (SAMs), functionalized silanes, Langmuir Blodgett, layer-by-layer polyelectrolytes deposition, and engineered peptides, polydopamine is neither limited by substrate types nor does require time-consuming multi-step processes or costly equipment to generate effective coating. Accordingly, the versatility of dopamine chemistry has been applied for many purposes, including surface functionalization,^{2,3} co-deposition with functional chemicals⁴⁻⁶, and post-polymerization modification of polymers for adhesive properties.^{7,8} Additionally, various modified polymerization conditions, such as oxidant variation,⁹ pH control,¹⁰ and incorporating UV photopatterning capability,¹¹ have been extensively explored.

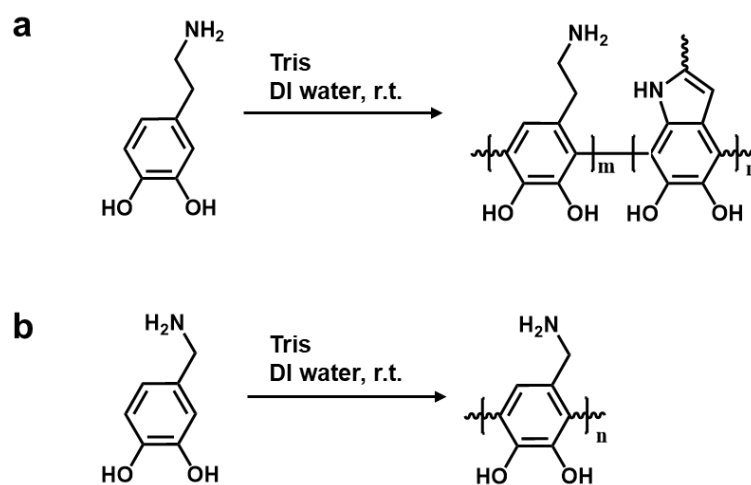
To understand the adhesion mechanism of PDA, we need to begin with mussel binding protein which motivated the use of PDA. Previous studies have shown that the unique adhesion property of mussel-binding proteins is derived from 3,4-dihydroxy-L-phenylalanine (DOPA, non-proteinogenic amino acid) and lysine amino acids that are uniquely rich in the plaque of mussels.¹² By forming strong covalent and noncovalent interactions with substrates, DOPA and lysine ensure unique surface-independent adhesion.¹³ Since the pioneering work by the Messersmith group, extensive studies have been devoted to understanding the origin of PDA adhesion behavior. First, phenolic compounds are investigated due to their universal adhesion by forming metal-phenolic network (MPN) assembly,¹⁴ Layer by Layer (LbL) assembly¹⁵, and PDA coatings. The catechol group of dopamine and its oxidized quinone were elucidated as the main chemical attributes owing to their capability of hydrogen bonding,^{16,17} metal chelating,¹⁸ as well as aryl-aryl coupling.^{13,19}

Recent studies suggested that the presence of the amine group is crucial to exhibit surface-independent coating properties via ionic bonding to negatively charged surfaces^{20,21} and to crosslink with quinones through Schiff-base reaction or Michael addition. Thus, it is postulated that both catechol and amine would synergistically aid the adhesion of PDA.

Although dopamine monomer consists of catechol and ethylamine, catecholamine is not the only building block of PDA. Dopamine monomer possesses several reactive sites (amine, benzene, or hydroxy), which are electrophiles or nucleophiles, respectively, and thus are prone to create various building blocks such as catecholamine, 5,6-dihydroxy indole (DHI), and dopamine quinone during self-polymerization.²² Among these components, catecholamine plays a crucial role in adhesion²³, whereas DHI interferes with adherence.^{24,25} Although DHI provides a cohesive behavior by promoting intermolecular π - π interaction, cation- π interactions through abundant π -electrons as well as covalent crosslinking at its 2-position, an abundance of DHIs decreases the adhesion behavior of PDA.²⁶ Therefore, we hypothesized that highly functionalized surface modification could be achieved by eliminating DHI units.

In this study, we utilized a PDA derivative, 3,4-dihydroxybenzylamine, containing aminomethyl group instead of the aminoethyl group in dopamine to prevent cyclization from forming DHI (Scheme 4-1). Recently, Liebscher group reported oxidative polymerization of 3,4-dihydroxybenzylamine in Tris buffer solution and confirmed the absence of DHI.²⁷ The conventional oxidative self-polymerization prepared the corresponding DHI-free poly(catecholamine) (PCA) and the resulting polymer was capable of surface-independent coating while showing more uniform morphology than PDA owing to the suppressed aggregation formation on the surface in the absence of DHI. We applied 3,4-dihydroxybenzylamine to graphene surface modification to achieve an interactive interface in the polymer-graphene

composites. The surface-functionalized graphene by DHI-free PCA exhibits, on average, 59% higher (maximum 87% higher) thermal conductivity than the untreated graphene-polymer composites having 5 – 10wt% graphene. We also investigated the possible application of 3,4-dihydroxybenzylamine as an amine functionalization agent to take advantage of its material-independent coating capability by conducting fluorescent dye attachment on the resulting DHI-free PCA surface.



Scheme 4-1 Self-polymerization of (a) dopamine and (b) 3,4-dihydroxybenzylamine in aqueous solution.

4.2 Result and Discussion

4.2.1 Design of DHI-free PCA

In conventional PDA synthesis, DHI is inevitably formed by oxidative ring closure of dopamine via the dopaquinone form. Although DHI enhances robust coating capability by facilitating various secondary interactions (π - π staking, cation- π interaction, as well as covalent crosslinking), there are some noticeable downsides of DHI. First, DHI limits the length of a polymer chain. Even though earlier models suggested that PDA should have a large molecular

weight with covalently linked catecholamine and DHI, recent studies predicted that a large amount of DHI would limit the degree of polymerization. Chen et al. employed computational methods to explore possible DHI oligomer formation. They concluded that DHI polymers are likely to have a low molecular weight due to the stable tetramer formation.²⁸ Secondly, DHI is less likely to have good adhesion. Della Vecchia et al. successfully synthesized a series of PDA with different building block ratios of uncyclized catecholamine/quinones to cyclized DHI units²⁹ and compared the adhesion of those three components on PET and PE substrates. They concluded that catecholamine has a superior coating capability than DHI. Lastly, the surface morphology of PDA depends on the presence of DHI. Due to the abundant π -electrons, DHI has a strong cohesion ability by π - π stacking and cation- π interaction³⁰ besides covalent crosslinking, thereby accelerating particle formation, which gives rise to a rough surface.

Considering the effects mentioned above of DHI, we wanted to explore a simple DHI-free PCA with surface-independent coating capability without forming DHI. A commercially available 3,4-dihydroxybenzylamine is an excellent candidate to exhibit self-polymerization and surface-independent coating without DHI formation in a conventional alkaline aqueous solution. UV-vis spectroscopy was used to monitor the polymerization progress.^{11,31} Figure 4-1a, b show time-dependent absorption spectra of PDA and DHI-free PCA, respectively. The observed increased absorption confirms the formation of these polymers. PDA has a broad absorption owing to its various building blocks having varying conjugation lengths and ensuring different absorptions (Figure 4-1a).

In contrast, DHI-free PCA exhibits distinct absorption at around 350 nm (Figure 4-1b), mainly attributed to the quinone units and a narrower absorption range. Hence, black color (PDA) and brown color (DHI-free PCA) were observed, respectively, after the polymerization. X-ray

Photoelectron Spectroscopy (XPS) was employed to analyze the potential amine based linkages. (Figure 4-1c). Due to the coexistence of catecholamine and DHI, the PDA coating exhibits both primary amines ($-\text{NH}_2$, 399.4 eV) and secondary aromatic amines ($-\text{NH}$ -401.1 eV). Although 3,4-dihydroxybenzylamine is not able to close the ring, the primary amine of 3,4-dihydroxybenzylamine can undergo Michael addition with the electrophilic carbon of quinone or participate in a Schiff-base reaction with the oxygen of quinone. Additionally, Tris can be incorporated into the catechol units by nucleophilic attack.^{32,33} However, the high-resolution N 1s XPS spectra of DHI-free PCA exhibited predominant primary amine ($-\text{NH}_2$ 399.4 eV), suggesting the absence of DHI and minimal formation of secondary amines through side reactions.

Investigation of the polymeric nature of PDA has been hindered by its poor solubility in both aqueous and organic solvents. Previous studies have used mass spectrometry to identify soluble oligomers in the early stages of polymerization.^{29,34} However, conventional mass spectrometry can be used for oligomers only. Interestingly, Messersmith group analyzed the polymeric nature of polydopamine by applying single-molecule force spectroscopy (SMFS).³⁵ In our study, we employed the time-of-flight (ToF) method to elucidate the structural models of 3,4-dihydroxybenzylamine under mild basic conditions. As shown in Figure 4-1d, oligomeric components up to the pentamer level were detected at m/z values of 413.2, 551.6, and 683.4. The suggested corresponding structures are available in the Supporting Information (Scheme S4-1). While ToF detects only oligomers, it is possible that longer oligomers or even polymers may also exist.

The polymerization process of DHI-free PCA was monitored using ^1H NMR in bicarbonate buffer (NaHCO_3) with D_2O at a pH of 8.5. As depicted in Figure 4-1e, the aromatic hydrogen shifted to the downfield due to increased electron density, and the monomer was

completely consumed after 7 hours. Additionally, the overall intensity gradually decreased due to the precipitation of oligomers as their molecular weight increased. As shown in Figure 4-2 we further conducted ^{13}C CP-MAS solid-state NMR of DHI-free PCA. The NMR spectra exhibit peaks in the aliphatic ($\sim 15\text{-}65$ ppm) and aromatic (~ 100 to 155 ppm) regions. Since MAS averages the anisotropic chemical shift interaction and proton RF decoupling removes the dipolar couplings between ^{13}C nuclei and protons, the observed broad peaks could be attributed to the presence of a mixture of species due to the heterogeneous nature of the polymerization chemical reaction; this is also confirmed by the multiple poorly resolved peaks at ~ 110 to ~ 130 ppm. According to the chemical reaction shown in Scheme 4-1b, the ^{13}C peaks at ~ 58 ppm, ~ 45 ppm, and ~ 19 ppm in the aliphatic region should be from the CH groups derived from imines, the CH_2 moiety of 3,4-dihydroxybenzylamine, and the CH_3 moiety at the terminal of the polymer. In an attempt to further enhance the spectral resolution, a short contact time (250us) was used to reduce any ^{13}C peaks associated with weaker dipolar couplings with protons. The resultant ^{13}C CP-MAS spectrum (the bottom trace) showed a significant reduction in the intensities of peaks at ~ 19 ppm and ~ 145 ppm. Overall, ^{13}C CP-MAS solid-state NMR spectra of DHI-free PCA supports the existence of DHI-free PCA subunits than other byproducts. In the ToF study, we observed that the majority of oligomers existed as a trimer, while tetramer and pentamer are relatively less abundant due to the increased hydrophobicity. The ^1H NMR spectra of DHI-free PCA after 7 hours match well with aromatic hydrogens ($\delta = 6.5\text{-}6.6$ ppm) of the trimer (Figure 4-1f). Furthermore, appearance of new peaks of methyl ($\delta = 2.5\text{-}4.3$ ppm) indicated the aliphatic hydrogens from trimer, tetramer and pentamer (Full spectra are available in the Supporting information Figure S4-3).

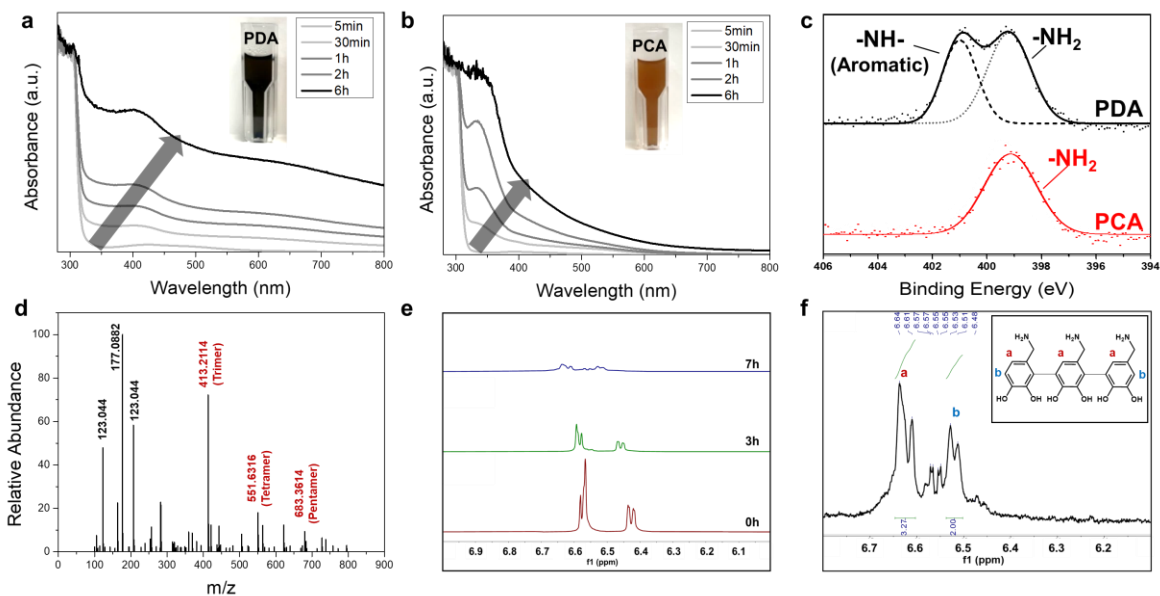


Figure 4-1 Structure analysis of DHI-free PCA. UV-vis spectra of (a) PDA and (b) DHI-free PCA in aqueous solution. (c) High-resolution XPS spectra of N 1s in the PDA and DHI-free PCA coatings. (d) Spectrum of ToF characterizations of DHI-free PCA film, (e) ^1H NMR spectra monitoring the reaction of DHI-free PCA in 10 mM $\text{NaHCO}_3/\text{D}_2\text{O}$ with time. (f) The aromatic region of the ^1H NMR spectra of DHI-free PCA after 7 hrs in $\text{NaHCO}_3/\text{D}_2\text{O}$

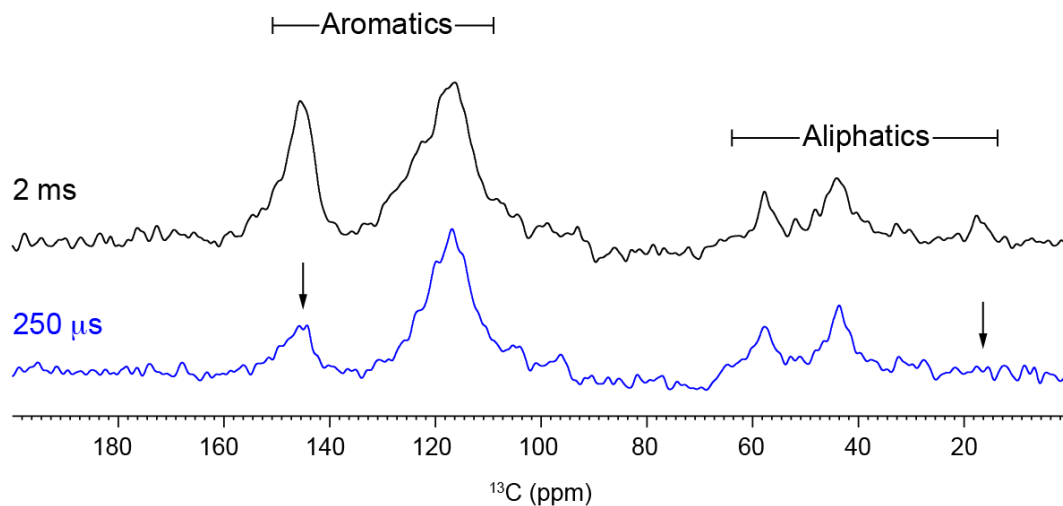


Figure 4-2 Carbon- ^{13}C CP-MAS NMR spectra of a powder sample of PDA polymer obtained under 15 kHz MAS. A ramp-CP pulse sequence was used with 2 ms (top trace) and 250 μs (bottom trace) contact times. The arrows indicate peaks from carbon nuclei associated with lesser ^1H - ^{13}C dipolar couplings.

4.2.2 Surface Independent Coating of DHI-free PCA and Morphology

As discussed above, the surface-independent coating capability stems from the combination of catechol and amine. Recently, Huamin et al. synthesized a series of dopamine analogs containing catechol and amine units as a building block. They revealed that the universal coating capability of dopamine could be reproduced as far as the dopamine analogs have both catechol and amine regardless of the aliphatic carbon length in the dopamine analogs.²⁵ Thus, we anticipated that 3,4-dihydroxybenzylamine would show good coating capability on various substrates. To confirm the coating capability of poly(3,4-dihydroxybenzylamine) in an alkaline solution, we dip-coated multiple substrates such as polymer, metal, and ceramic surfaces in the alkaline solution (Figure 4-3a, b). Both dopamine hydrochloride and 3,4-dihydroxybenzylamine hydrobromide exhibit good coating properties on all substrates, including adhesion-resistant materials such as poly(tetrafluoroethylene) (PTFE). Dark brown color of PDA represents the presence of DHI. In contrast, the orange color of DHI-free PCA indicates the presence of a catecholamine unit only.

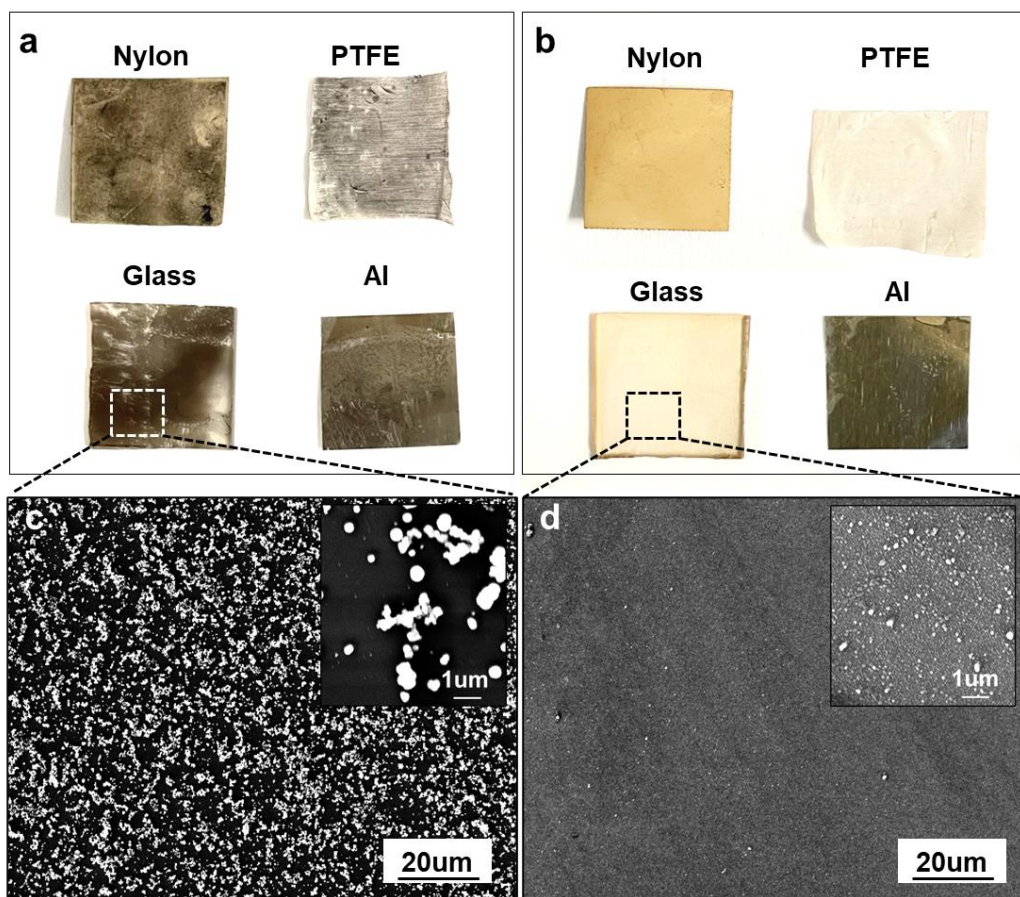
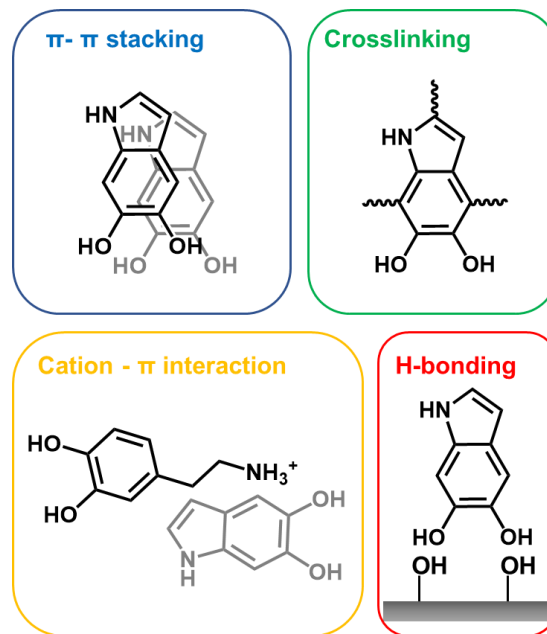


Figure 4- 3 Surface independent coating of polydopamine and DHI-free PCA. Polydopamine coating on Nylon, PTFE, Glass, and Aluminum (a) and the corresponding SEM image on the glass substrate (c). DHI-free PCA coating on various substrates (b) and its corresponding SEM image on the glass substrate (d).

The most visible difference between PDA and DHI-free PCA we observed is that uneven PDA coating was formed on each substrate while DHI-free PCA coating was relatively smoother and more uniform (Figure 4-3 c, d). As we discussed, during the deposition of PDA on a substrate, DHI enables diverse intermolecular interactions, inducing aggregation and ensuring a rough surface morphology (Scheme 4-2). Therefore, a smoother and more homogeneous surface is

anticipated when PCA is free of DHI. The scanning electron microscope (SEM) image (Figure 4-3c) of a PDA film clearly shows large particles ($d = 200\text{--}700\text{nm}$), while the SEM image of DHI-free PCA exhibits an even surface with small particles ($d = <50\text{nm}$) (Figure 4-3d).



Scheme 4-2 Diverse interactions of DHI.

4.2.3 Primary Amine Functionalization via DHI-free PCA

We further investigated a potential application of the universal coating capability of DHI-free PCA having abundant primary amine groups as a surface modifying strategy to endow surface amine-functionalization. Primary amine functionalization is widely used in various fields owing to the reactivity of amine with diverse groups (e.g., carboxylic acids, alkyl halides, sulfonyl chloride, etc.), its ability to form hydrogen bonding and electrostatic interactions,³⁶ and the abundance of available amine group in biological tissues.³⁷⁻³⁹ Furthermore, primary amine coating on porous materials efficiently captures carbon dioxide (CO_2) by forming carbamate through reversible reactions with CO_2 .⁴⁰ Aminoalkyl-containing silanes are the most widely used chemicals to achieve an amine-rich surface due to their simplicity and affordability.^{41,42} The process generates amine functionalized monolayer by covalent silanization. However, silanization requires hydroxyl groups on the substrate for surface modification, usually formed by hydrolysis of alkoxy groups, thereby limiting the applicable substrates to glass or silicon wafers.

Polyethyleneimine (PEI) coating is another method to give an amine rich surface. Abundant primary and secondary amine provide hydrophilic property as well as superior CO₂ capturing behavior.⁴³ Nevertheless, PEI is a viscous liquid at room temperature and is soluble in water, that restricts its application.

Therefore, DHI-free PCA's material-independent amine coating capability has immense potential as a universal surface amine functionalization agent. Hence, we attached a fluorescence dye on the DHI-free PCA-coated glass to verify the primary amine functionality using N-hydroxysuccinimide (NHS) esters reaction. Because of the fluorescence quenching effect of PDA by Förster resonance energy transfer (FRET)⁴⁴ and photoinduced electron transfer (PET),⁴⁵ we carefully chose the polydiacetylene liposome as a fluorescence dye because the supramolecular structure of the polydiacetylene liposome effectively prevents fluorescence quenching. As shown in Figure 4-4a, amine groups of DHI-free PCA react with NHS-ester-modified polydiacetylene liposome exhibiting red fluorescence (Figure 4-4c), while bare glass did not show any fluorescence (Figure 4-4a). Moreover, carboxylic acid functionalized polydiacetylene liposome was added as a negative control to check the physisorption of the liposome. Although carboxylic acid of the polydiacetylene liposome could form hydrogen bonding with amine groups, only a tiny amount of the liposomes were observed after rinsing the surface with deionized water (Figure 4-4d), indicating that the non-specific binding of a liposome is negligible. Consequently, DHI-free PCA's simple and surface-independent amine functionalization method was verified.

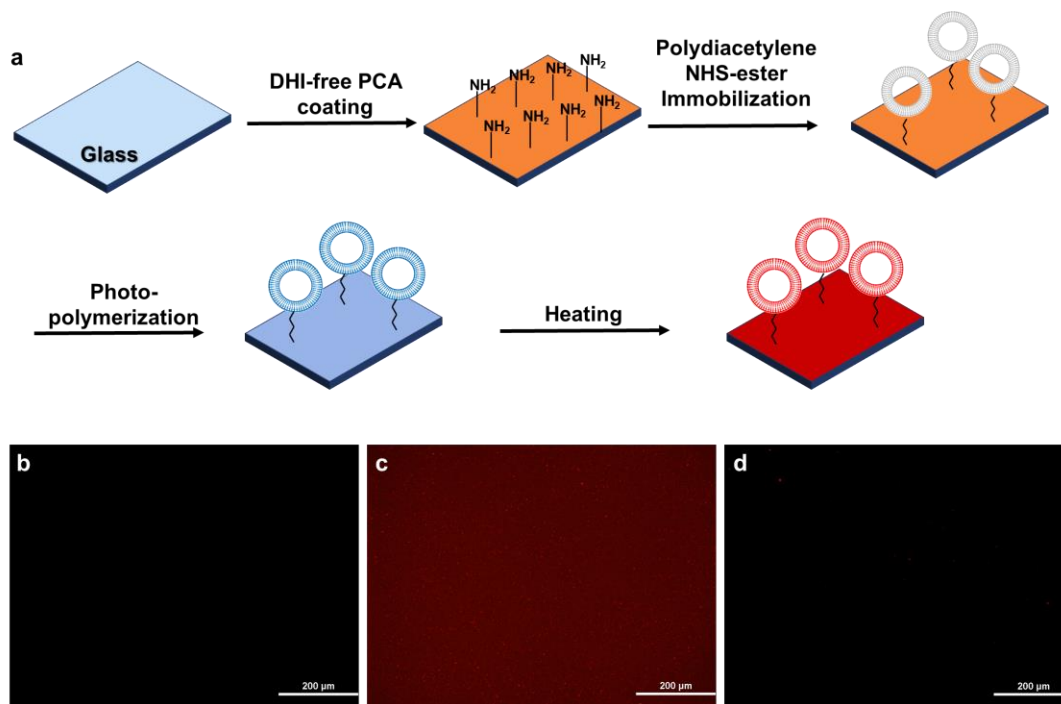


Figure 4-4 Primary amine functionalization by using DHI-free PCA. (a) Schematic illustration of polydiacetylene dye tethering procedure on DHI-free PCA. Fluorescence microscopy images on (b) NHS-ester polydiacetylene@bare glass, (c) NHS-ester-polydiacetylene@DHI-free PCA coated glass, and (d) COOH-polydiacetylene@DHI-free PCA coated glass.

4.2.4 DHI-free PCA-coated Graphene for Polymer Composites with Enhanced Thermal

Conductivity

We investigated DHI-free PCA's application to develop graphene-polymer composites with enhanced thermal conductivity. We anticipated an amine functionalization of the graphene to alleviate thermal resistance at the interface with PAA. Owing to the ultra-high thermal conductivity (1500 to 5800 W/mK),⁴⁶⁻⁴⁹ graphene has been used as a thermal filler in polymer composites.⁵⁰⁻⁵³ However, when graphene is mixed with a polymer, the thermal conductivity of the resulting composite does not increase significantly because the graphene-polymer composite does not follow the rule-of-mixture due to the interfacial thermal resistance (or Kapitza resistance⁵⁴) which means a large portion of thermal energy is scattered at the dissimilar interface. Therefore,

reducing the thermal barrier at the interface by inducing strong interaction is crucial to achieving high thermal conductivity of composites.⁵⁵⁻⁵⁷ PDA-assisted graphene modification has been elucidated due to its strong π - π bonding capability with graphene.^{58,59} Unlike the covalent functionalization of graphene via graphene oxide, PDA coating does not sacrifice the intrinsic thermal conductivity of graphene by preserving the homogeneous sp^2 carbons of pristine graphene. Two times higher thermal conductivity has been reported from the poly(vinyl alcohol) (PVA) composite having PDA-passivated graphene compared to pure PVA. The enhanced thermal conductivity was attributed to the H-bonding among NH_2 and OH groups in PDA and OH of PVA. We hypothesized that DHI-free PCA would facilitate efficient heat transfer at the graphene-polymer interface by providing smooth contact and strong secondary binding via hydrogen bonding and electrostatic interaction. To validate our hypothesis, we prepared a series of composites using PAA, which has carboxylic acid ($-COOH$) side groups that can be ionized to a carboxylate ($-COO^-$) at a pH above its pK_a value. Considering the basicity of primary amine, we anticipate that strong coulombic interactions would be formed between carboxylate($-COO^-$) and ammoniumyl ($-NH_3^+$), which would closely bind the polymer and graphene together. For this purpose, graphene was coated with PDA and DHI-free PCA by the conventional self-polymerization in an alkaline aqueous solution with vigorous stirring. The surface modification of graphene was then confirmed by SEM/EDX and Thermogravimetric Analysis (TGA). SEM/EDX results (Figure 4-5e-h) show widespread nitrogen atoms, which represent the presence of PDA and DHI-free PCA on the graphene surface. Although both PDA and DHI-free PCA successfully covered graphene, PDA aggregates on the surface were observed due to the DHI-induced aggregation that prevents close contact with a matrix polymer. (Figure 4-5e). On the other hand, uniform coating of DHI-free PCA (Figure 4-5g) enables direct contact with a matrix polymer that

would facilitate better heat transfer at the interface. TGA results supported that PDA formed a relatively thicker coating (8 wt%) due to surface aggregation compared to DHI-free PCA, which formed 5wt% coating on the graphene surface (Figure 4-5i).

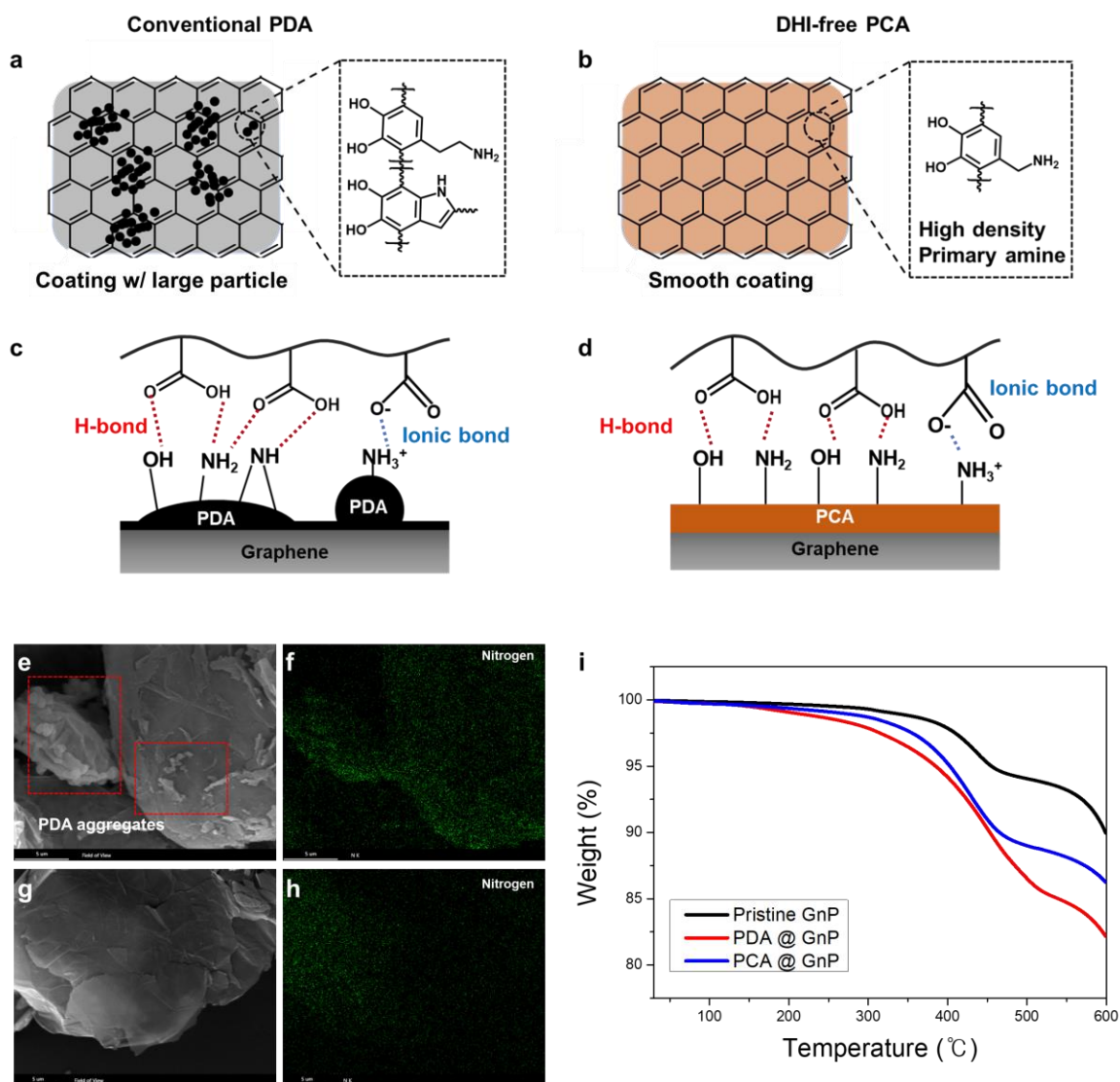


Figure 4-5 DHI-free PCA coating on graphene. Schematic illustration of (a) conventional PDA and (b) DHI-free PCA coating on graphene and (c, d) Corresponding intermolecular interaction (H-bonding, electrostatic interaction) between functionalized graphene and PAA. DHI-free PCA coating on graphene. SEM images of (e) PDA and (g) DHI-free PCA-coated graphene and their corresponding EDX images (f, h) confirming the presence of nitrogen from the surface. (i) Thermogravimetric Analysis (TGA) on PDA and DHI-free PCA-coated graphene.

PAA-graphene composites with different graphene contents were fabricated by solution processing and subsequent hot-pressing, which are described in the experimental section. Then, a differential 3- ω method^{60,61} was applied to measure the thermal conductivity after gold electrode deposition. The measurement details are described in the experimental section. Table 4-1 and Figure 4-6 summarize the measured thermal conductivities of the PAA composites with pristine GnP, PDA-coated GnP, and DHI-free PCA-coated GnP, having various graphene contents. PDA/GnP shows a trend of increased k (avg. 39% \uparrow), which we attribute to efficient interface heat transport by hydrogen bonding and electrostatic interaction between PDA and PAA (Figure 4-5 c,d). Further increase in k was observed in DHI-free PCA/GnP (avg. 59% \uparrow), and the maximally increased k was found at 15wt% PCA coating (87% \uparrow). The enhanced k from PCA/GnP is attributed to the abundant primary amine, which forms strong electrostatic interaction with carboxylate (-COO-) in an aqueous condition to reduce the interfacial thermal resistance.

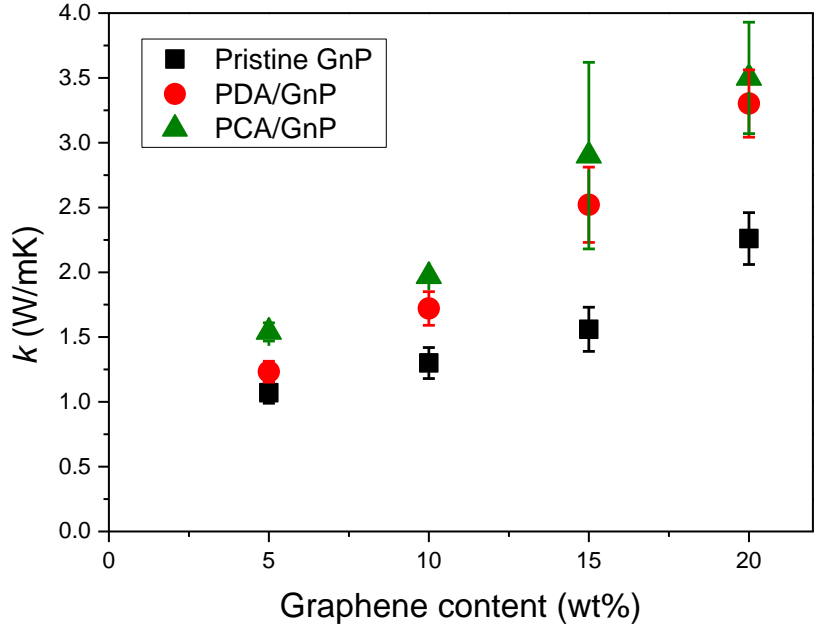


Figure 4-6 Thermal conductivities of GnP-poly(acrylic acid) composites as a function of graphene content.

Table 4-1 Thermal conductivity of graphene nanoplatelet-poly(acrylic acid) composites

GnP Content In PAA [wt%]	Thermal Conductivity [W/mK]		
	Pristine GnP	PDA/GnP	PCA/GnP
5	1.069 (0.08)	1.233 (0.08)	1.539 (0.07)
10	1.298 (0.12)	1.722 (0.13)	1.972 (0.02)
15	1.556 (0.17)	2.522 (0.29)	2.903 (0.72)
20	2.261 (0.20)	3.321 (0.26)	3.502 (0.43)

4.3 Conclusion

We explored a DHI-free universal coating strategy using 3,4-dihydroxybenzylamine hydrobromide in a mild basic aqueous solution. 3,4-dihydroxybenzylamine hydrobromide has a one-carbon length shorter linkage between catechol and amine than conventional dopamine, thereby cannot form the indole ring. Since the DHI formation is the origin of the polydopamine aggregation, preventing the DHI formation of DHI-free PCA renders not only smooth and uniform surface morphology but also primary amine-rich surface coating. The UV-vis spectroscopy, SEM/EDX, NMR, and XPS results confirmed the absence of DHI and the presence of a primary amine. We exploited this primary amine functionality to modify the surface of graphene nanoplates to maintain graphene's high thermal conductivity and lower the thermal barrier at the interface between the PCA-coated graphene and PAA matrix by inducing strong intermolecular interactions. Compared to PDA, the PCA-coated graphene exhibited a smoother surface, efficient interfacial hydrogen bonding, and electrostatic interactions, resulting in a 15% increase in thermal conductivity of the graphene composite. These results demonstrate the potential of DHI-free PCA as an unconditional primary amine functionalization method.

4.4 Publication Information

Jiwon Lim, Shuo Zhang, Luyang Wang, Deokwon Seo, Malitha C. Dickwella Widanage, Kevin P. Pipe, Ayyalusamy Ramamoorthy, Jinsang Kim* “Dihydroxy indole (DHI)-free poly(catecholamine) for smooth surface coating with amine functionality”

Contents in this chapter was published in *ACS Appl. Polym. Mater.* **2023**, 5, 8, 6133–6142.

4.5 Experimental Section

4.5.1 Materials

Dopamine hydrochloride, 3,4-dihydroxybenzylamine hydrobromide, tris, and poly(acrylic acid) (PAA) solution (Mw~100,000, 35wt% in H₂O) were purchased from Sigma-Aldrich. Graphene nanoplates (GnPs) with the size of 25 μm (xGnP-M-25) were produced by XG Science. These chemicals were used without further purification.

4.5.2 Method

4.5.2.1 Preparation of PDA and DHI-free PCA Coatings on Various Substrates

First, a dopamine hydrochloride solution (2 mg/mL) dissolved in tris buffer (pH 8.5) was prepared (DA/Tris solution). Then various substrates (1x1 cm²) were placed in a petri dish containing 5 mL of the DA/Tris solution. After 24h, the PDA -coated substrates were rinsed with DI water and methanol and then dried by blowing air. DHI-free PCA coatings were prepared in the same way.

4.5.2.2 Polydiacetylene Liposome Assembly

The polydiacetylene liposomes were assembled by the following injection method.^{62,63} 10,12-pentacosadiynoic acid PCDA(3.75 g) were in the 300 μl of tetrahydrofuran and the solution was injected to 20 ml of 5mM HEPES buffer at pH 8. The liposome solution was probesonicated at 120 W for 20 min and was filtrated through a 0.8 μm cellulose acetate syringe filter. The filtrate was stored at 5 °C before use.

4.5.2.3 10,12-pentacosadiynoic Acid (PCDA)-NHS Liposome Assembly

PCDA (75 mg) and PCDA-NHS (25 mg) were co-dissolved in the 1 ml of dichloromethane and added to a 20 ml glass vial. The mixture was dried under vacuum and obtained thin white film from the bottom of the vial. The film was hydrated with 20 ml of 5mM HEPES buffer at pH 8, and probe-sonicated at 120W for 1 hr. The solution was filtrated through a 0.8 μm cellulose acetate syringe filter and stored at 5 $^{\circ}\text{C}$ before use.

4.5.2.4 Preparation of Polydopamine Derivatives Coated Graphene Nanoplatelets

The reaction was carried out in a 500 ml flask equipped with a magnetic stirrer in room temperature. Tris (0.3 g) was added to 250 ml of deionized water. GnPs (1 g) was dispersed in the Tris buffer solution in an ultrasonic bath for 30 min. Then, dopamine (0.25 g) was added under gentle magnetic stirring. Finally, the mixture was continuously stirred for 24 h. Subsequently, the suspension was filtered through a 0.22 μm polytetrafluoroethylene membranes and washed several times with deionized water and ethanol until the filtrate became colorless and neutral. Finally, the resulting product was dried in a vacuum at 40 $^{\circ}\text{C}$ for 24 h to a constant weight. DHI-free PCA-coated GnPs were prepared in the same way.

4.5.2.5 Preparation of Composites Film

GnPs coated with the PDA derivatives (17mg, 36mg, 58mg, and 83 mg, respectively) were dispersed in a 20 ml vial having 10 ml of DI water under ultrasonic condition for 30 min. Then an aqueous PAA solution (0.86g in 2.16 ml of water) was added and vigorously stirred for 24h at room temperature. After pouring the mixture into a Teflon sheet, the mixture was dried in a vacuum oven at 60 $^{\circ}\text{C}$ for overnight. The resulting composite chunks were placed between two Teflon

sheets with a $300 \pm \mu\text{m}$ spacer, followed by hot-pressing at 150°C for 1 min to obtain a composite film having a smooth surface and a uniform thickness ($300 \pm 20 \mu\text{m}$).

4.5.2.6 Characterization Methods

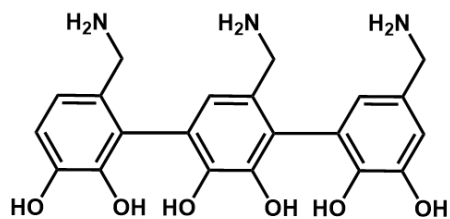
UV-vis absorbance spectra were obtained on Varian Cary50 UV/Vis spectrophotometer. XPS analysis were performed using a Kratos Axis Ultra XPS. NMR: ^1H spectra were collected at 500 MHz on a Varian Vnmrs 500. ^{13}C cross-polarization Magic angle spinning (CP-MAS) solid-state NMR experiments were conducted on a 400 MHz (9.4 T) Bruker Avance NMR spectrometer. Positive ion mode of Time-of-Flight (ToF) was performed using Agilent 6230 TOF. Scanning Electron Microscopy with Energy Dispersive X-ray spectroscopy (SEM/EDX) results were prepared by TESCAN MIRA-3 FEG. TGA curves of graphene nanoplatelets were measured under nitrogen gas by a TA Instruments Discovery Series TGA.

4.5.2.7 Thermal Conductivity Measurement

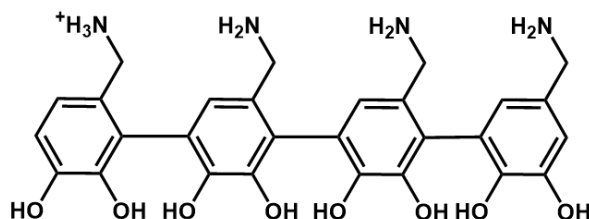
Thin metal lines were patterned by electron-beam deposition (40 nm thick Ti/400 nm thick Au) using shadow-masking ($50 \mu\text{m}$) on both sample and reference. κ in the composite films was measured using the conventional differential 3ω method in ambient conditions.

4.6 Supporting Information

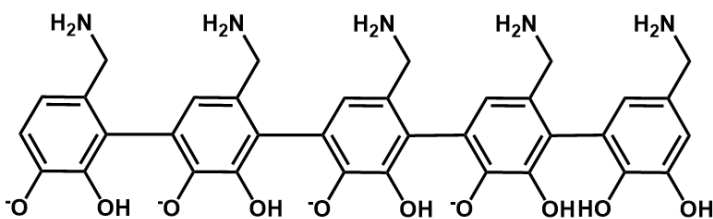
4.6.1 Proposed structure of 3,4-dihydroxybenzylamine Oligomers Based on the ToF Spectrum



Calcd. : 413.43
Found : 413.21



Calcd. : 551.58
Found : 551.63



Calcd. : 683.68
Found : 683.36

Scheme S4-1 Calculated and found molecular weight of trimer, tetramer, and pentamer and their corresponding molecular structures.

4.6.2 ^1H NMR spectra of DHI-free PCA During 7 hrs in $\text{NaHCO}_3/\text{D}_2\text{O}$

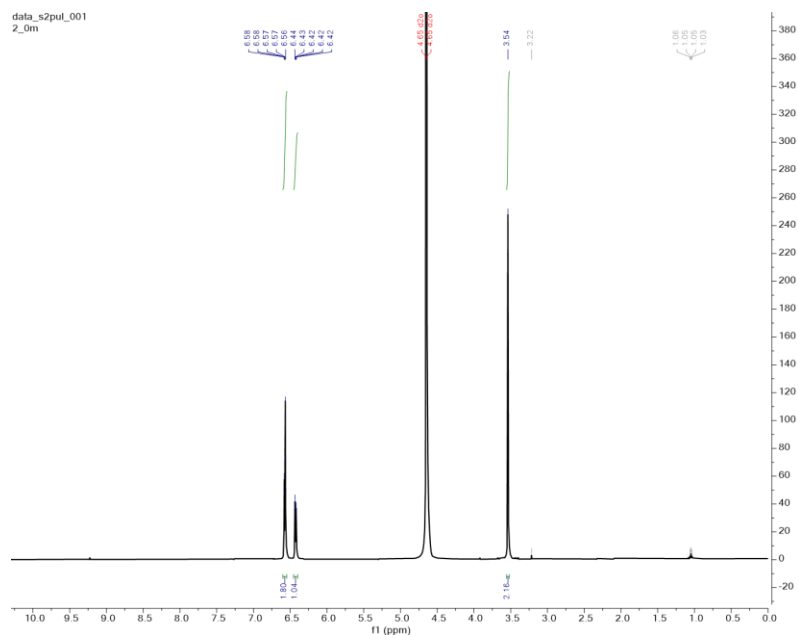


Figure S4-1 ^1H NMR spectra of DHI-free PCA after 0 min.

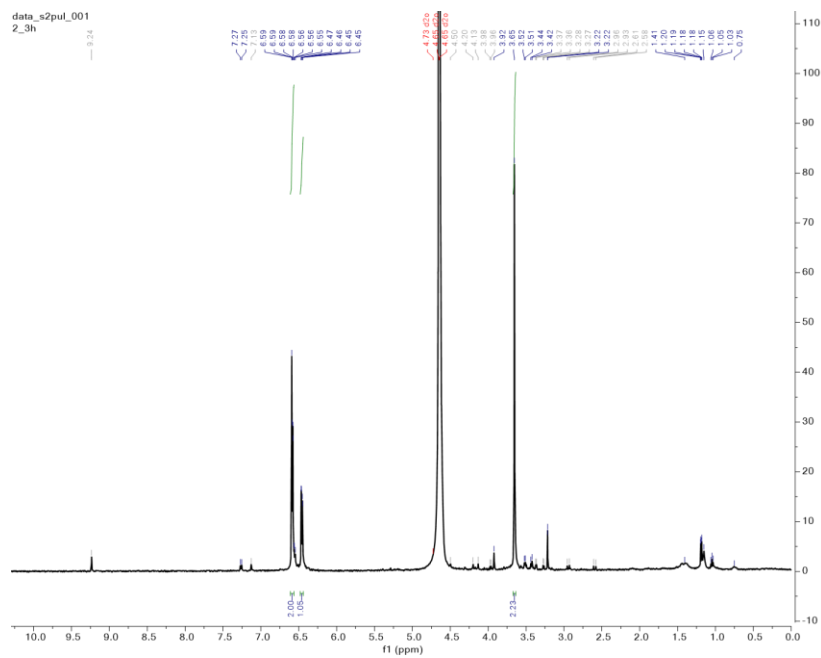


Figure S4-2 ^1H NMR spectra of DHI-free PCA after 3 hrs.

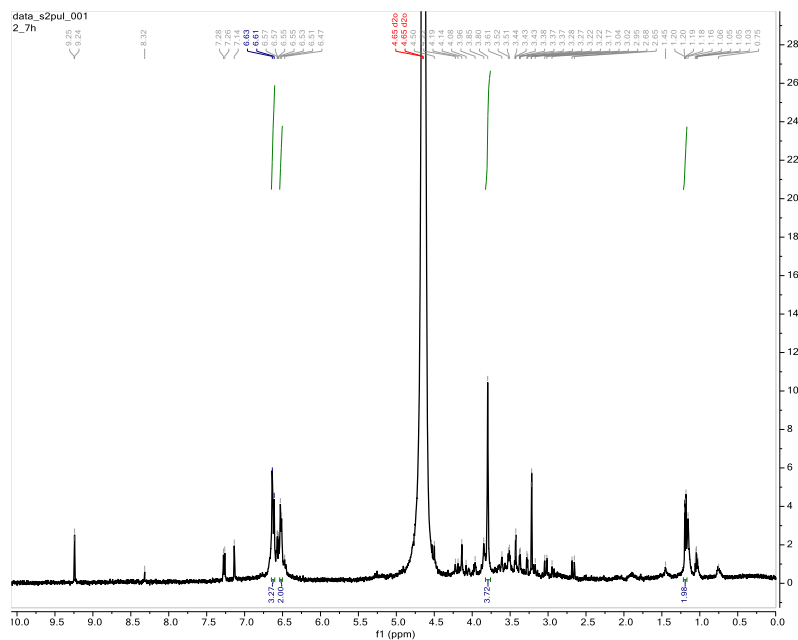
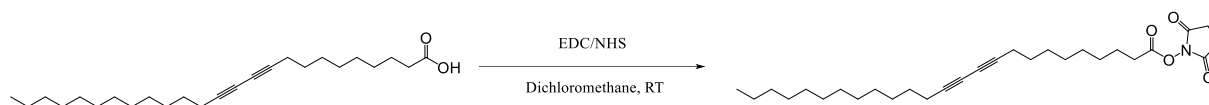


Figure S4-3 ^1H NMR spectra of DHI-free PCA after 7 hrs.

4.6.3 Solid-state NMR Spectroscopy

Proton to carbon-13 cross-polarization Magic angle spinning (CP-MAS) solid-state NMR experiments were conducted on a 400 MHz (9.4 T) Bruker Avance NMR spectrometer with 400.16 MHz and 100.62 MHz resonance frequencies for ^1H and ^{13}C nuclei, respectively. A 2.5 mm HCN triple-resonance MAS probe from Bruker was used to acquire ^{13}C CP-MAS NMR spectra under 15 kHz MAS at 295 K. ^{13}C chemical shifts were externally referenced to adamantane's $^{13}\text{CH}_2$ peak at 38.48 ppm with 0 ppm for ^{13}C peak of tetramethylsilane (TMS). A ramp-CP pulse sequence was used to enhance the sensitivity with a 100 kHz radiofrequency (RF) field for ^1H 90° and 1H decoupling pulses. The RF field on the 1H RF channel was ramped from 42 to 84 kHz, while it was 63 kHz on the ^{13}C RF channel. One-dimensional ^{13}C NMR spectra of a powder sample of PDA polymer were obtained using 2 ms and 250 μs contact times with 46,000 scans and a recycle delay of 2 s.

4.6.4 Synthesis of 10,12-pentacosadiynoic Acid (PCDA)-NHS²



Scheme S4- 2 Synthetic route of PCDA-NHS.

10, 12-pentacosadiynoic acid (2.0 g, 5.34 mmol) was dissolved in dichloromethane (20 ml) and 1-Ethyl-3-(3-dimethylaminopropyl)carbodiimide(EDC) (0.80 g, 6.94 mmol), and N-Hydroxysuccinimide(NHS) (1.33 g, 6.94 mmol) dissolved in the solution. The mixture was stirred at room temperature for 2 h. The mixture was dried using rotary evaporation under vacuum at room temperature. The mixture was transferred to a funnel using 50 ml of Ethyl acetate and washed with distilled water. The organic phase was concentrated in vacuo and yielded a white solid. ¹H NMR (300 MHz, CDCl₃): δ(ppm) 0.86 (t, 3H), 1.21-1.65 (m, 32H), 2.21 (t, 4H), 2.60 (t, 2H), 2.87 (s, 4H).

4.7 Reference

- (1) Lee, H.; Dellatore, S. M.; Miller, W. M.; Messersmith, P. B. Mussel-Inspired Surface Chemistry for Multifunctional Coatings. *Science*. **2007**, *318* (5849), 426–430.
<https://doi.org/10.1126/science.1147241>.
- (2) Black, K. C. L.; Yi, J.; Rivera, J. G.; Zelasko-Leon, D. C.; Messersmith, P. B. Polydopamine-Enabled Surface Functionalization of Gold Nanorods for Cancer Cell-Targeted Imaging and Photothermal Therapy. *Nanomedicine* **2013**, *8* (1), 17–28.
<https://doi.org/10.2217/nnm.12.82>.

- (3) Zhang, Z.; Zhang, J.; Zhang, B.; Tang, J. Mussel-Inspired Functionalization of Graphene for Synthesizing Ag-Polydopamine-Graphene Nanosheets as Antibacterial Materials. *Nanoscale* **2012**, *5* (1), 118–123. <https://doi.org/10.1039/c2nr32092d>.
- (4) Suárez-García, S.; Sedó, J.; Saiz-Poseu, J. ; Ruiz-Molina, D. Copolymerization of a Catechol and a Diamine as a Versatile Polydopamine-Like Platform for Surface Functionalization: The Case of a Hydrophobic Coating. *Biomimetics* **2017**, *2* (4), 22. <https://doi.org/10.3390/biomimetics2040022>.
- (5) Lv, Y.; Yang, S. J.; Du, Y.; Yang, H. C.; Xu, Z. K. Co-Deposition Kinetics of Polydopamine/Polyethyleneimine Coatings: Effects of Solution Composition and Substrate Surface. *Langmuir* **2018**, *34* (44), 13123–13131. <https://doi.org/10.1021/acs.langmuir.8b02454>.
- (6) Kang, D. H.; Jung, H. S.; Kim, K.; Kim, J. Mussel-Inspired Universal Bioconjugation of Polydiacetylene Liposome for Droplet-Array Biosensors. *ACS Appl. Mater. Interfaces* **2017**, *9* (48), 42210–42216. <https://doi.org/10.1021/acsami.7b14086>.
- (7) Matos-Pérez, C. R.; White, J. D.; Wilker, J. J. Polymer Composition and Substrate Influences on the Adhesive Bonding of a Biomimetic, Cross-Linking Polymer. *J. Am. Chem. Soc.* **2012**, *134* (22), 9498–9505. <https://doi.org/10.1021/ja303369p>.
- (8) Liebscher, J. Chemistry of Polydopamine – Scope, Variation, and Limitation. *European J. Org. Chem.* **2019**, *2019* (31–32), 4976–4994. <https://doi.org/10.1002/ejoc.201900445>.
- (9) Ponzio, F.; Barthès, J.; Bour, J.; Michel, M.; Bertani, P.; Hemmerlé, J.; D’Ischia, M.; Ball, V. Oxidant Control of Polydopamine Surface Chemistry in Acids: A Mechanism-Based Entry to Superhydrophilic-Superoleophobic Coatings. *Chem. Mater.* **2016**, *28* (13), 4697–4705. <https://doi.org/10.1021/acs.chemmater.6b01587>.
- (10) Chen, T. P.; Liu, T.; Su, T. L.; Liang, J. Self-Polymerization of Dopamine in Acidic Environments without Oxygen. *Langmuir* **2017**, *33* (23), 5863–5871. <https://doi.org/10.1021/acs.langmuir.7b01127>.

- (11) Du, X.; Li, L.; Li, J.; Yang, C.; Frenkel, N.; Welle, A.; Heissler, S.; Nefedov, A.; Grunze, M.; Levkin, P. UV-Triggered Dopamine Polymerization: Control of Polymerization, Surface Coating, and Photopatterning. *Adv. Mater.* **2014**, *26* (47), 8029–8033. <https://doi.org/10.1002/adma.201403709>.
- (12) Waite, J. H.; Tanzer, M. L. Polyphenolic Substance of *Mytilus Edulis*: Novel Adhesive Containing L-Dopa and Hydroxyproline. *Science* **1981**, *212* (4498), 1038–1040. <https://doi.org/10.1126/science.212.4498.1038>.
- (13) Yu, M.; Hwang, J.; Deming, T. J. Role of 1-3,4-Dihydroxyphenylalanine in Mussel Adhesive Proteins. *J. Am. Chem. Soc.* **1999**, *121* (24), 5825–5826. <https://doi.org/10.1021/ja990469y>.
- (14) Ejima, H.; Richardson, J. J.; Liang, K.; Best, J. P.; Van Koeverden, M. P.; Such, G. K.; Cui, J.; Caruso, F. One-Step Assembly of Coordination Complexes for Versatile Film and Particle Engineering. *Science* **2013**, *341* (6142), 154–157. <https://doi.org/10.1126/science.1237265>.
- (15) Shutava, T.; Prouty, M.; Kommireddy, D.; Lvov, Y. PH Responsive Decomposable Layer-by-Layer Nanofilms and Capsules on the Basis of Tannic Acid. *Macromolecules* **2005**, *38* (7), 2850–2858. <https://doi.org/10.1021/ma047629x>.
- (16) Waite, J. H.; Andersen, N. H.; Jewhurst, S.; Sun, C. Mussel Adhesion: Finding the Tricks Worth Mimicking. *The Journal of Adhesion* **2006**, *81*, 297–317. <https://doi.org/10.1080/00218460590944602>.
- (17) Lee, H.; Scherer, N. F.; Messersmith, P. B. Single-Molecule Mechanics of Mussel Adhesion. *Proc. Natl. Acad. Sci. U. S. A.* **2006**, *103* (35), 12999. <https://doi.org/10.1073/pnas.0605552103>.
- (18) Fant, C.; Hedlund, J.; Höök, F.; Berglin, M.; Fridell, E.; Elwing, H. Investigation of Adsorption and Cross-Linking of a Mussel Adhesive Protein Using Attenuated Total Internal Reflection Fourier Transform Infrared Spectroscopy (ATR-FTIR). *The Journal of Adhesion* **2010**, *86* (1), 25–38. <https://doi.org/10.1080/00218460903417768>.

- (19) Sedó, J.; Saiz-Poseu, J.; Busqué, F.; Ruiz-Molina, D. Catechol-Based Biomimetic Functional Materials. *Adv. Mater.* **2013**, *25* (5), 653–701.
<https://doi.org/10.1002/adma.201202343>.
- (20) Olivieri, M. P.; Wollman, R. M.; Hurley, M. I.; Swartz, M. F. Using Conformational Analysis to Identify Structurally Conserved Regions of MAP Peptides That Exhibit Cellular Attachment Ability. *Biofouling* **2010**, *18* (2), 149-159.
<https://doi.org/10.1080/08927010290013035>.
- (21) Suci, P. A.; Geesey, G. G. Influence of Sodium Periodate and Tyrosinase on Binding of Alginate to Adlayers of *Mytilus Edulis* Foot Protein 1. *J. Colloid Interface Sci.* **2000**, *230* (2), 340–348. <https://doi.org/10.1006/jcis.2000.7120>.
- (22) Hemmatpour, H.; De Luca, O.; Crestani, D.; Stuart, M. C. A.; Lasorsa, A.; van der Wel, P. C. A.; Loos, K.; Giouisis, T.; Haddadi-Asl, V.; Rudolf, P. New Insights in Polydopamine Formation via Surface Adsorption. *Nat. Commun.* **2023**, *14* (1), 1–12.
<https://doi.org/10.1038/s41467-023-36303-8>.
- (23) Hong, S.; Yeom, J.; Song, I. T.; Kang, S. M.; Lee, H.; Lee, H. Pyrogallol 2-Aminoethane: A Plant Flavonoid-Inspired Molecule for Material-Independent Surface Chemistry. *Adv. Mater. Interfaces* **2014**, *1* (4). <https://doi.org/10.1002/admi.201400113>.
- (24) Della Vecchia, N. F.; Avolio, R.; Alfè, M.; Errico, M. E.; Napolitano, A.; D’Ischia, M. Building-Block Diversity in Polydopamine Underpins a Multifunctional Eumelanin-Type Platform Tunable Through a Quinone Control Point. *Adv. Funct. Mater.* **2013**, *23* (10), 1331–1340. <https://doi.org/10.1002/adfm.201202127>.
- (25) Hu, H.; Dyke, J. C.; Bowman, B. A.; Ko, C.-C.; You, W. Investigation of Dopamine Analogues: Synthesis, Mechanistic Understanding, and Structure–Property Relationship. *Langmuir* **2016**, *32* (38), 9873–9882. <https://doi.org/10.1021/acs.langmuir.6b02141>.
- (26) Lyu, Q.; Hsueh, N.; Chai, C. L. L. Direct Evidence for the Critical Role of 5,6-Dihydroxyindole in Polydopamine Deposition and Aggregation. *Langmuir* **2019**, *35* (15), 5191–5201. <https://doi.org/10.1021/ACS.LANGMUIR.9B00392>.

- (27) Petran, A.; Filip, C.; Bogdan, D.; Zimmerer, C.; Beck, S.; Radu, T.; Liebscher, J. Oxidative Polymerization of 3,4-Dihydroxybenzylamine—The Lower Homolog of Dopamine. *Langmuir* **2023**, *39* (15), 5610–5620 <https://doi.org/10.1021/acs.langmuir.3c00604>.
- (28) Seo, D.; Ansari, R.; Lee, K.; Kieffer, J.; Kim, J. Amplifying the Sensitivity of Polydiacetylene Sensors: The Dummy Molecule Approach. *ACS Appl. Mater. Interfaces* **2022**, *14*, 14561–14567. <https://doi.org/10.1021/acsami.1c25066>.
- (29) Seo, D.; Major, T. C.; Kang, D. H.; Seo, S.; Lee, K.; Bartlett, R. H.; Kim, J. Polydiacetylene Liposome Microarray toward Facile Measurement of Platelet Activation in Whole Blood. *ACS Sensors* **2021**, *6* (9), 3170–3175. <https://doi.org/10.1021/acssensors.1C01167>.
- (30) Chen, C. T.; Martin-Martinez, F. J.; Jung, G. S.; Buehler, M. J. Polydopamine and Eumelanin Molecular Structures Investigated with Ab Initio Calculations. *Chem. Sci.* **2017**, *8* (2), 1631–1641. <https://doi.org/10.1039/c6sc04692d>.
- (31) Della Vecchia, N. F.; Avolio, R.; Alfè, M.; Errico, M. E.; Napolitano, A.; D’Ischia, M. Building-Block Diversity in Polydopamine Underpins a Multifunctional Eumelanin-Type Platform Tunable through a Quinone Control Point. *Adv. Funct. Mater.* **2013**, *23* (10), 1331–1340. <https://doi.org/10.1002/adfm.201202127>.
- (32) Hong, S.; Wang, Y.; Park, S. Y.; Lee, H. Progressive Fuzzy Cation- Assembly of Biological Catecholamines. *Sci. Adv.* **2018**, *4* (9), 1–11. <https://doi.org/10.1126/sciadv.aat7457>.
- (33) Wei, Q.; Zhang, F.; Li, J.; Li, B.; Zhao, C. Oxidant-Induced Dopamine Polymerization for Multifunctional Coatings. *Polym. Chem.* **2010**, *1* (9), 1430–1433. <https://doi.org/10.1039/c0py00215a>.
- (34) Mrówczyński, R.; Markiewicz, R.; Liebscher, J. Chemistry of Polydopamine Analogues. *Polym. Int.* **2016**, *65* (11), 1288–1299. <https://doi.org/10.1002/pi.5193>.

- (35) Miao, Z.-H.; Wang, H.; Yang, H.; Li, Z.-L.; Zhen, L.; Xu, C.-Y. Intrinsically Mn²⁺-Chelated Polydopamine Nanoparticles for Simultaneous Magnetic Resonance Imaging and Photothermal Ablation of Cancer Cells. *ACS Appl. Mater. Interfaces* **2015**, *7* (31), 16946–16952. <https://doi.org/10.1021/acsami.5b06265>.
- (36) Liebscher, J.; Mrówczyński, R.; Scheidt, H. A.; Filip, C.; Haidade, N. D.; Turcu, R.; Bende, A.; Beck, S. Structure of Polydopamine: A Never-Ending Story? *Langmuir* **2013**, *29* (33), 10539–10548. <https://doi.org/10.1021/la4020288>.
- (37) Delparastan, P.; Malollari, K. G.; Lee, H.; Messersmith, P. B. Direct Evidence for the Polymeric Nature of Polydopamine. *Angew. Chemie Int. Ed.* **2019**, *58* (4), 1077–1082. <https://doi.org/10.1002/anie.201811763>.
- (38) Schreiber, H. P.; Qin, R.; Sengupta, A. The Effectiveness of Silane Adhesion Promoters in the Performance of Polyurethane Adhesives. *The Journal of Adhesion* **2006**, *68*, 31–44. <https://doi.org/10.1080/00218469808029578>.
- (39) Gan, D.; Xing, W.; Jiang, L.; Fang, J.; Zhao, C.; Ren, F.; Fang, L.; Wang, K.; Lu, X. Plant-Inspired Adhesive and Tough Hydrogel Based on Ag-Lignin Nanoparticles-Triggered Dynamic Redox Catechol Chemistry. *Nat. Commun* **2019**, *10* (1), 1–10. <https://doi.org/10.1038/s41467-019-09351-2>.
- (40) Wang, Y.; Jia, K.; Xiang, C.; Yang, J.; Yao, X.; Suo, Z. Instant, Tough, Noncovalent Adhesion. *ACS Appl. Mater. Interfaces* **2019**, *11* (43), 40749–40757. <https://doi.org/10.1021/acsami.9B10995>.
- (41) Chen, J.; Wang, D.; Wang, L.-H.; Liu, W.; Chiu, A.; Shariati, K.; Liu, Q.; Wang, X.; Zhong, Z.; Webb, J.; Schwartz, R. E.; Bouklas, N.; Ma, M. An Adhesive Hydrogel with “Load-Sharing” Effect as Tissue Bandages for Drug and Cell Delivery. *Adv. Mater.* **2020**, *32* (43), 2001628. <https://doi.org/10.1002/adma.202001628>.
- (42) Patel, H. A.; Byun, J.; Yavuz, C. T. Carbon Dioxide Capture Adsorbents: Chemistry and Methods. *ChemSusChem* **2017**, *10* (7), 1303–1317. <https://doi.org/10.1002/CSSC.201601545>.

- (43) Janeta, M.; John, Ł.; Ejfler, J.; Szafet, S. High-Yield Synthesis of Amido-Functionalized Polyoctahedral Oligomeric Silsesquioxanes by Using Acyl Chlorides. *Chem. – A Eur. J.* **2014**, *20* (48), 15966–15974. <https://doi.org/10.1002/chem.201404153>.
- (44) Xie, Y.; Hill, C. A. S.; Xiao, Z.; Militz, H.; Mai, C. Silane Coupling Agents Used for Natural Fiber/Polymer Composites: A Review. *Compos. Part A Appl. Sci. Manuf.* **2010**, *41* (7), 806–819. <https://doi.org/10.1016/j.compositesa.2010.03.005>.
- (45) Xu, X.; Song, C.; Andresen, J. M.; Miller, B. G.; Scaroni, A. W. Novel Polyethylenimine-Modified Mesoporous Molecular Sieve of MCM-41 Type as High-Capacity Adsorbent for CO₂ Capture. *Energy and Fuels* **2002**, *16* (6), 1463–1469. <https://doi.org/10.1021/ef020058u>.
- (46) Jiang, Y.; Tang, Y.; Miao, P. Polydopamine Nanosphere@silver Nanoclusters for Fluorescence Detection of Multiplex Tumor Markers. *Nanoscale* **2019**, *11* (17), 8119–8123. <https://doi.org/10.1039/c9nr01307e>.
- (47) Ji, X.; Palui, G.; Avellini, T.; Na, H. Bin; Yi, C.; Knappenberger, K. L.; Mattoussi, H. On the PH-Dependent Quenching of Quantum Dot Photoluminescence by Redox Active Dopamine. *J. Am. Chem. Soc.* **2012**, *134* (13), 6006–6017. <https://doi.org/10.1021/ja300724x>.
- (48) Balandin, A. A.; Ghosh, S.; Bao, W.; Calizo, I.; Teweldebrhan, D.; Miao, F.; Lau, C. N. Superior Thermal Conductivity of Single-Layer Graphene. *Nano Lett.* **2008**, *8*, 3, 902–907. <https://doi.org/10.1021/nl0731872>.
- (49) Cai, W.; Moore, A. L.; Zhu, Y.; Li, X.; Chen, S.; Shi, L.; Ruoff, R. S. Thermal Transport in Suspended and Supported Monolayer Graphene Grown by Chemical Vapor Deposition. *Nano Lett.* **2010**, *10* (5), 1645–1651. <https://doi.org/10.1021/nl9041966>.
- (50) Chen, S.; Moore, A. L.; Cai, W.; Suk, J. W.; An, J.; Mishra, C.; Amos, C.; Magnuson, C. W.; Kang, J.; Shi, L.; Ruoff, R. S. Raman Measurements of Thermal Transport in Suspended Monolayer Graphene of Variable Sizes in Vacuum and Gaseous Environments. *ACS Nano* **2011**, *5* (1), 321–328. <https://doi.org/10.1021/nn102915x>.

- (51) Lee, J.-U.; Yoon, D.; Kim, H.; Lee, S. W.; Cheong, H. Thermal Conductivity of Suspended Pristine Graphene Measured by Raman Spectroscopy. *RAPID Commun. Phys. Rev. B* **2011**, *83*, 81419. <https://doi.org/10.1103/PhysRevB.83.081419>.
- (52) Kulkarni, H. B.; Tambe, P.; M. Joshi, G. Influence of Covalent and Non-Covalent Modification of Graphene on the Mechanical, Thermal and Electrical Properties of Epoxy/Graphene Nanocomposites: A Review. *Compos. Interfaces* **2018**, *25*, 381–414. <https://doi.org/10.1080/09276440.2017.1361711>.
- (53) Cho, E. C.; Huang, J. H.; Li, C. P.; Chang-Jian, C. W.; Lee, K. C.; Hsiao, Y. S.; Huang, J. H. Graphene-Based Thermoplastic Composites and Their Application for LED Thermal Management. *Carbon N. Y.* **2016**, *102*, 66–73. <https://doi.org/10.1016/j.carbon.2016.01.097>.
- (54) Shim, S. H.; Kim, K. T.; Lee, J. U.; Jo, W. H. Facile Method to Functionalize Graphene Oxide and Its Application to Poly(Ethylene Terephthalate)/Graphene Composite. *ACS Appl. Mater. Interfaces* **2012**, *4* (8), 4184–4191. <https://doi.org/10.1021/am300906z>.
- (55) Cheng, H. K. F.; Sahoo, N. G.; Tan, Y. P.; Pan, Y.; Bao, H.; Li, L.; Chan, S. H.; Zhao, J. Poly(Vinyl Alcohol) Nanocomposites Filled with Poly(Vinyl Alcohol)-Grafted Graphene Oxide. *ACS Appl. Mater. Interfaces* **2012**, *4* (5), 2387–2394. <https://doi.org/10.1021/am300550n>.
- (56) Pollack, G. L. Kapitza Resistance. *Rev. Mod. Phys.* **1969**, *41* (1), 48. <https://doi.org/10.1103/RevModPhys.41.48>.
- (57) Gao, Y.; Müller-Plathe, F. Increasing the Thermal Conductivity of Graphene-Polyamide-6,6 Nanocomposites by Surface-Grafted Polymer Chains: Calculation with Molecular Dynamics and Effective-Medium Approximation. *J. Phys. Chem. B* **2016**, *120* (7), 1336–1346. <https://doi.org/10.1021/acs.jpcc.5b08398>.
- (58) Wang, Y.; Zhan, H. F.; Xiang, Y.; Yang, C.; Wang, C. M.; Zhang, Y. Y. Effect of Covalent Functionalization on Thermal Transport across Graphene-Polymer Interfaces. *J. Phys. Chem. C* **2015**, *119* (22), 12731–12738. <https://doi.org/10.1021/acs.jpcc.5b02920>.

- (59) Sayed, S. Y.; Fereiro, J. A.; Yan, H.; McCreery, R. L.; Bergren, A. J. Charge Transport in Molecular Electronic Junctions: Compression of the Molecular Tunnel Barrier in the Strong Coupling Regime. *Proc. Natl. Acad. Sci. U. S. A.* **2012**, *109* (29), 11498–11503. <https://doi.org/10.1073/pnas.1201557109>.
- (60) Liu, Y.; Wu, K.; Luo, F.; Lu, M.; Xiao, F.; Du, X.; Zhang, S.; Liang, L.; Lu, M. Significantly Enhanced Thermal Conductivity in Polyvinyl Alcohol Composites Enabled by Dopamine Modified Graphene Nanoplatelets. *Compos. Part A Appl. Sci. Manuf.* **2019**, *117*, 134–143. <https://doi.org/10.1016/j.compositesa.2018.11.015>.
- (61) Ren, Y.; Ren, L.; Li, J.; Lv, R.; Wei, L.; An, D.; Maqbool, M.; Bai, S.; Wong, C. P. Enhanced Thermal Conductivity in Polyamide 6 Composites Based on the Compatibilization Effect of Polyether-Grafted Graphene. *Compos. Sci. Technol.* **2020**, *199*, 108340. <https://doi.org/10.1016/j.compscitech.2020.108340>.
- (62) Koh, Y. K.; Singer, S. L.; Kim, W.; Zide, J. M. O.; Lu, H.; Cahill, D. G.; Majumdar, A.; Gossard, A. C. Comparison of the 3ω Method and Time-Domain Thermoreflectance for Measurements of the Cross-Plane Thermal Conductivity of Epitaxial Semiconductors. *J. Appl. Phys.* **2009**, *105* (5), 054303. <https://doi.org/10.1063/1.3078808>.
- (63) Borca-Tasciuc, T.; Kumar, A. R.; Chen, G. Data Reduction in 3ω Method for Thin-Film Thermal Conductivity Determination. *Rev. Sci. Instrum.* **2001**, *72* (4), 2139. <https://doi.org/10.1063/1.1353189>.

Chapter 5 Summary and Outlook

In this dissertation, we embarked on a comprehensive exploration of polydopamine (PDA) chemistry, beginning with its historical context in studies of mussel adhesion mechanisms and its emergence as a material with a facile application method. Since the introduction of PDA in 2007, it has inspired over twenty thousand subsequent research efforts, largely due to its unconditional binding properties. Yet, the intricate chemical structure and structure-property relationships of PDA continue to elude full comprehension. Existing theories have only partially unraveled binding mechanisms such as the roles of catechol and dihydroxyindole (DHI), DHI-induced aggregation, and amine-mediated underwater adhesion.

Chapter 2 contributed fresh insights into the PDA binding mechanism through rational molecular design. We built on prior models that compared PDA to the combination of DOPA and lysine in mussel adhesive proteins but lacked a definitive mechanism. Devising a series of molecular analogs—including catechol, catecholamine, and DHI constituents—allowed us to deconvolve the building blocks of PDA. By observing particle formation in aqueous solutions and conducting morphological analyses with scanning electron microscopy (SEM) and atomic force microscopy (AFM), we discovered that binding occurs beyond the solubility limit of agglomerates in polar solvents. The pivotal roles of amine and DHI in facilitating particle aggregation via π - π and cation- π interactions were identified. We validated our hypothesis by demonstrating the aggregation-induced adhesion of polycatechol/qPVP nanoparticles upon surface deposition.

Chapter 3 built upon the newfound knowledge of PDA binding to devise a phenolic compound-alkanedithiol copolymer system, which expands the applicability of PDA chemistry

to encompass a variety of polyphenols. The adhesive traits of catechol or gallol moieties, in tandem with hydrophobic linkers, effectively mimic the mussel adhesive protein's flexible backbone and its active binding groups, such as DOPA. This system's remarkable outcome is its surface-independent coating ability, overcoming categorical limitations associated with catecholamine-based polymers. By incorporating diverse functionalities, such as amine, acid, and aldehyde groups, to surfaces, this copolymer enhanced versatility. Moreover, this copolymer exhibits enhanced solvent resistance, outperforming the PDA, which depends on cohesive forces derived from secondary interactions, especially upon integrating a multi-functional cross-linker.

In Chapter 4, we introduced a DHI-free polycatecholamine coating that exhibits smoother surface morphology relative to PDA coatings. This study leveraged our observation from Chapter 1, which highlighted the necessity of particle formation in PDA adhesion, and reinforced the critical role of amine groups in enabling such aggregates. By preventing DHI production during self-polymerization, we not only achieved smoother surfaces but also increased primary amine functionalities, pioneering a potential substitute for conventional amine-functionalizing agents like APTES. Subsequent applications for surface amine-functionalization validated our approach through fluorescent dye-based assessments. Extending this innovation to graphene, we applied the coating method to enhance the thermal conductivity of the polymer-graphene composite, which exhibited up to an 87% increase when compared to untreated graphene-polymer composites, thereby markedly reducing interfacial thermal resistance.

Looking ahead, we designed an extended amine-bearing catechol molecule inspired by DHI-free polycatecholamine. This design stems from the observation that in the latter polymer, most amines are obscured by the benzene ring or engaged in cation- π interactions, hence

inaccessible on the surface. Introducing a longer alkyl chain augments the steric freedom of the amine, potentially maximizing surface functionality for diverse aminations.

Additionally, to augment the polyphenol-alkanedithiol copolymer research, we designed a monomer incorporating a catechol and a carbene moiety to produce a robust coating. Carbenes, known for their reactivity with hydrocarbons, should enable adjacent carbon atoms to form covalent bonds. We hypothesize that combining carbene-catechol with traditional catecholamine monomers could increase the molecular weight and, consequently, the adhesive layer's cohesiveness and robustness.

Conclusively, this work provides not only a deeper understanding of PDA and related systems but also paves the way for future innovations in adhesive chemistry and materials science.